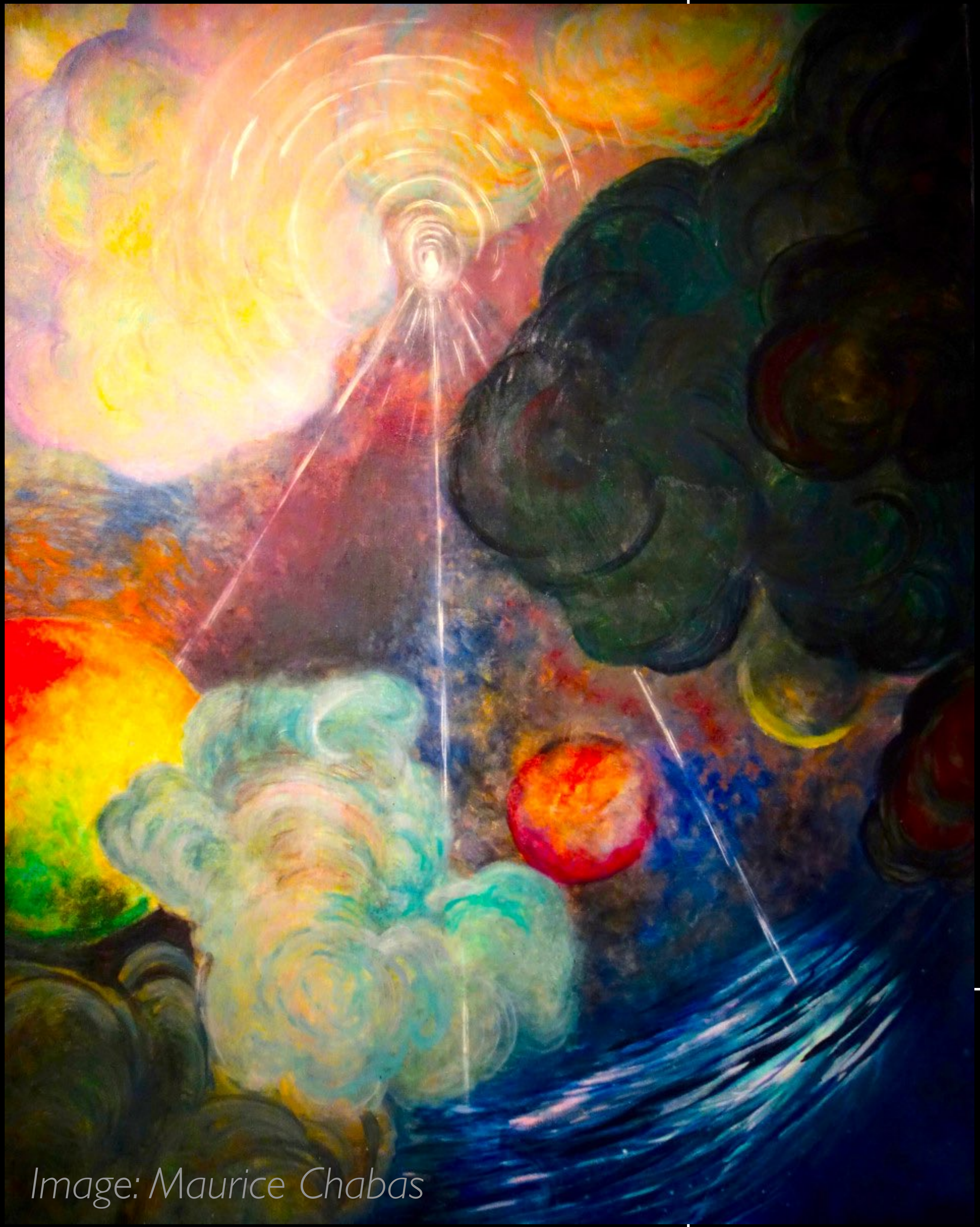

Image: Maurice Chabas

D. Ehlert[1], F. Oikonomou[1], M. Unger[2,1]

1. Norwegian University of Science and Technology, 2. Karlsruhe Institute of Technology

UHECRs from a population of sources

PRD [Editor's suggestion] arXiv:2207.10691

NTNU
Norwegian University of Science and Technology

KIT
Karlsruhe Institute of Technology

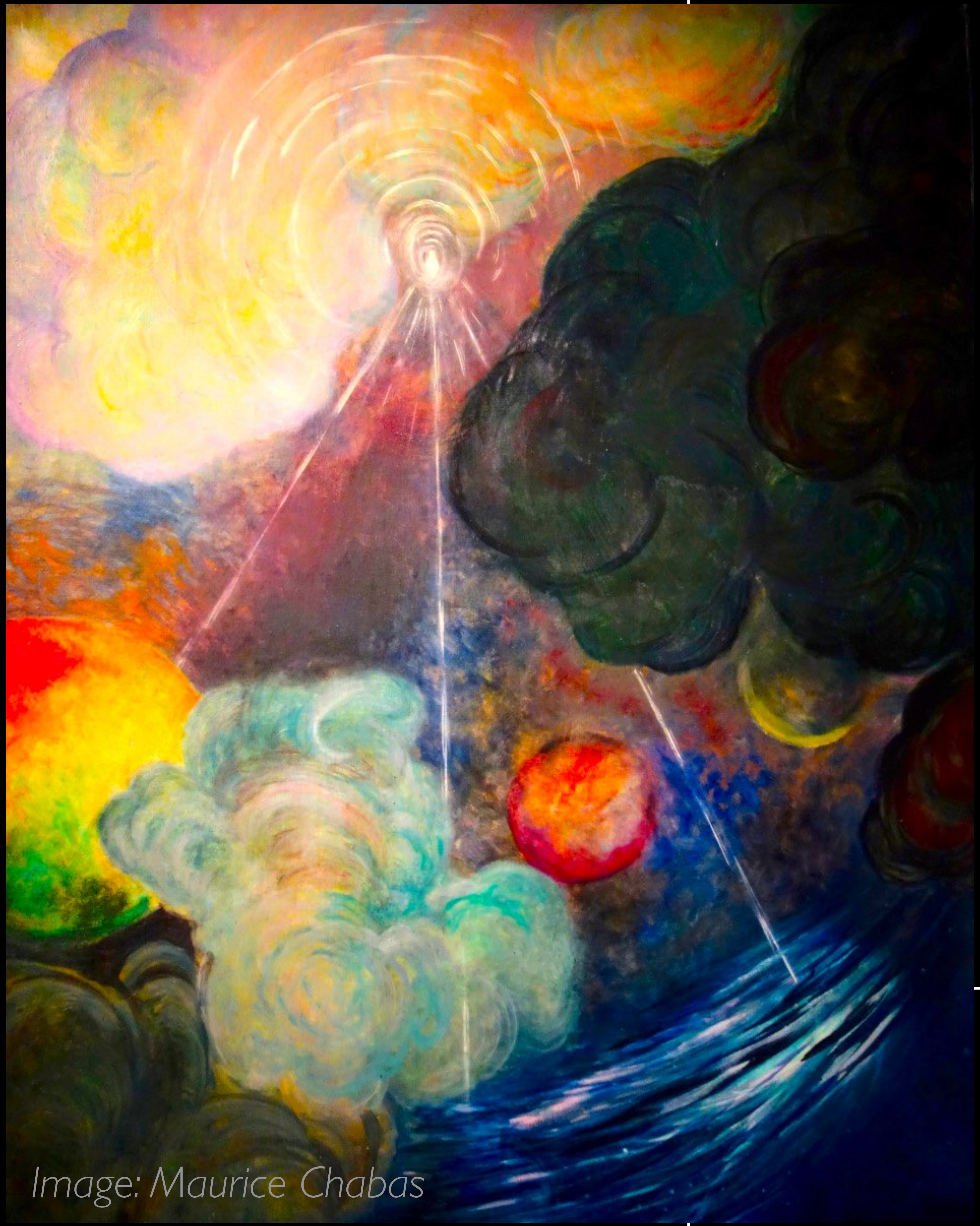

D. Ehlert[1], F. Oikonomou[1], M. Unger[2,1]

1. Norwegian University of Science and Technology, 2. Karlsruhe Institute of Technology

UHECRs from a population of sources

PRD [Editor's suggestion] arXiv:2207.10691

NTNU
Norwegian University of Science and Technology

KIT
Karlsruhe Institute of Technology

What we know about the sources of UHECRs

Arrival directions

Auger Coll. 2017 Science 357 6357

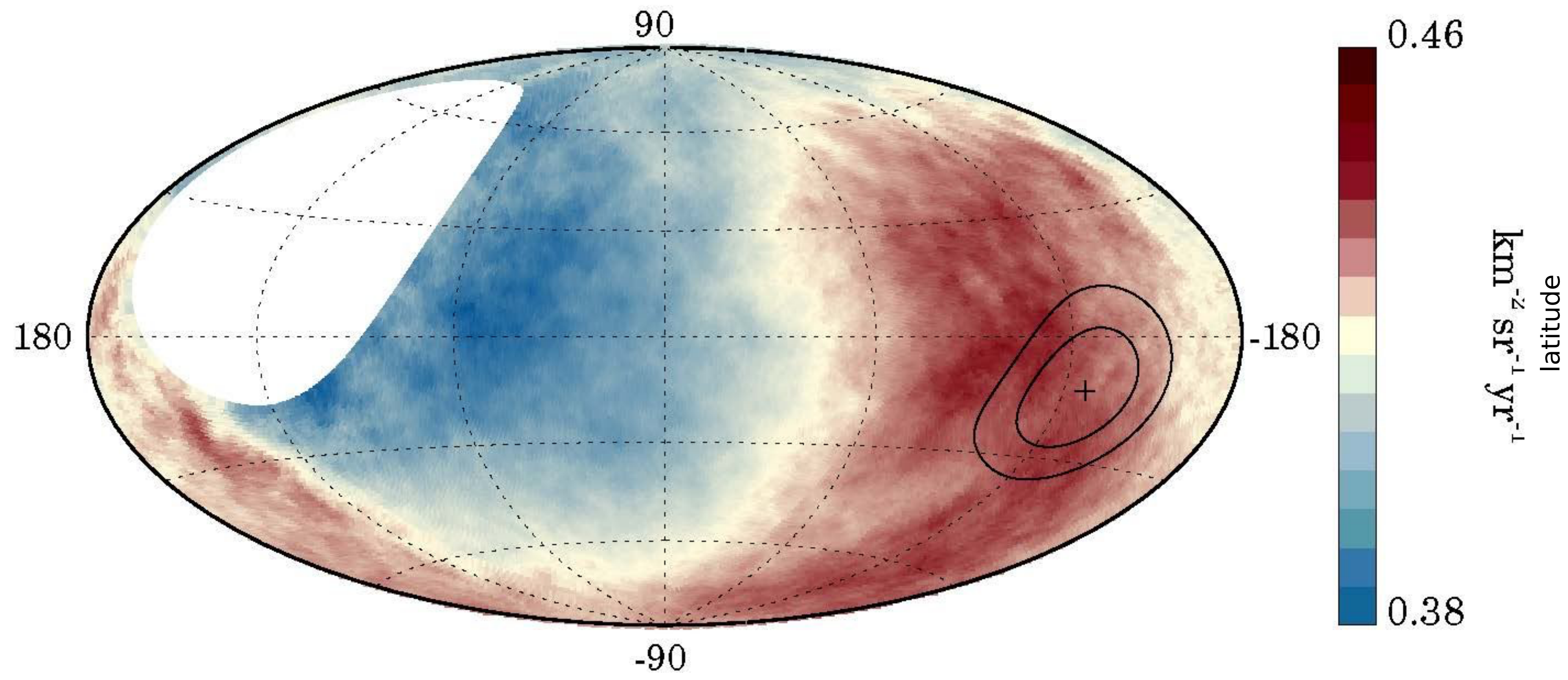

Auger Coll. 2017 ApJ 935 (2022) 170

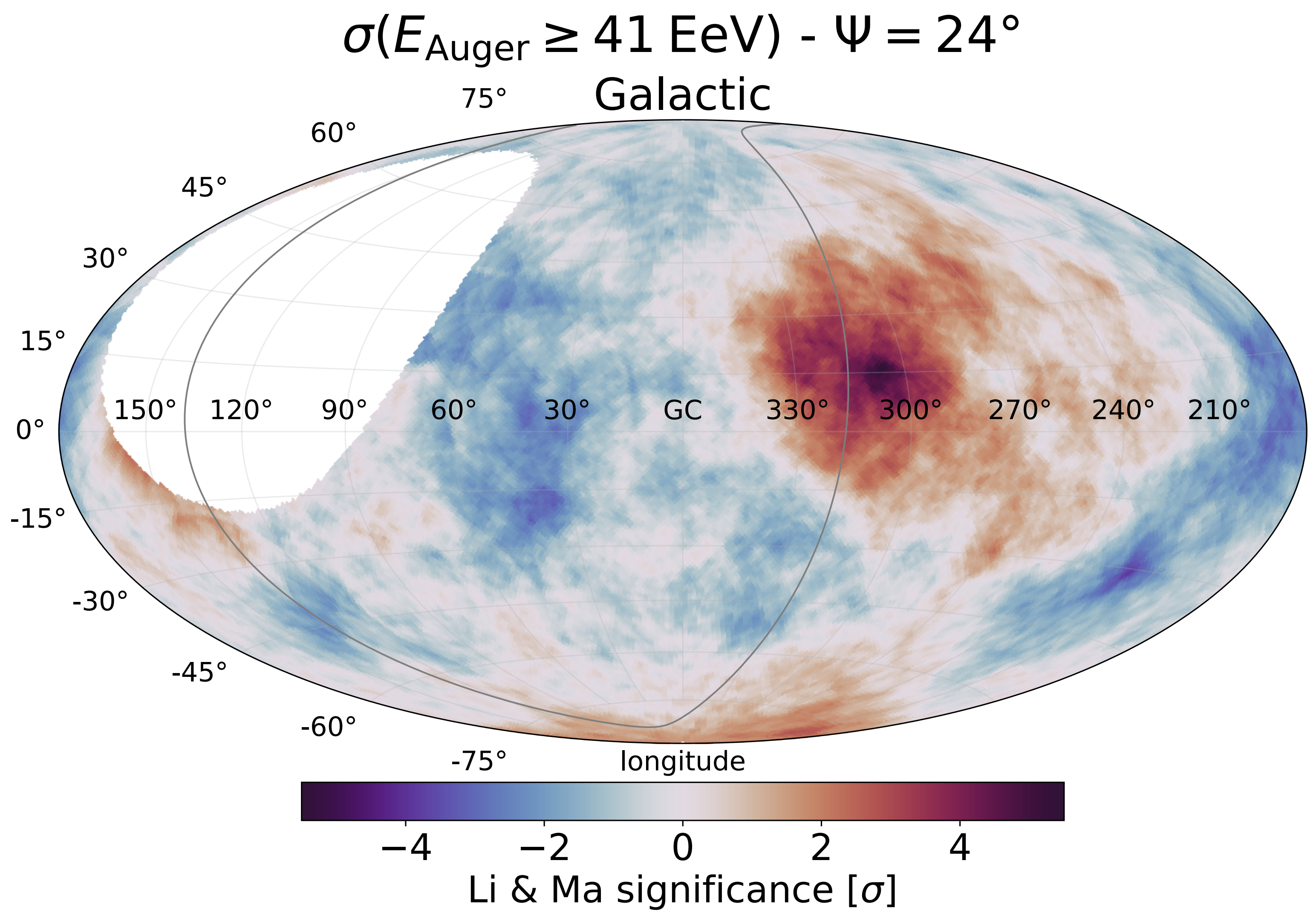

Auger Coll, JCAP05(2013)009

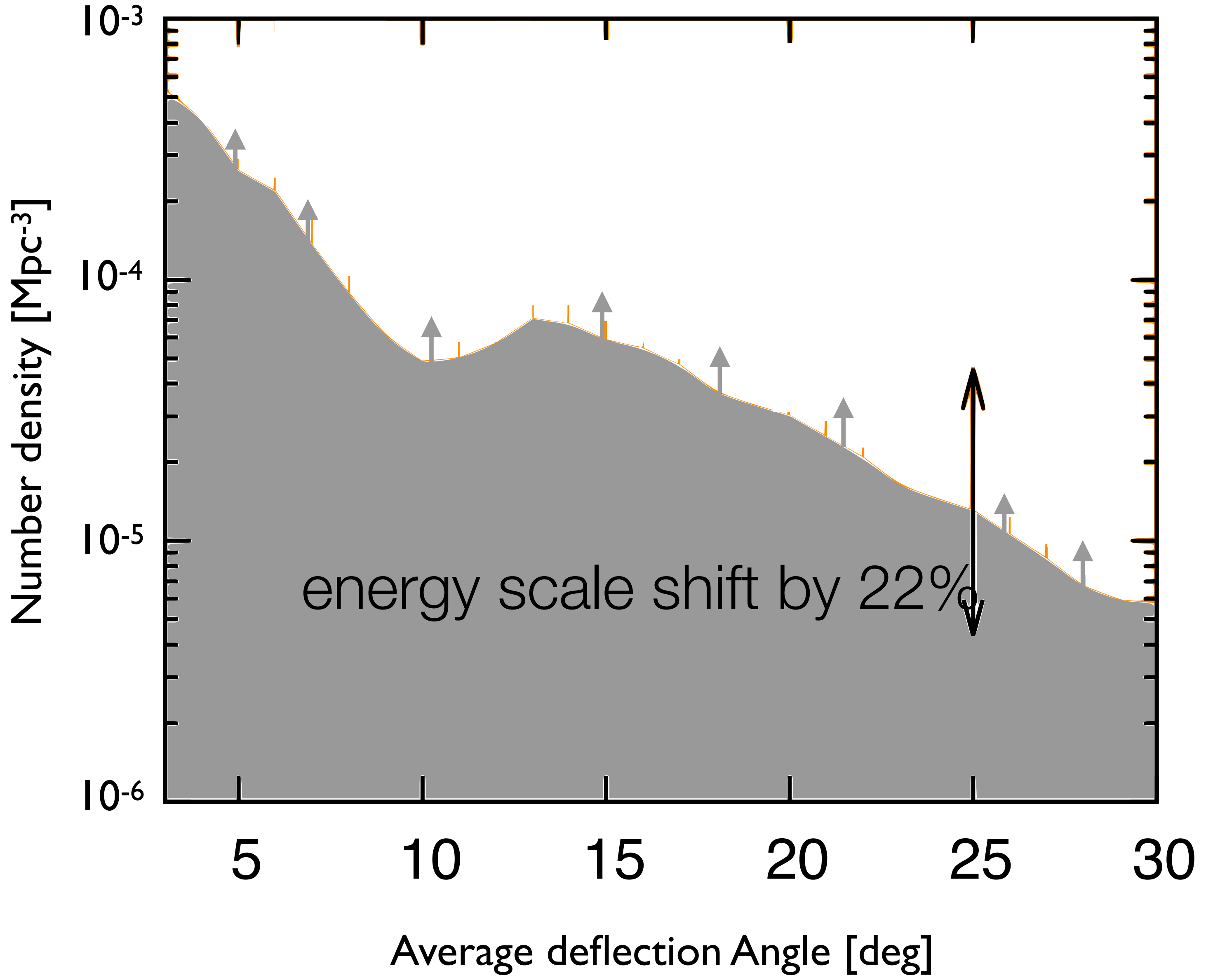

Dipole: Consistent with local galaxy distribution or local extragalactic sources (e.g. jetted AGN) *(Giacinti 2011,, Harari et al 2014,2015,2021, Mollerach et al 2017, 2021, Auger Coll 2017, Ding et al 2021, Allard et al 2022, Eichmann, Kachelriess, FO 2022)*

E > 32 EeV: Consistent with jetted AGN, Starburst galaxies, infrared galaxies, non-jetted AGN *(Auger Coll 2018, 2022, ApJ)*

Number density: 10^{-5} Mpc^{-3}, E > 70 EeV, $\langle\theta\rangle \lesssim 30°$

What we know about the sources of UHECRs

Jansson, Farrar 2012

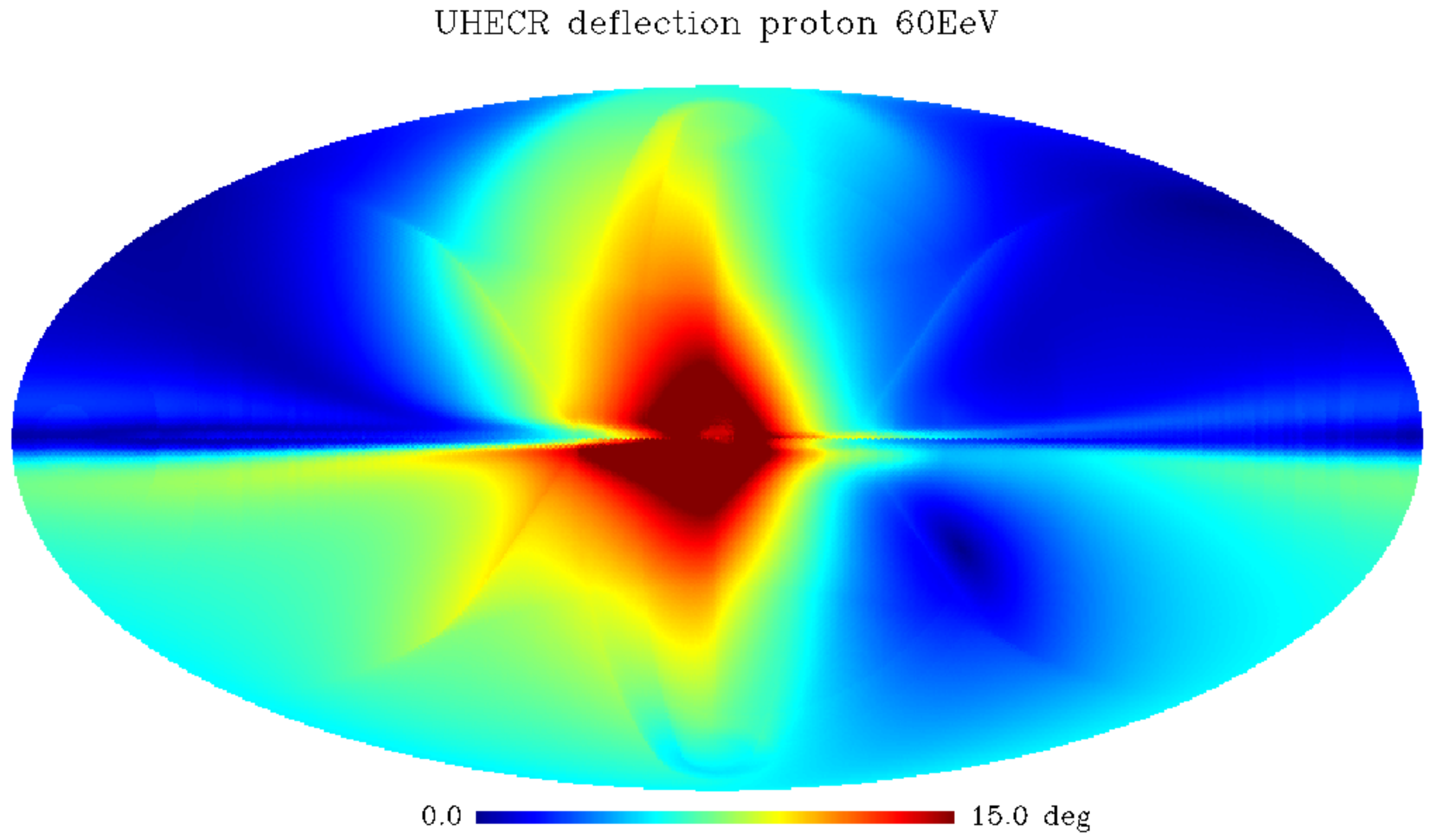

Beck et al 2014

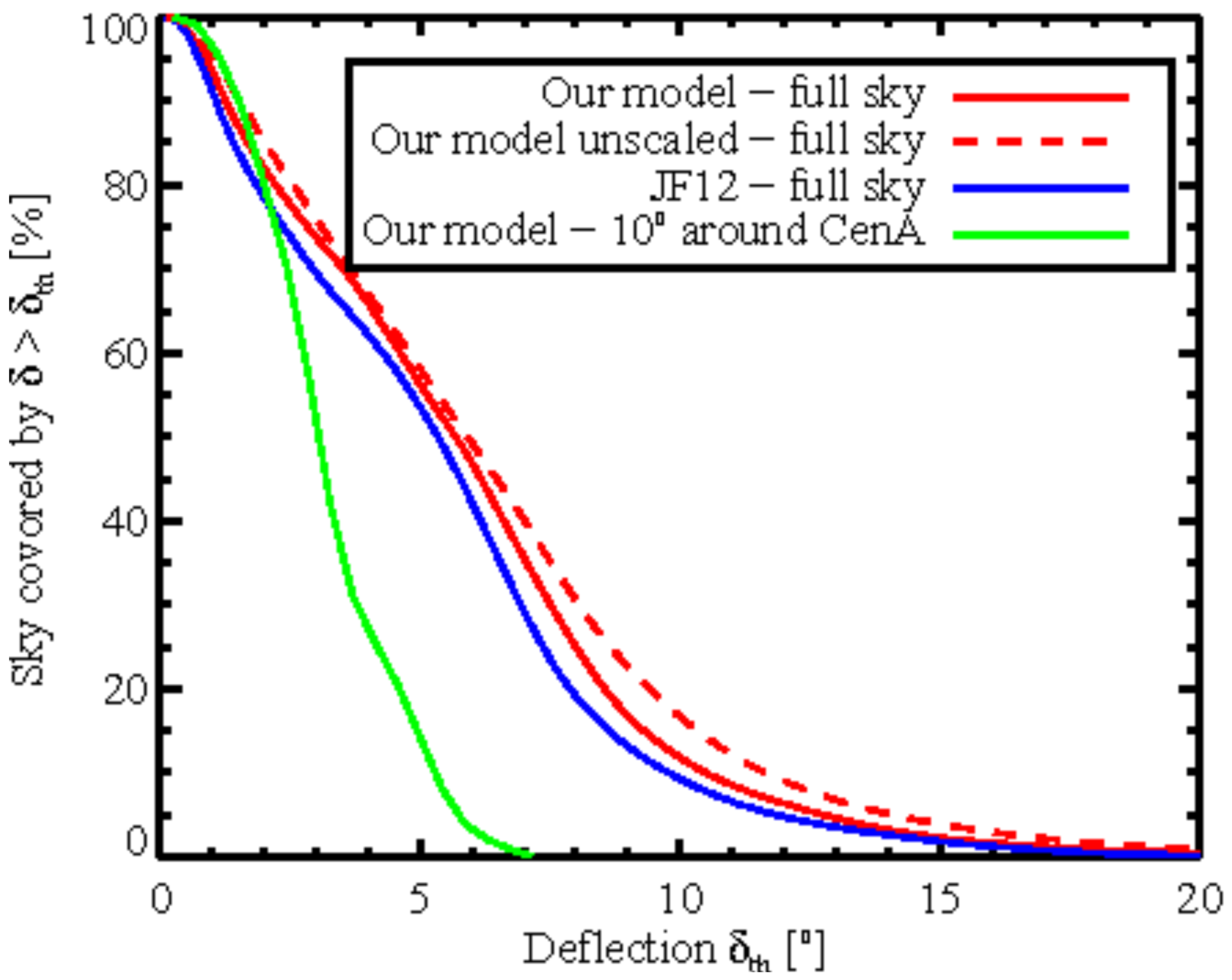

Auger Coll, JCAP05(2013)009

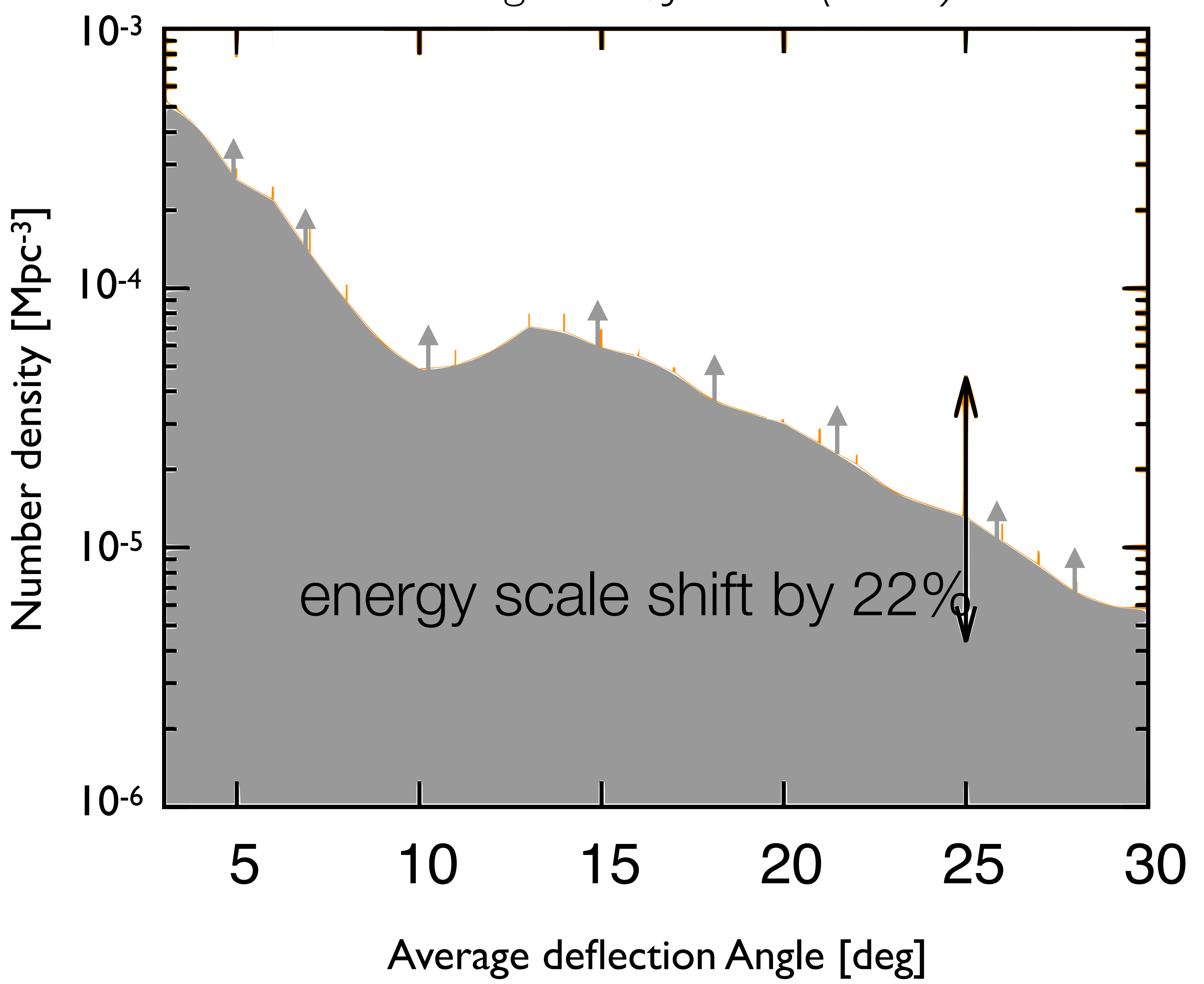

Median Deflection: $\theta_{1/2}^{\mathrm{JF12}} \sim 5^{\circ} \left(\frac{60 \text{ EV}}{R} \right)$

Number density: 10^{-5} Mpc^{-3}, E > 70 EeV, $\langle\theta\rangle \lesssim 30^{\circ}$

What we know about the sources of UHECRs

Spectrum & Composition

Auger Coll. 2022, JCAP

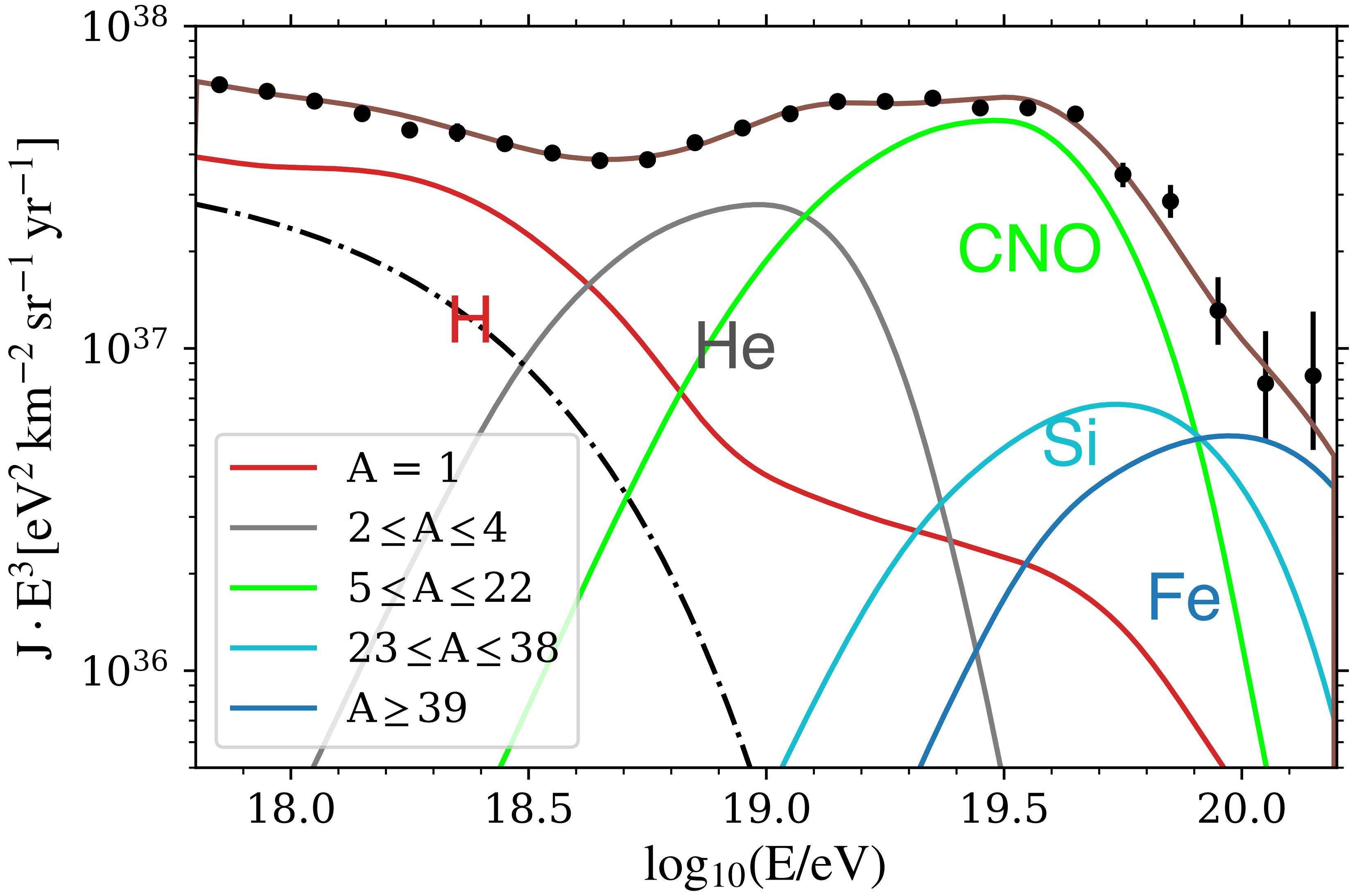

Muzio et al 2021

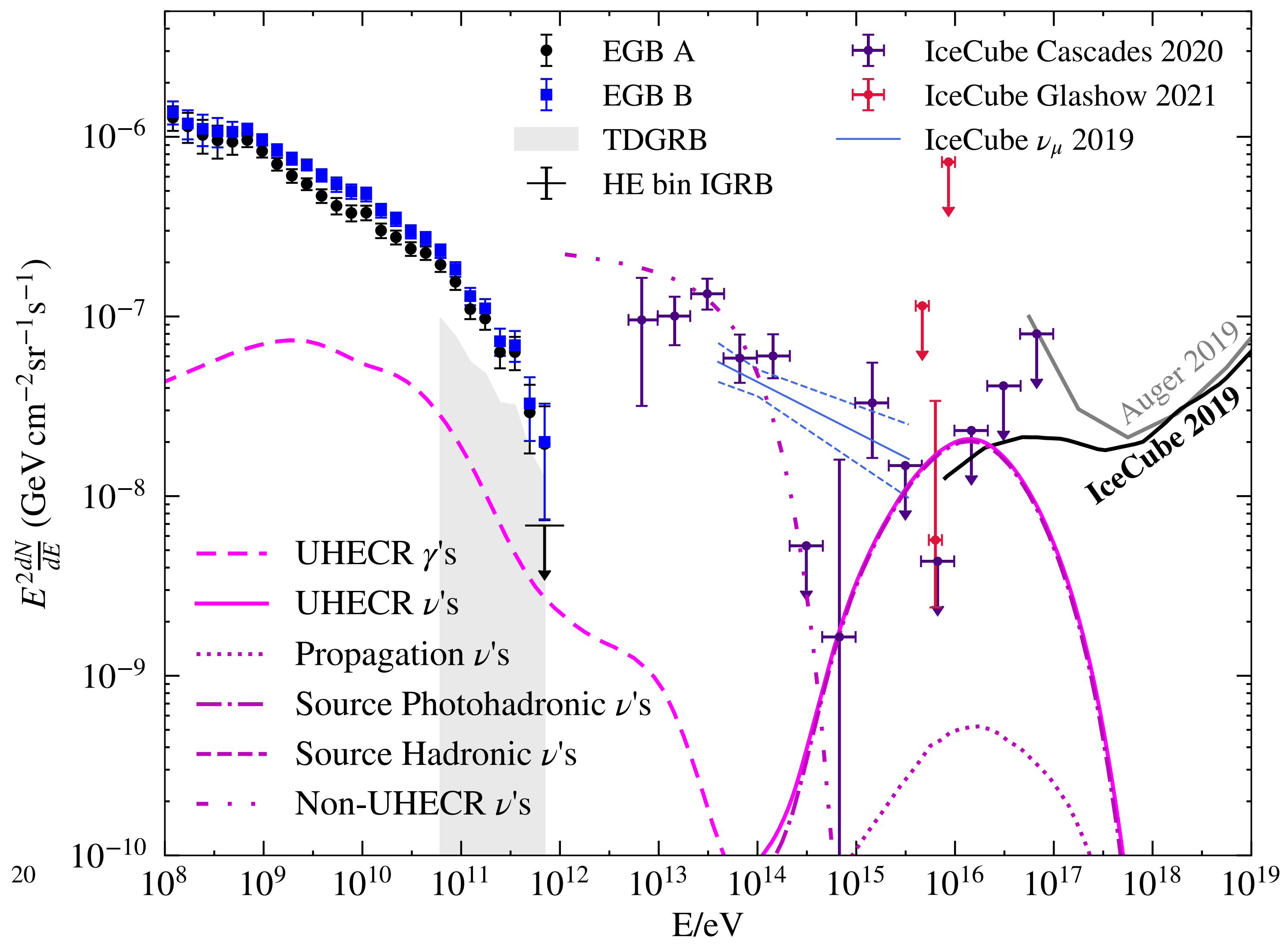

Composition: Increasingly heavy with increasing energy, consistent with "Peters Cycle"

Sources: Joint origin with PeV neutrinos possible

Possible second "light" population
(*Muzio et al 2021, Das et al 2021, Auger Coll 2022, Ehlert et al 2023*)

Searching for the sources of UHECRs

Auger Coll. 2022, JCAP

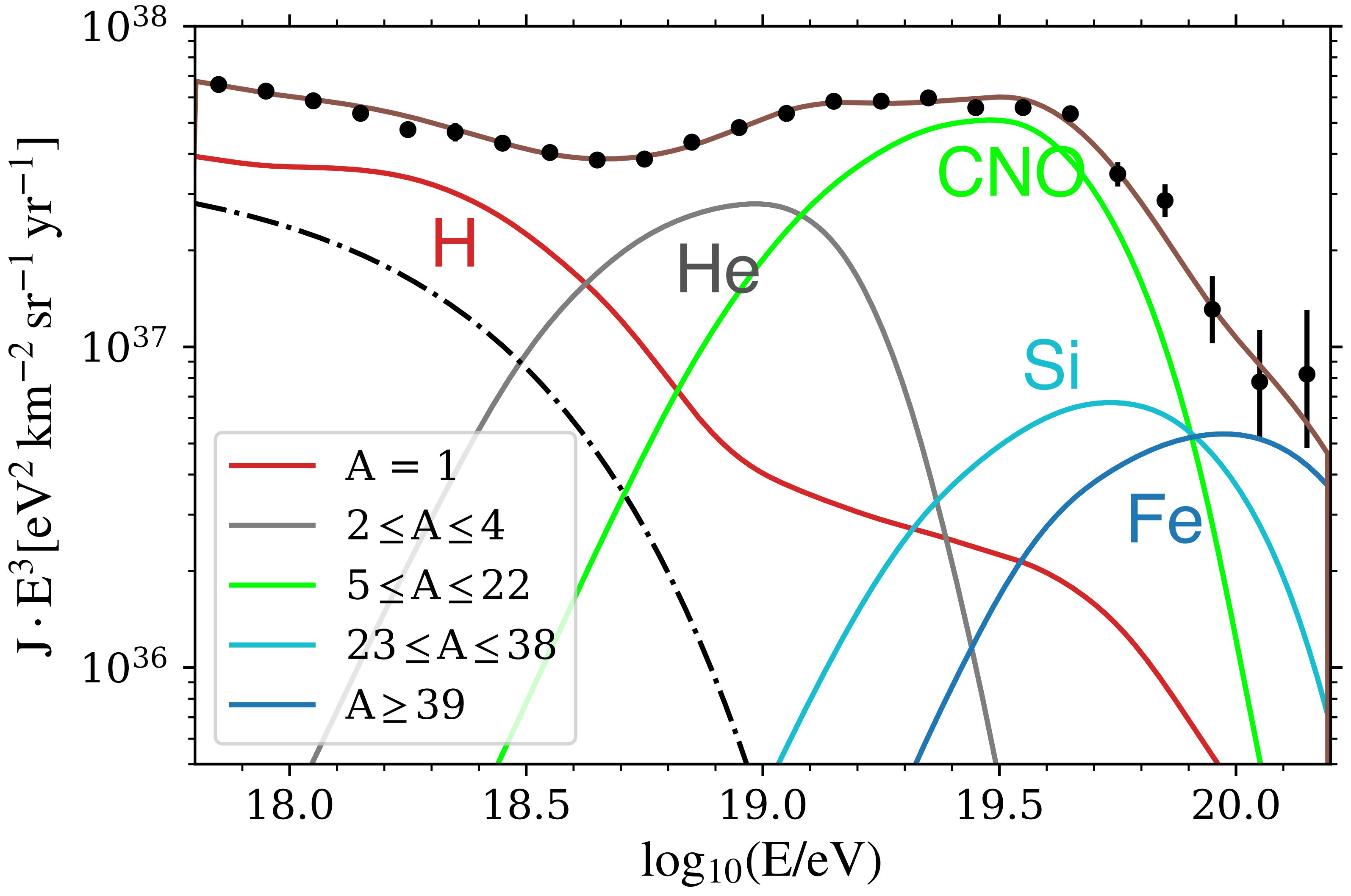

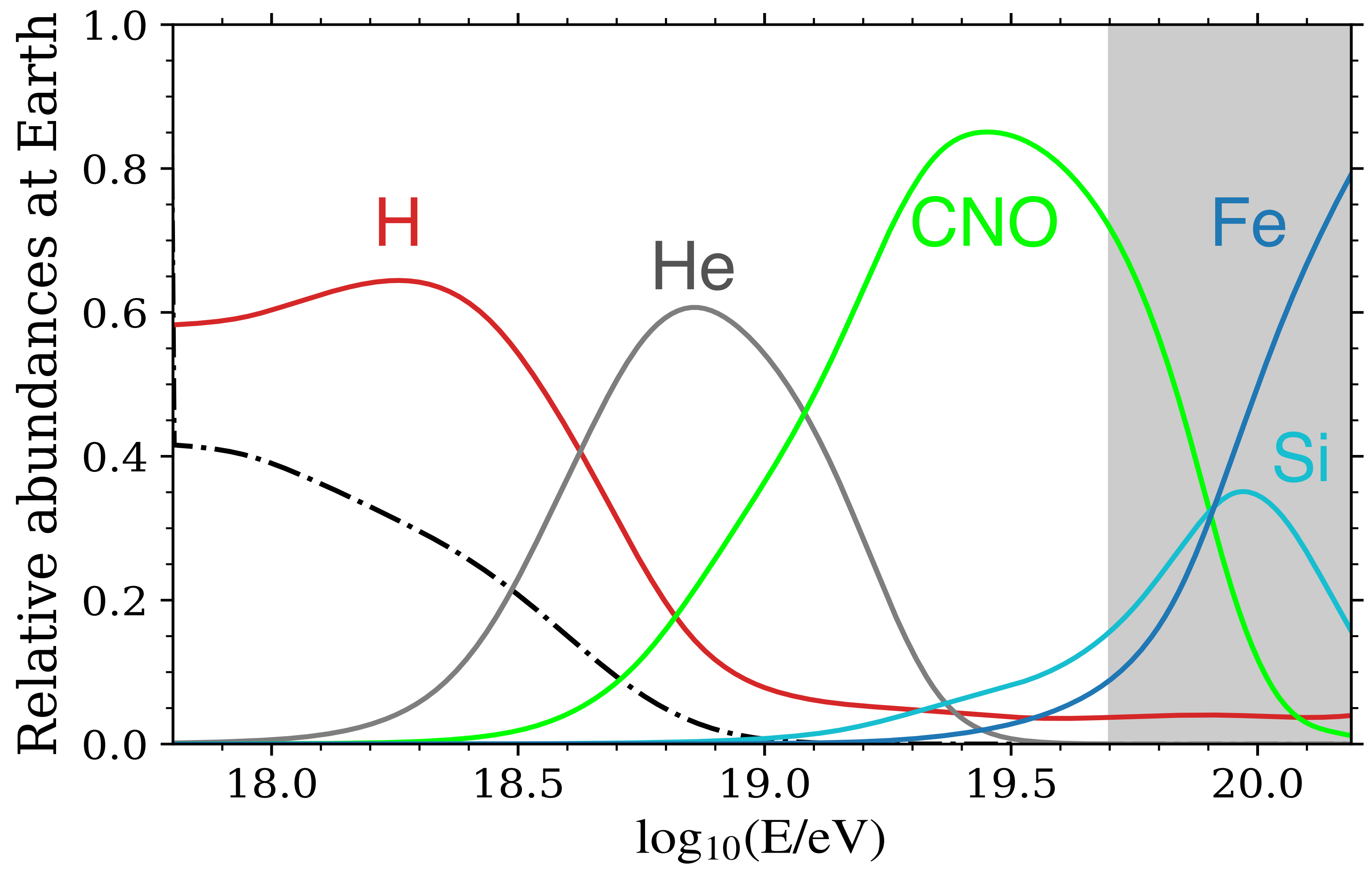

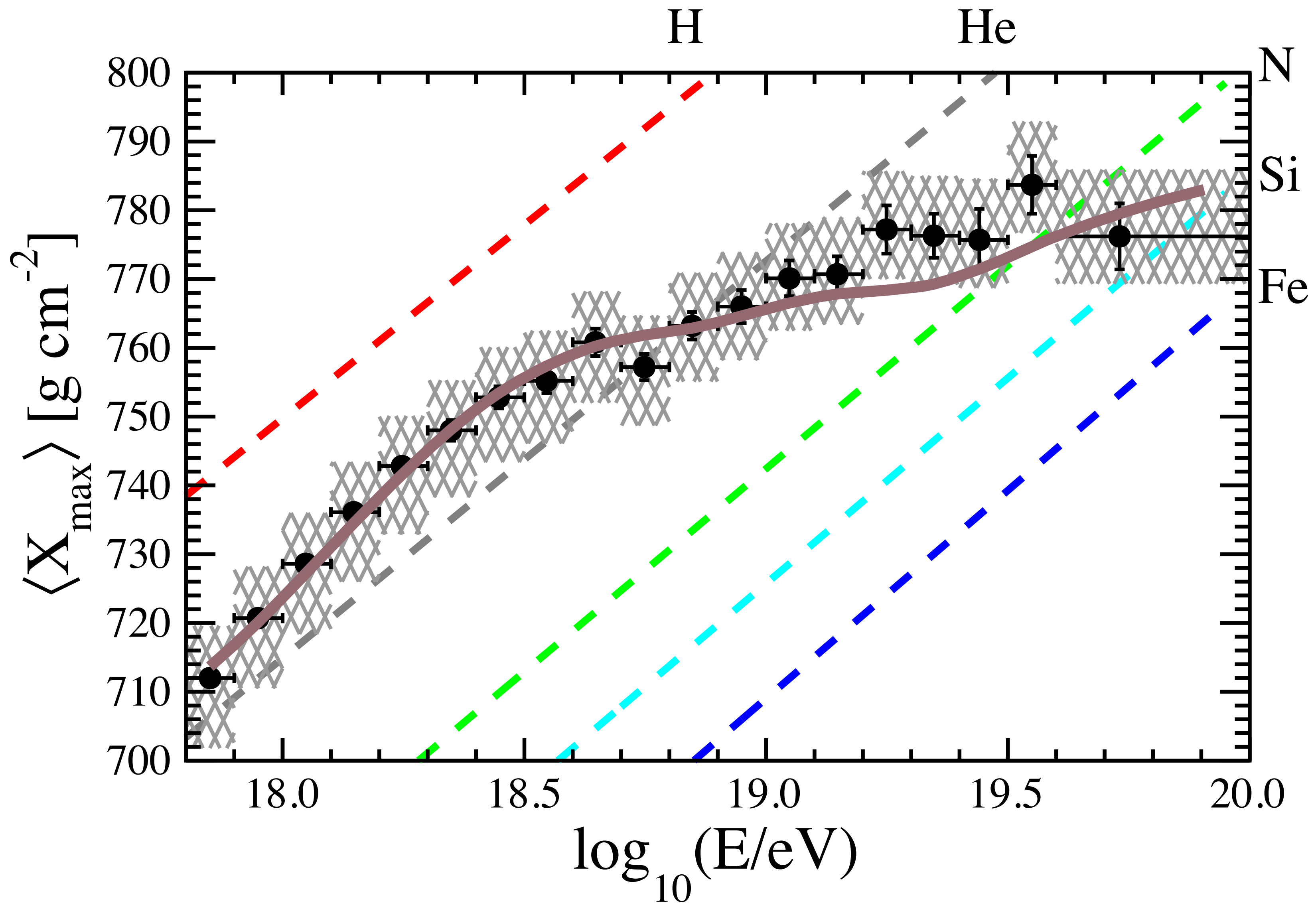

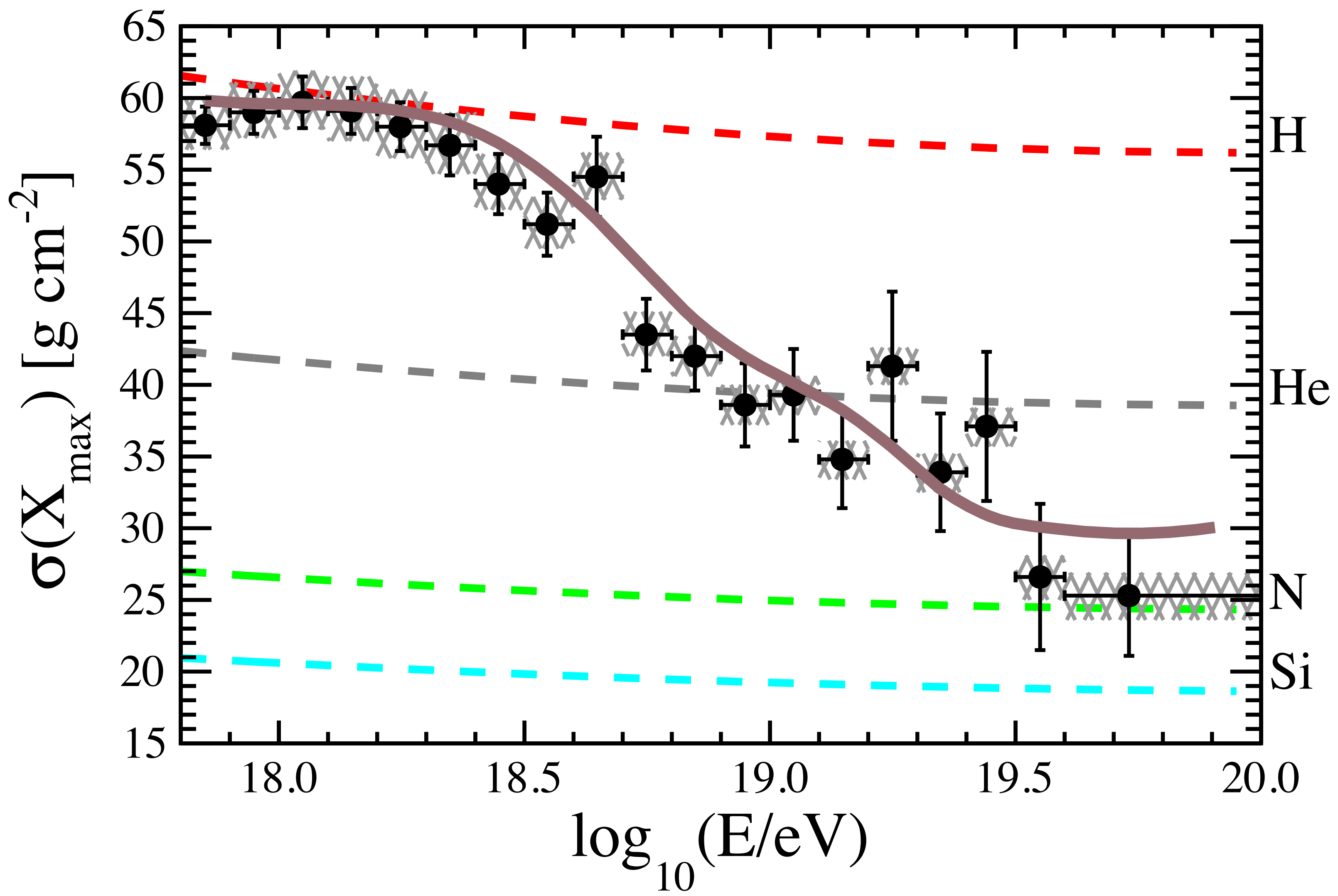

Generic Source Properties:
Allard et al 2007, 8, Hooper et al 2007, Unger et al 2015, Auger Coll 2016, Kachelriess et al 2017, Muzio et al 2019, 2022, Mollerach et al 2020, Das et al 2021.

Specific source classes:
Jetted AGN - *Eichmann et al 2017, 2022, Fang et al 2018, Kimura et al 2018, Rodrigues et al 2021*
GRBs - *Globus et al 2015, Biehl et al 2017, Zhang et al 2018, Boncioli et al 2018, 2019, Rudolf 2019,2022, Heinze et al 2020,*
TDEs - *Biehl et al 2017, Guepin et al 2017, Zhang et al 2019*
Transrelativistic Supernovae - *Zhang & Murase 2019*
Starburst galaxies - *Condorelli et al 2022*

Sources generally assumed to be intrinsically identical

Distribution of maximum energies:
UHECR protons: *Kachelriess & Semikoz 2007*
Galactic sources: *Shibata et al 2010*
Discrete AGN: *Eichmann, Kachelriess, FO 2022*

Maximum UHECR energy

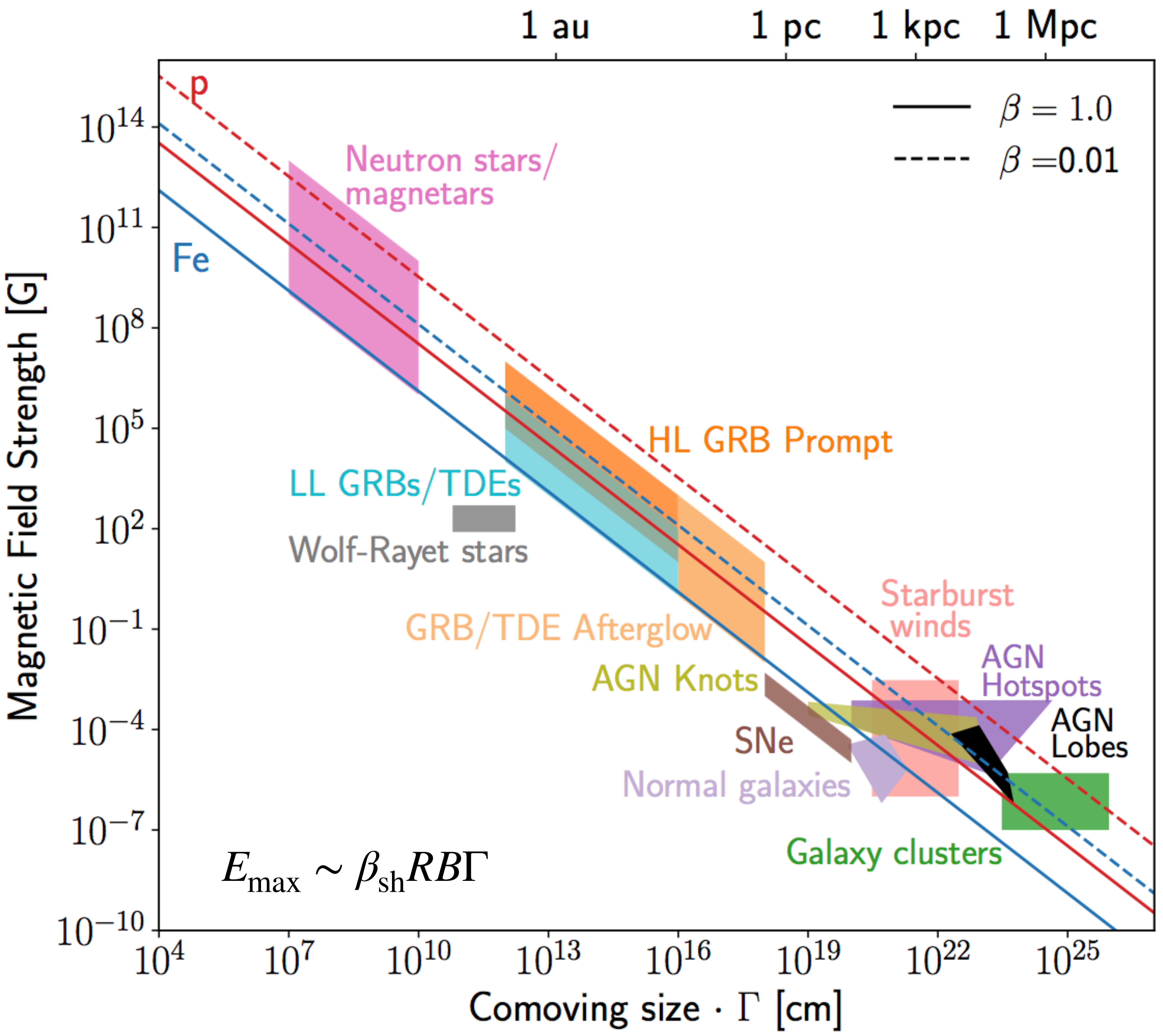

Alves Batista et al 2019, FrASS, 6, 23

Maximum UHECR energy

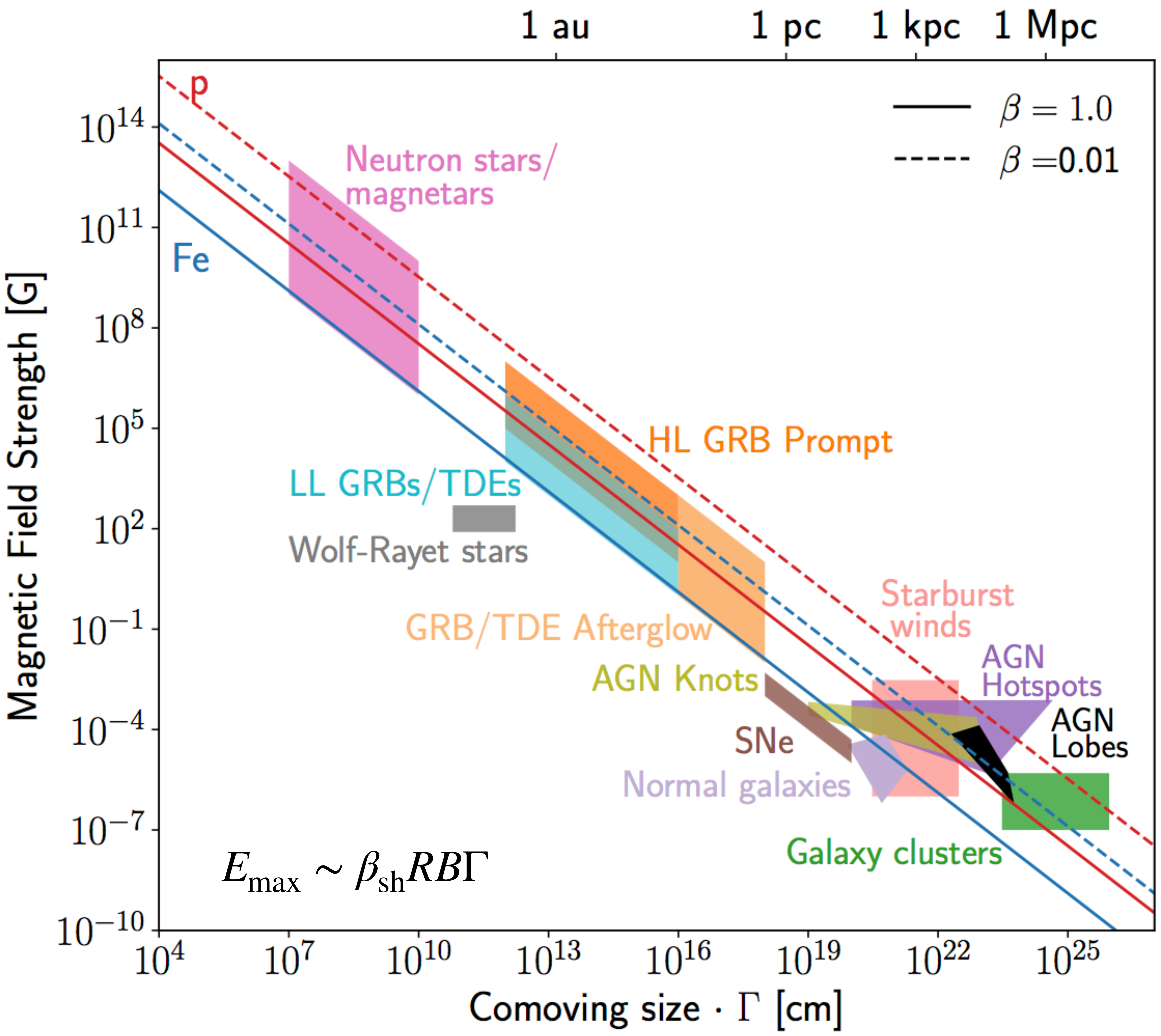

Alves Batista et al 2019, FrASS, 6, 23

$E_{max} \sim \beta_{sh} R B \Gamma$

e.g. 43 TeV emitting blazars in minimal SSC model

$B \sim 10^{-4}$ - 10 G

$R \sim 10^{15}$ - 10^{17} cm

$\Gamma \sim$ 10-50

$E_{max} \sim 10^{17}$ - 10^{20} eV

Tavecchio, FO, Righi 2019

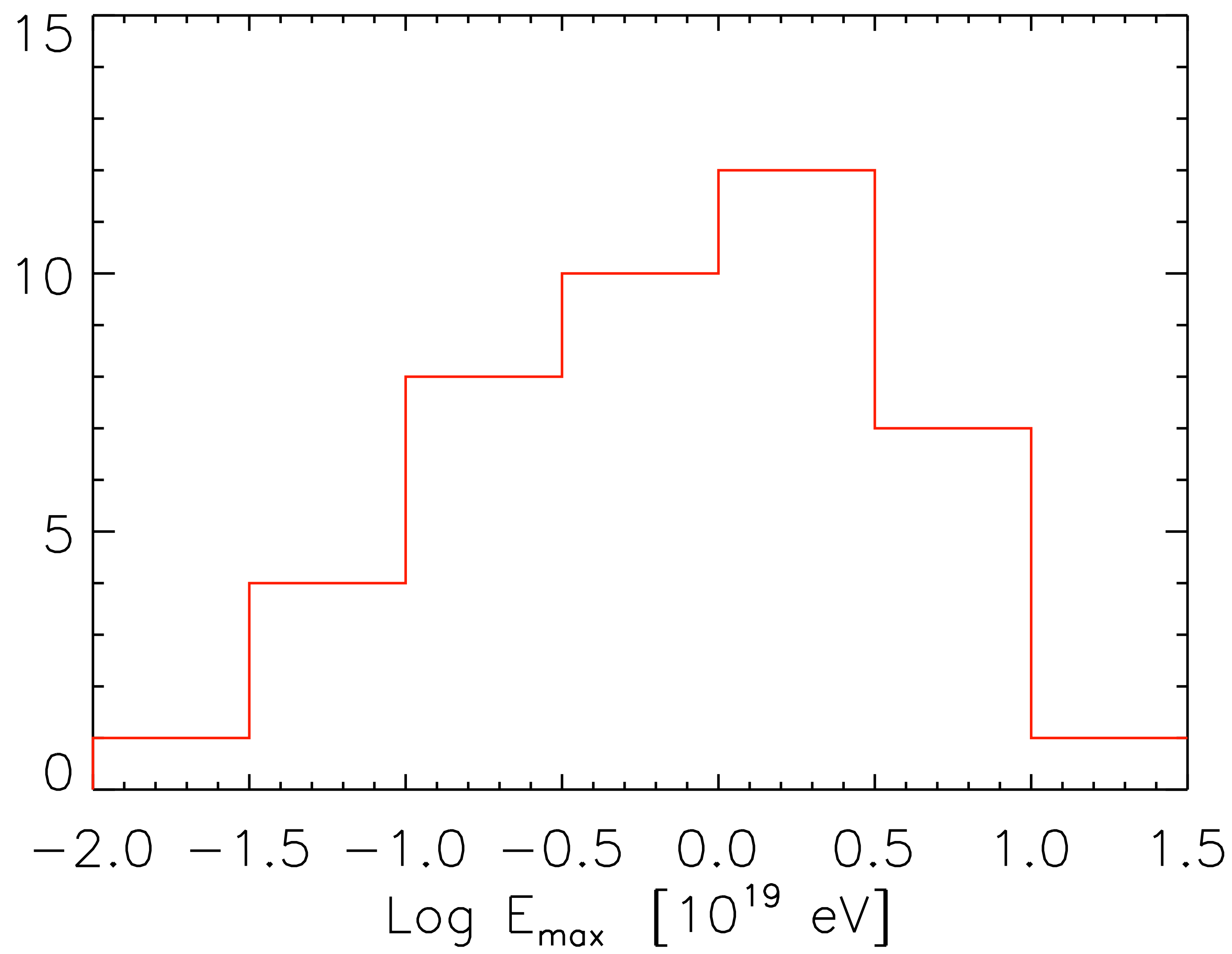

Maximum UHECR energy

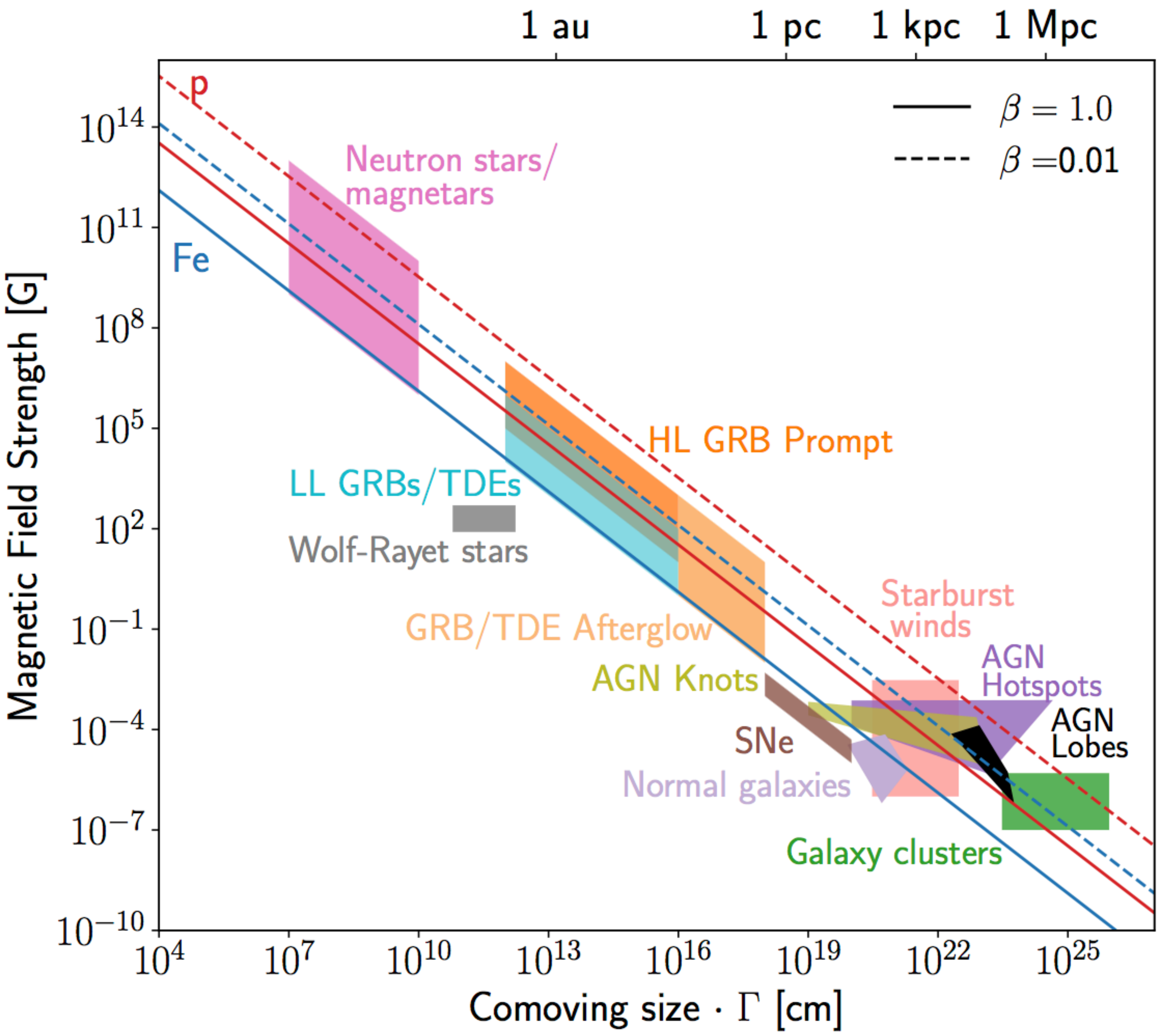

Alves Batista et al 2019, FrASS, 6, 23

Hillas energy *(Hillas 1984):*

$$E_{\max} \sim \beta_{\rm sh} R B \Gamma Z e$$

Espresso acceleration *(Caprioli 2015)*:

$$\langle E_{\max} \rangle \sim \Gamma^2 E_{\max,\rm Galactic}$$

In general $E_{\max} \propto \Gamma^{\alpha}$

In the blazar population

(Lister et al 2019, MOJAVE program, ~200 blazars tracked over 5 years)

$$dN(\Gamma)/d\Gamma = \Gamma^{-\eta}, 1.25 < \Gamma < 50, \ \eta \approx 1.4$$

Therefore

$$\frac{dN}{dE_{\max}} = \frac{dN}{d\Gamma}\left|\frac{d\Gamma}{dE_{\max}}\right| \propto E_{\max}^{\frac{1-\eta}{\alpha}-1} \begin{cases} E_{\max}^{-1.4} & \text{Hillas} \\ E_{\max}^{-1.2} & \text{Espresso} \end{cases}$$

Maximum UHECR energy

Marcotulli et al 2022, Swift BAT Blazar Luminosity Function

$$L \gtrsim L_B \sim \frac{U_{\rm mag} R^3}{t} \sim B^2 R^2 \beta$$

$$L_{\rm min} \sim \frac{10^{45.5}\ {\rm erg/s}}{\beta} \left(\frac{E}{100\ {\rm EeV}}\right)^2$$

$$E_{\rm max} \sim 100\ {\rm EeV}\ \beta^{1/2} \left(\frac{L}{10^{45.5}\ {\rm erg/s}}\right)^{1/2}$$

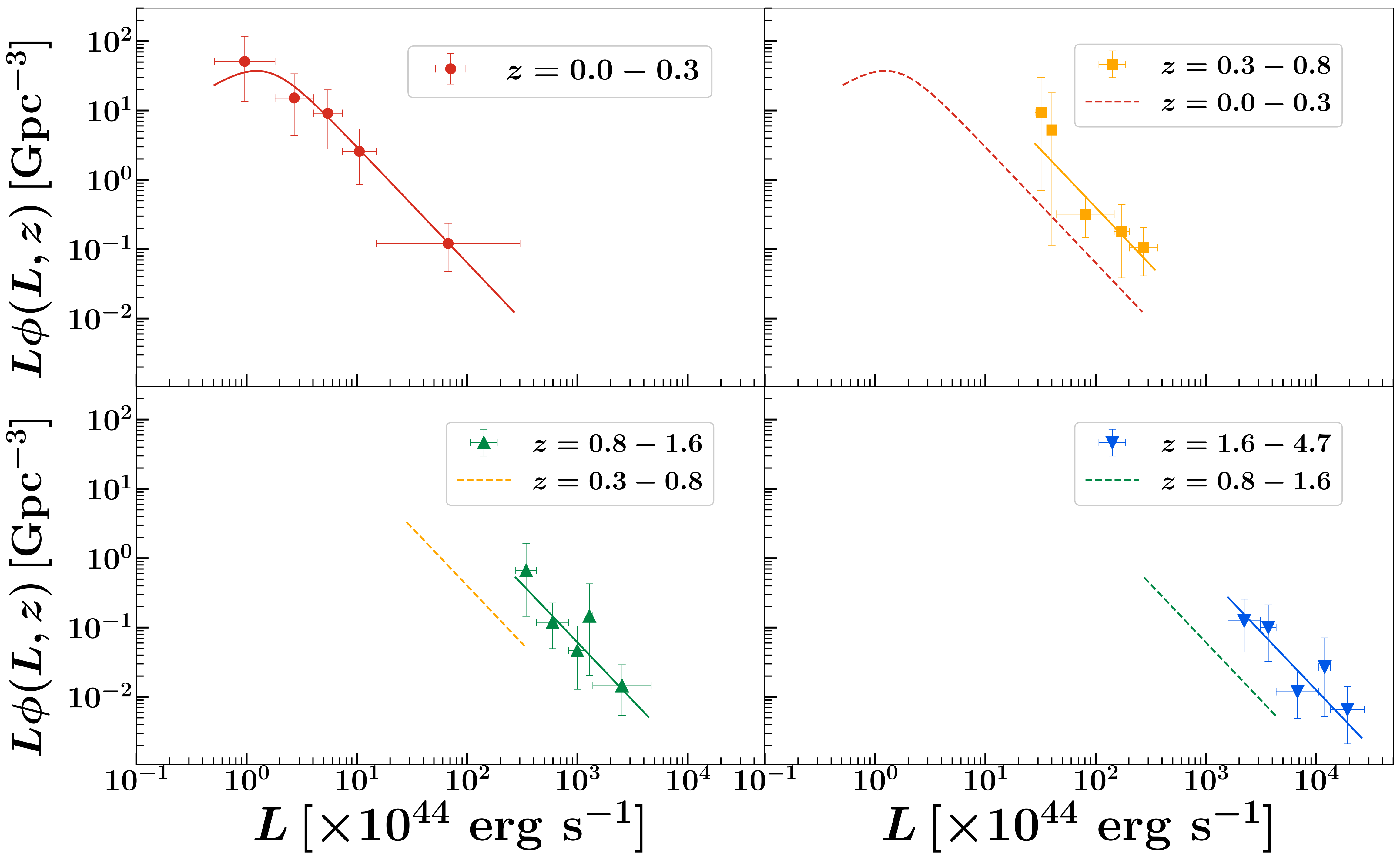

Lovelace 1976, Waxman 1995, 2001, Blandford 2000, Lemoine & Waxman 2009

UHECRs from a population with a range of maximum energies

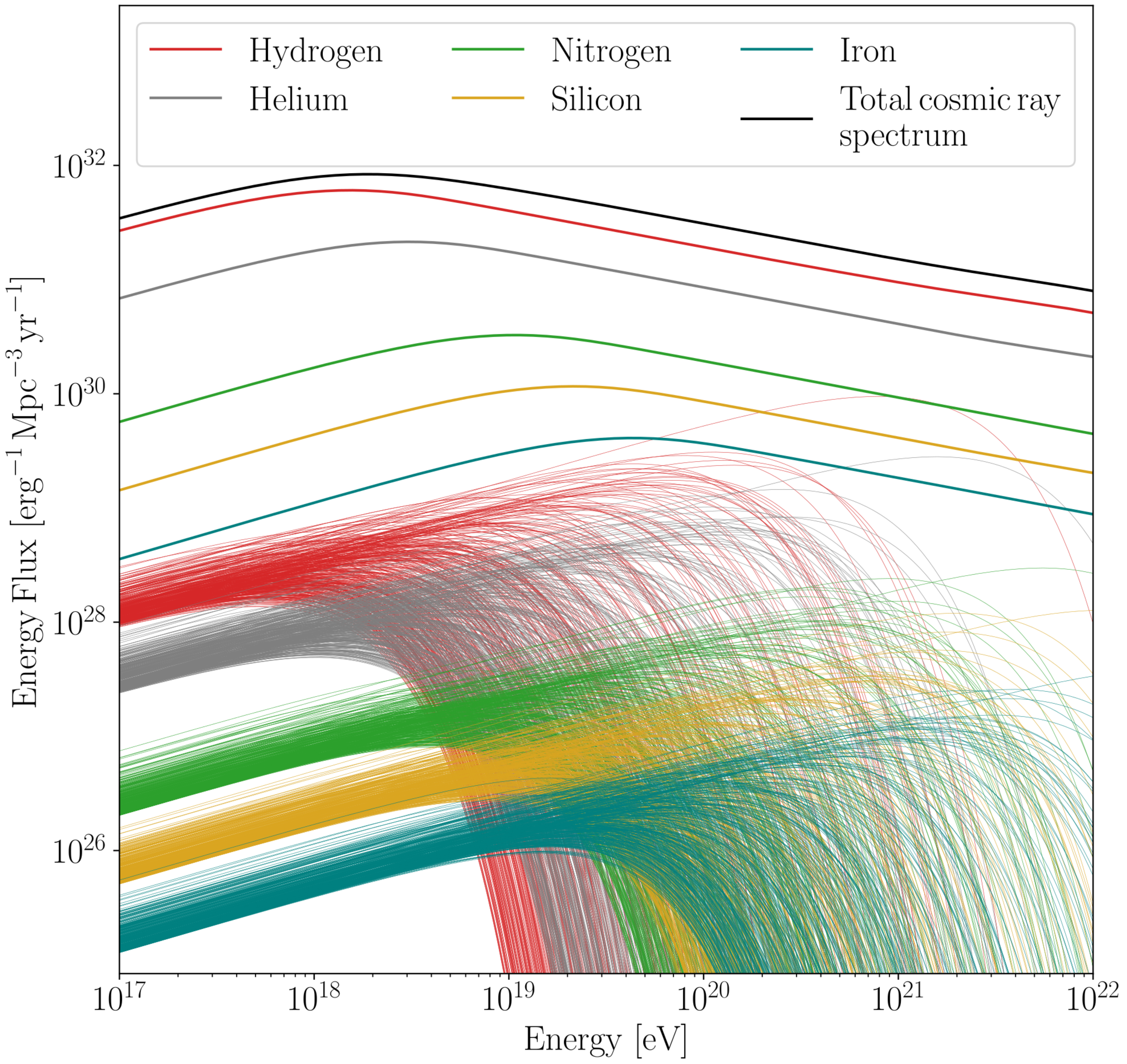

- Fit UHECR spectrum and composition observables
- Assume a Peters Cycle
- Large number of sources
- Above-ankle fit (no source interactions or second source population)
- Quantify the allowed "diversity" in maximum rigidity in the UHECR source population

From identical sources to a rigidity distribution

Rigidity, $R = \frac{\text{Energy}}{Z}$

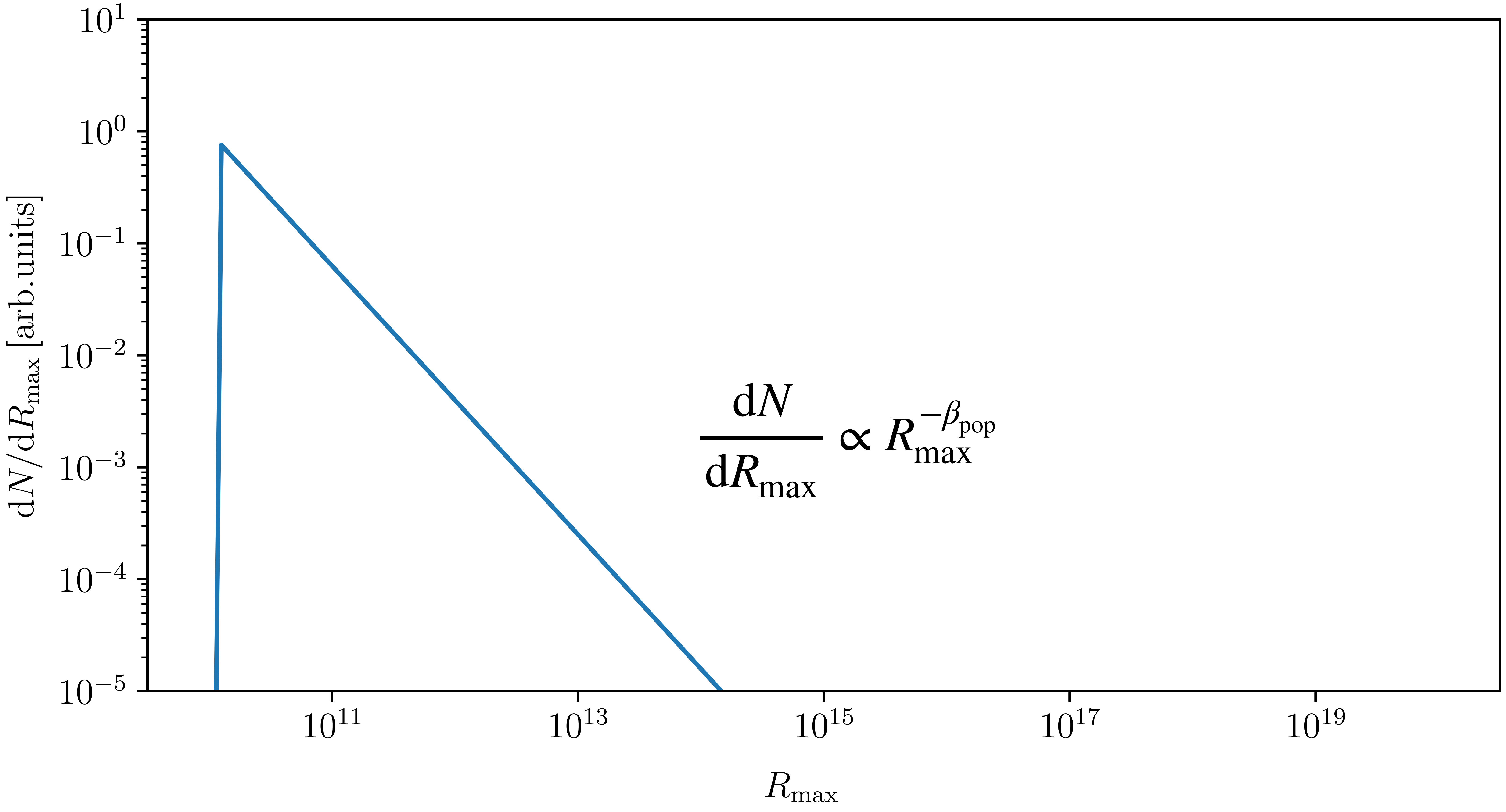

From single source to population spectrum

Single Source UHECR Spectrum

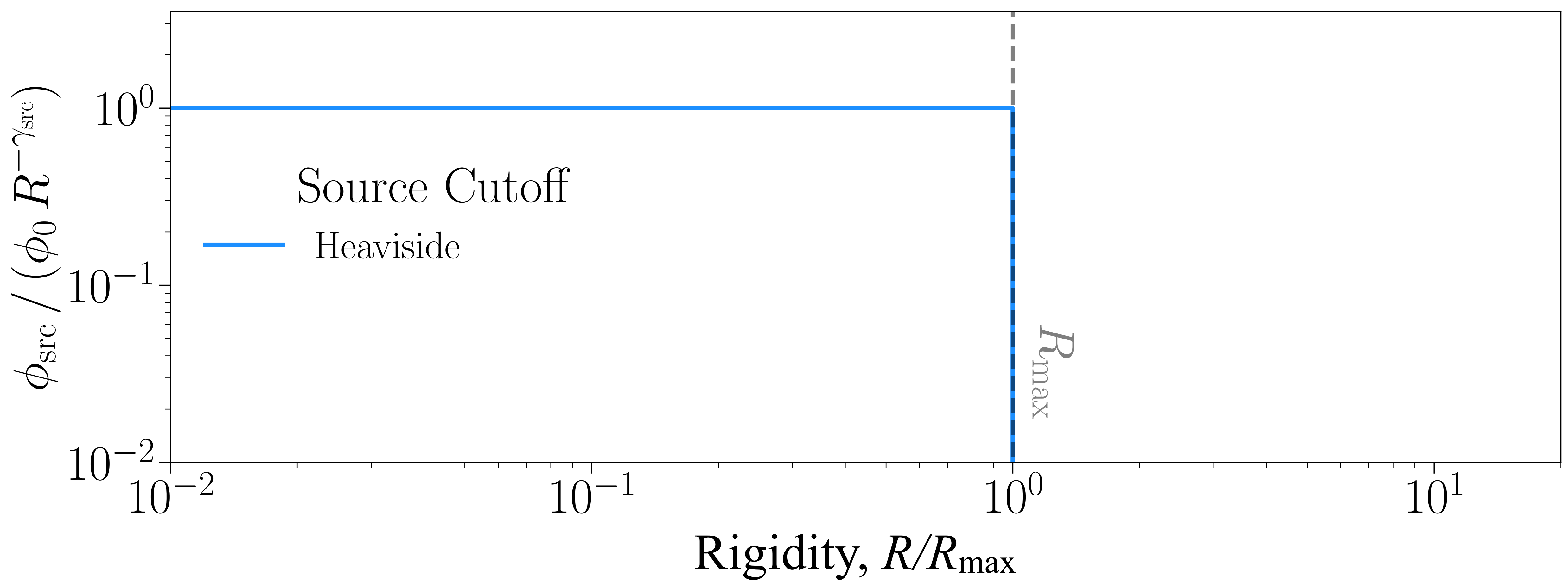

From single source to population spectrum

Single Source UHECR Spectrum

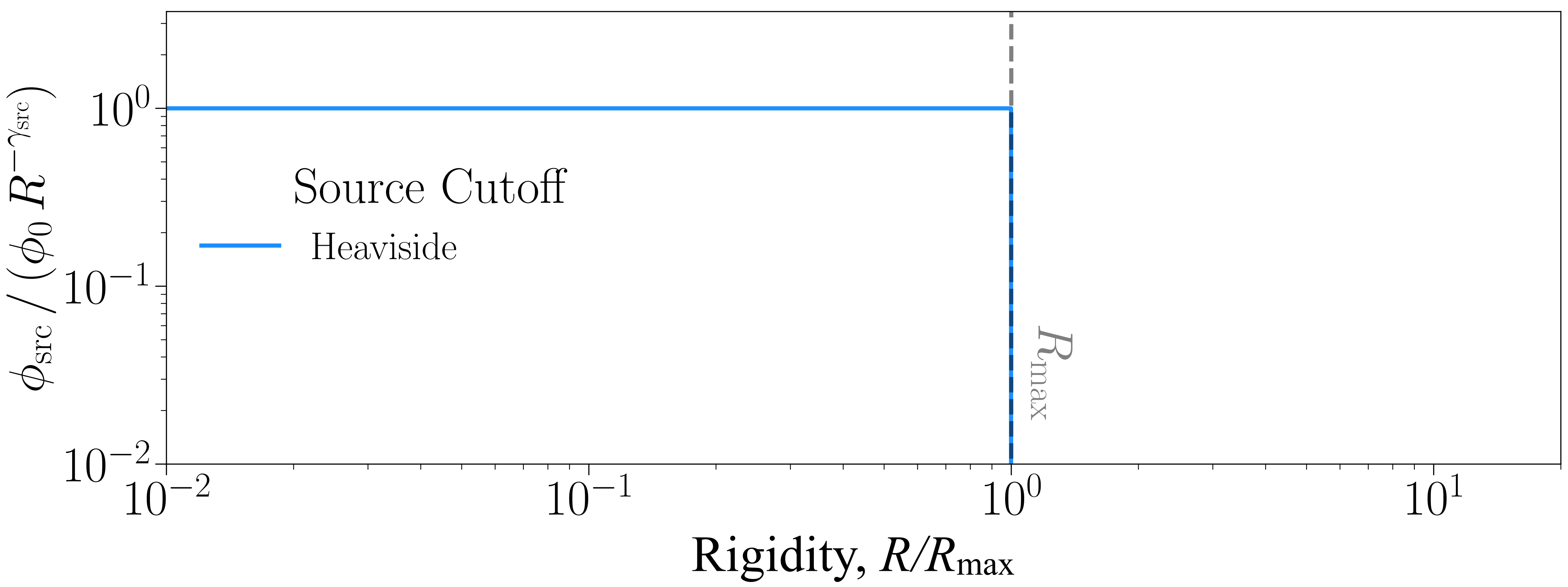

Population Spectrum

Power-law distributed maximum rigidity

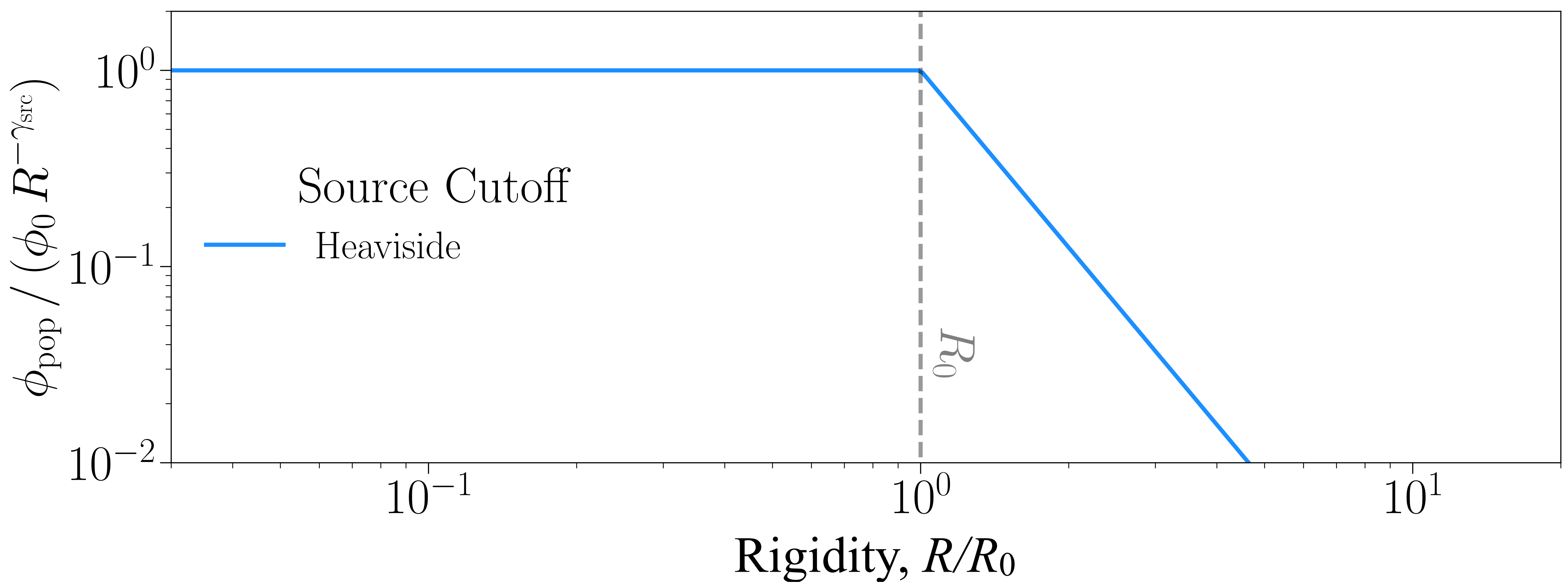

From single source to population spectrum

Single Source UHECR Spectrum

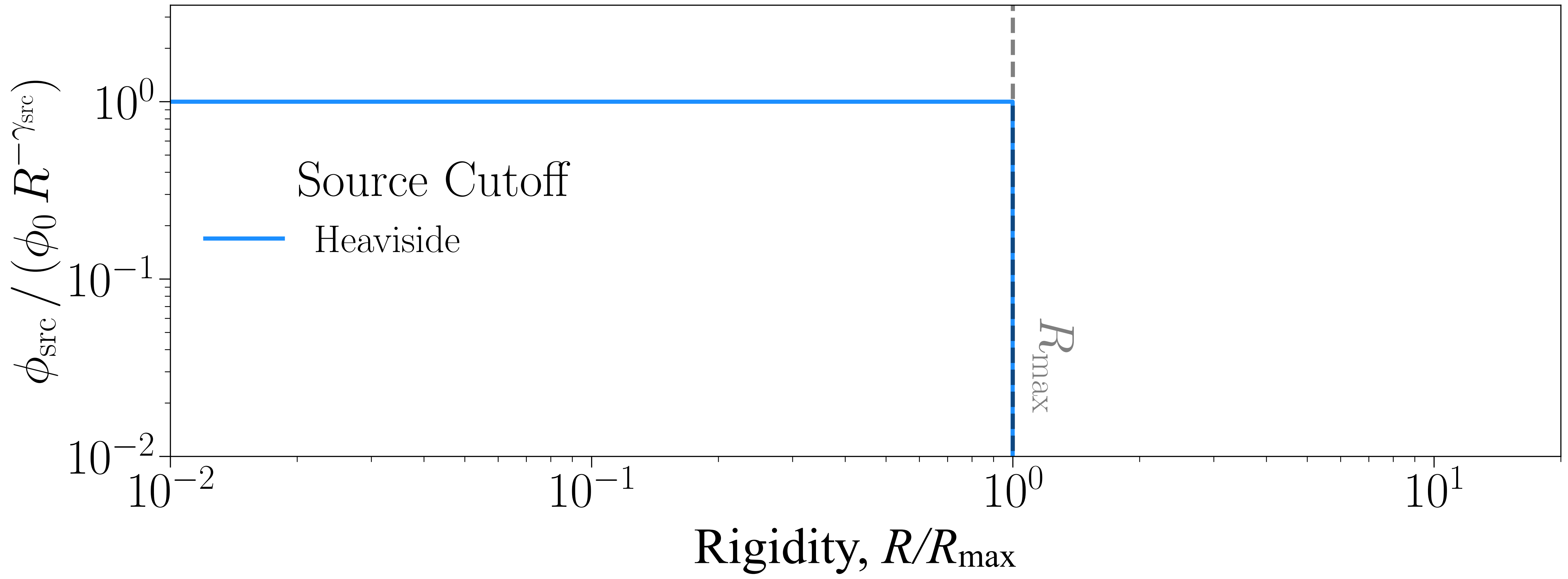

$$\frac{\mathrm{d}N}{\mathrm{d}R} \propto R^{-\gamma_{\mathrm{src}}}$$

$$\frac{\mathrm{d}N}{\mathrm{d}R_{\max}} \propto R_{\max}^{-\beta_{\mathrm{pop}}}$$

Population Spectrum

Power-law distributed maximum rigidity

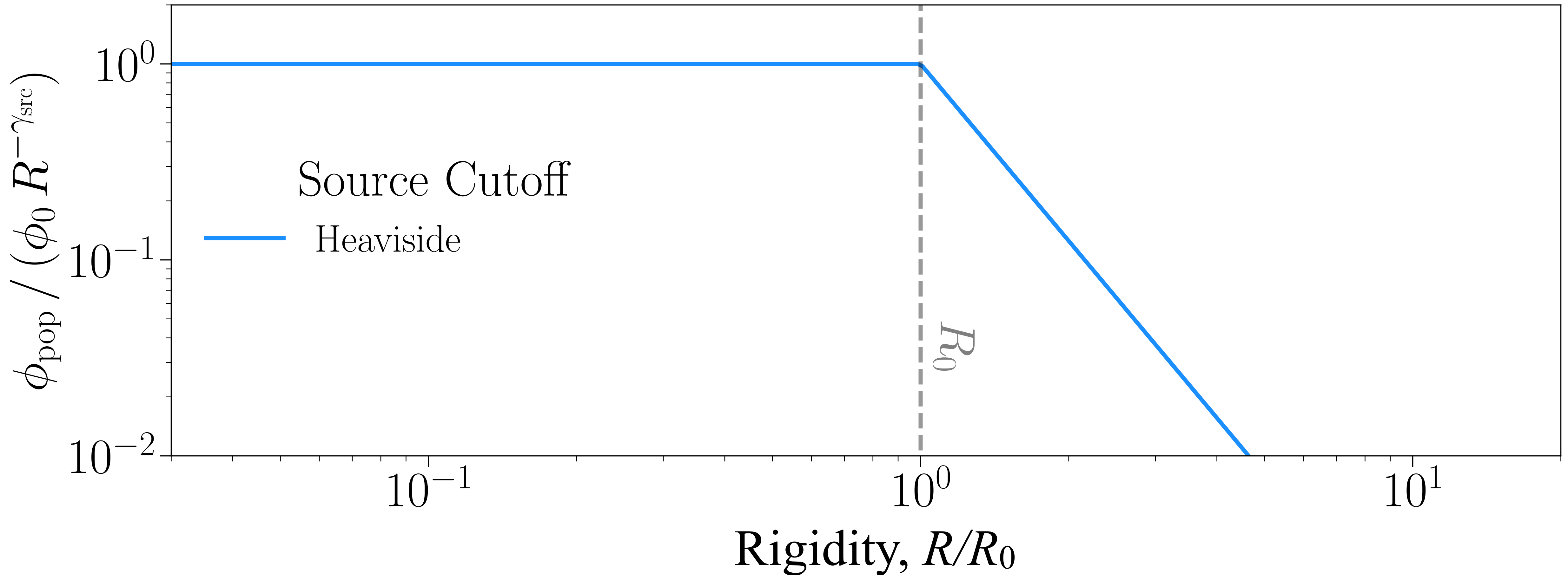

$$\phi_{\mathrm{pop}} \propto \begin{cases} R^{-\gamma_{\mathrm{src}}} & R \ll R_0 \\ R^{-\gamma_{\mathrm{src}}-\beta_{\mathrm{pop}}+1} & R \gg R_0 \end{cases}$$

From single source to population spectrum

Single Source UHECR Spectrum

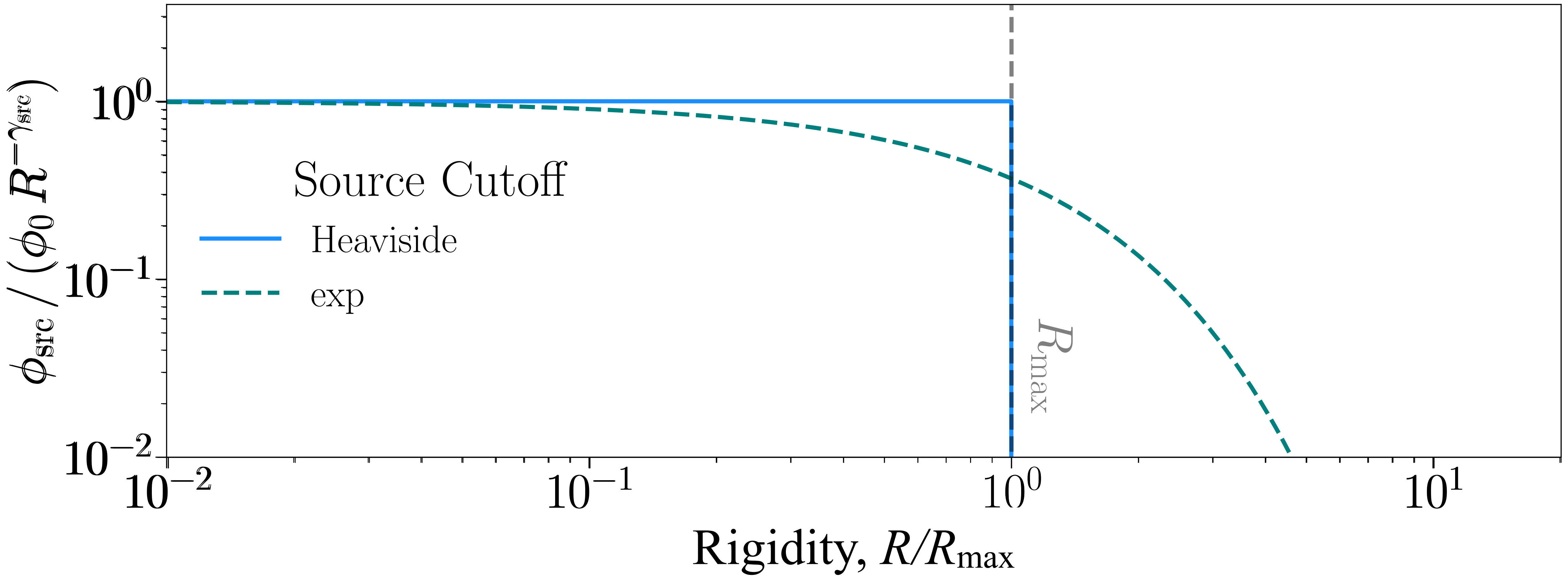

$$\frac{\mathrm{d}N}{\mathrm{d}R} \propto R^{-\gamma_{\rm src}}$$

$$\frac{\mathrm{d}N}{\mathrm{d}R_{\max}} \propto R_{\max}^{-\beta_{\rm pop}}$$

Population Spectrum

Power-law distributed maximum rigidity

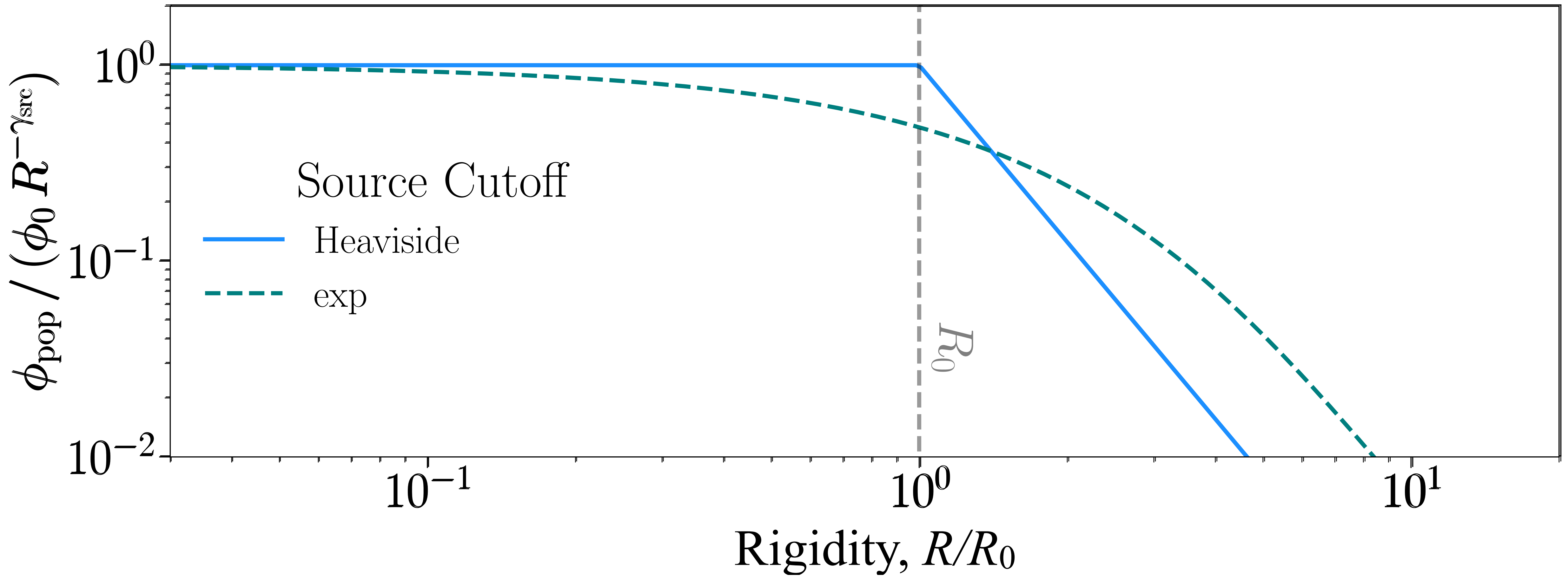

$$\phi_{\rm pop} \propto \begin{cases} R^{-\gamma_{\rm src}} & R \ll R_0 \\ R^{-\gamma_{\rm src}-\beta_{\rm pop}+1} & R \gg R_0 \end{cases}$$

From single source to population spectrum

Single Source UHECR Spectrum

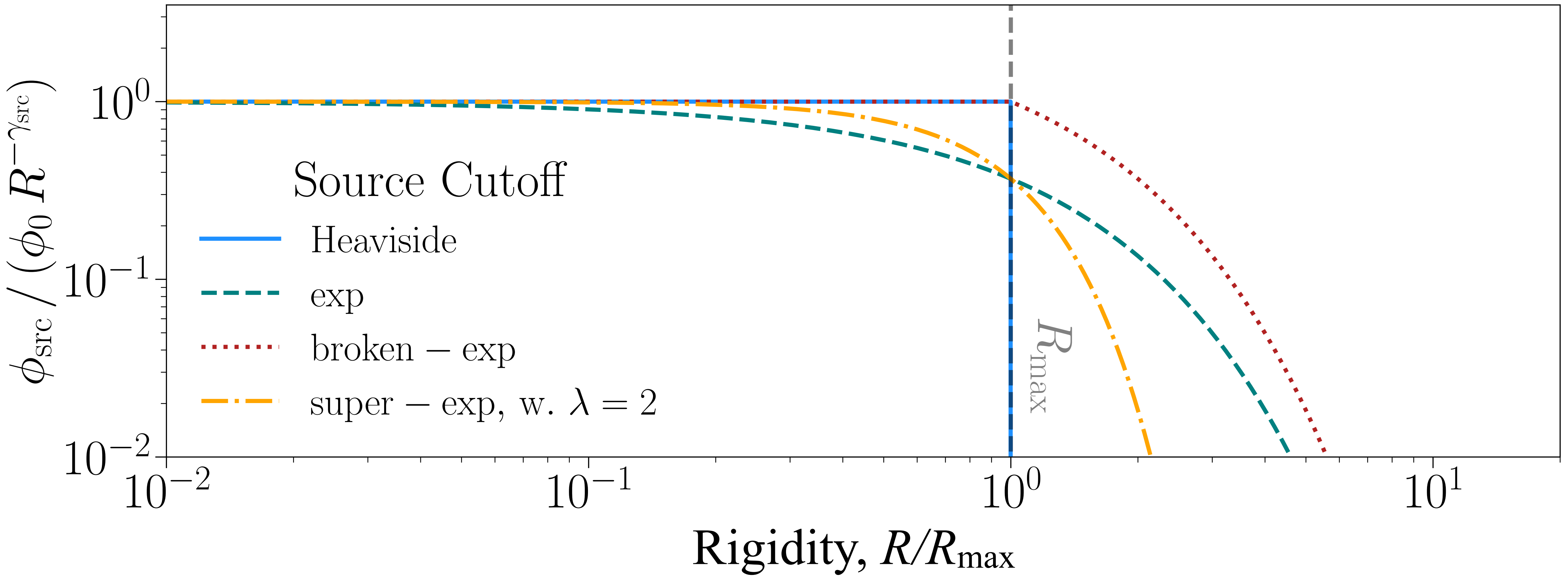

$$\frac{dN}{dR} \propto R^{-\gamma_{src}}$$

Population Spectrum

Power-law distributed maximum rigidity

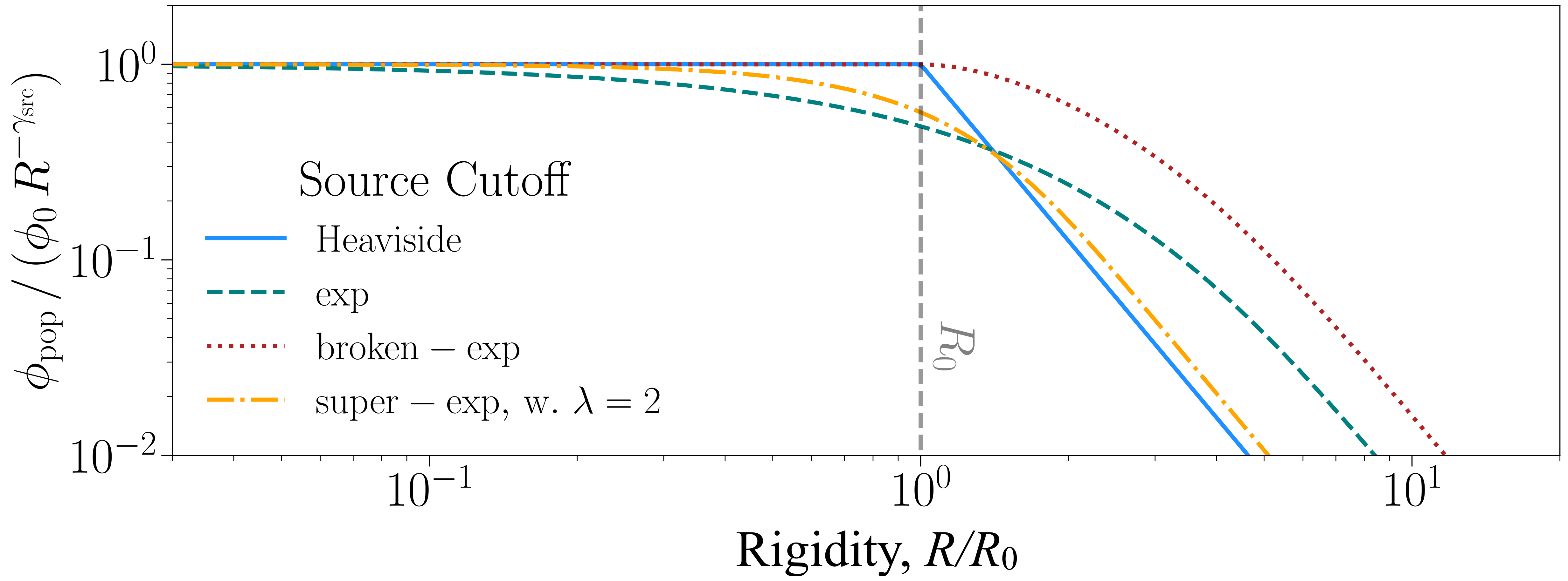

$$\frac{dN}{dR_{max}} \propto R_{max}^{-\beta_{pop}}$$

$$\phi_{pop} \propto \begin{cases} R^{-\gamma_{src}} & R \ll R_0 \\ R^{-\gamma_{src}-\beta_{pop}+1} & R \gg R_0 \end{cases}$$

Broken exponential, e.g. Auger Combined Fit (Aab et al 2017)

Super exponential in case of DSA with synchrotron losses with $dN/dR \propto \exp - R^{\lambda}, \lambda = 2$ *e.g. Zirakasvili & Aharonian 2007*

Single-power-law distributed maximum rigidity

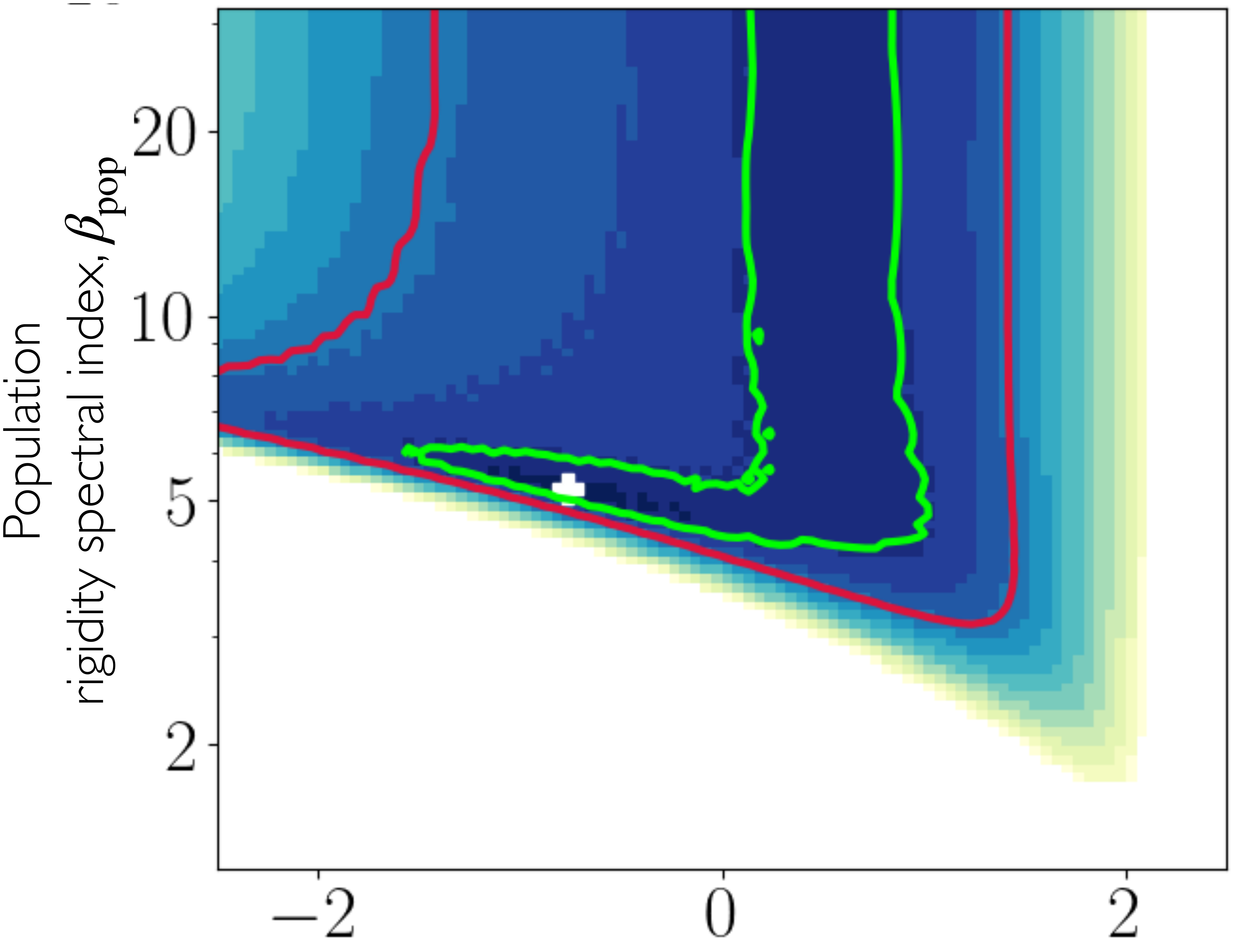

Inverted Spectra

Individual energy spectral index, $\gamma_{\rm src}$

Shock Acceleration

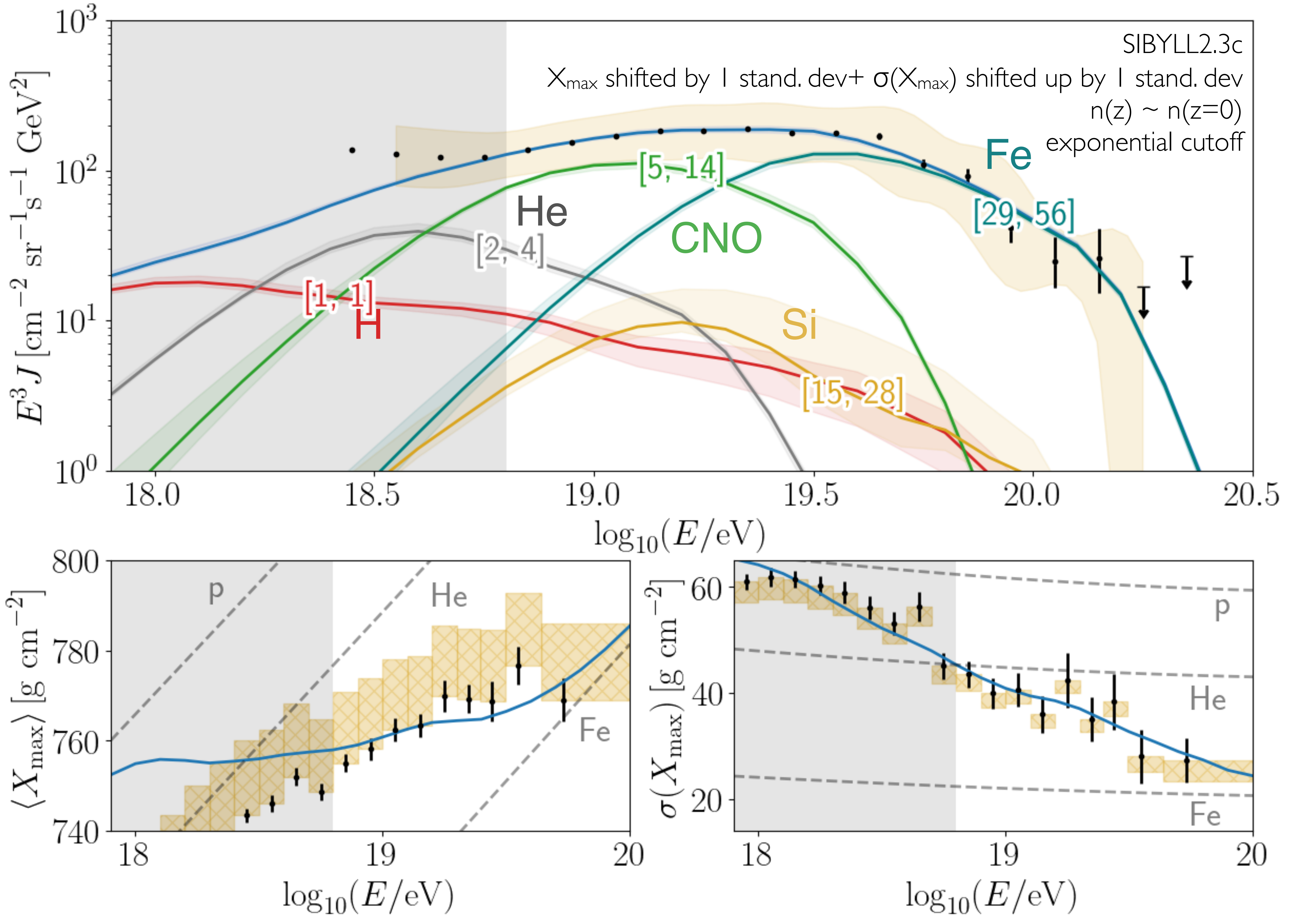

$$\frac{\mathrm{d}N}{\mathrm{d}R} \propto R^{-\gamma_{\rm src}} \qquad \frac{\mathrm{d}N}{\mathrm{d}R_{\rm max}} \propto R_{\rm max}^{-\beta_{\rm pop}} \qquad \phi_{\rm pop} \propto \begin{cases} R^{-\gamma_{\rm src}} & R \ll R_0 \\ R^{-\gamma_{\rm src}-\beta_{\rm pop}+1} & R \gg R_0 \end{cases}$$

Single-power-law distributed maximum rigidity

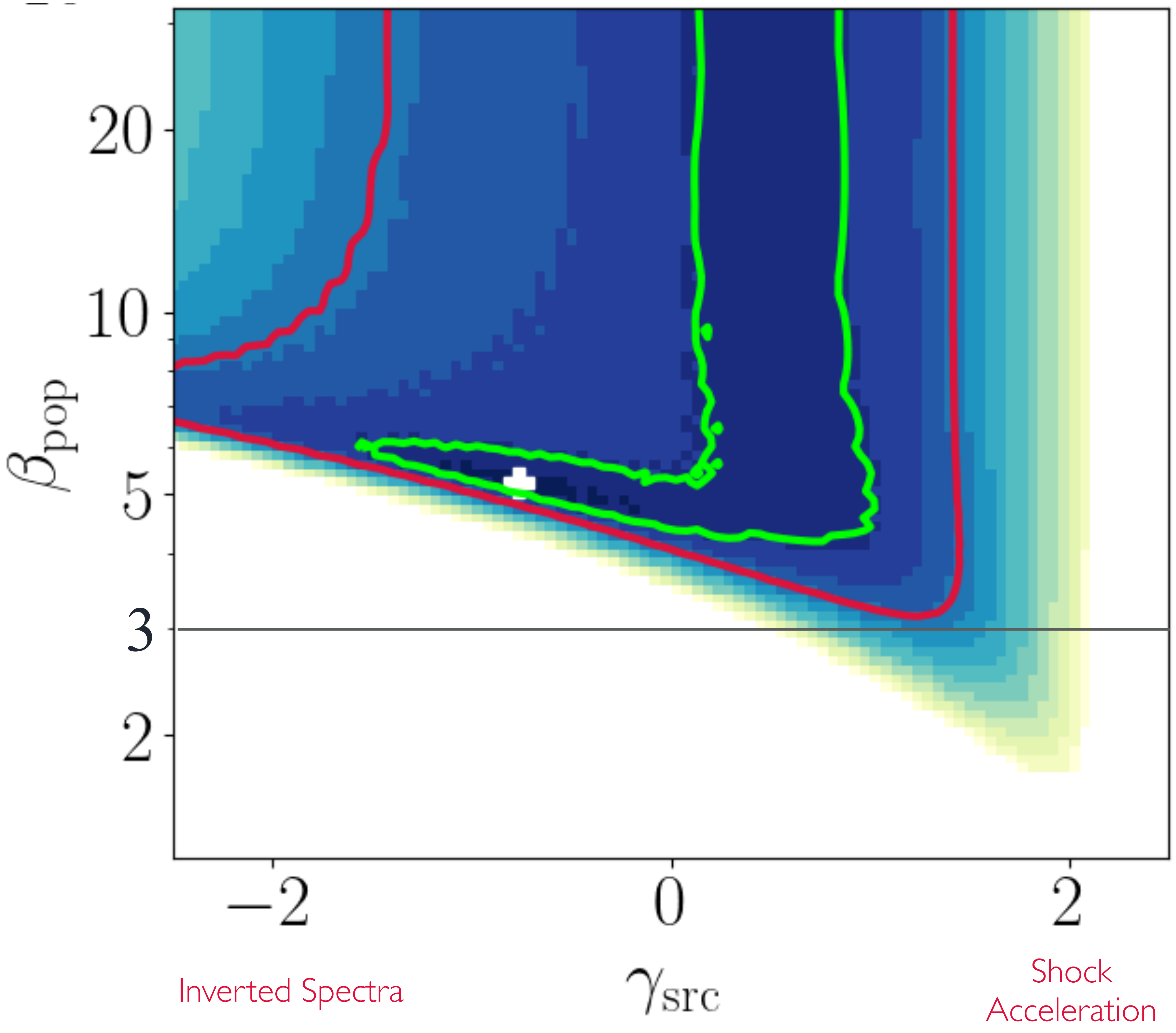

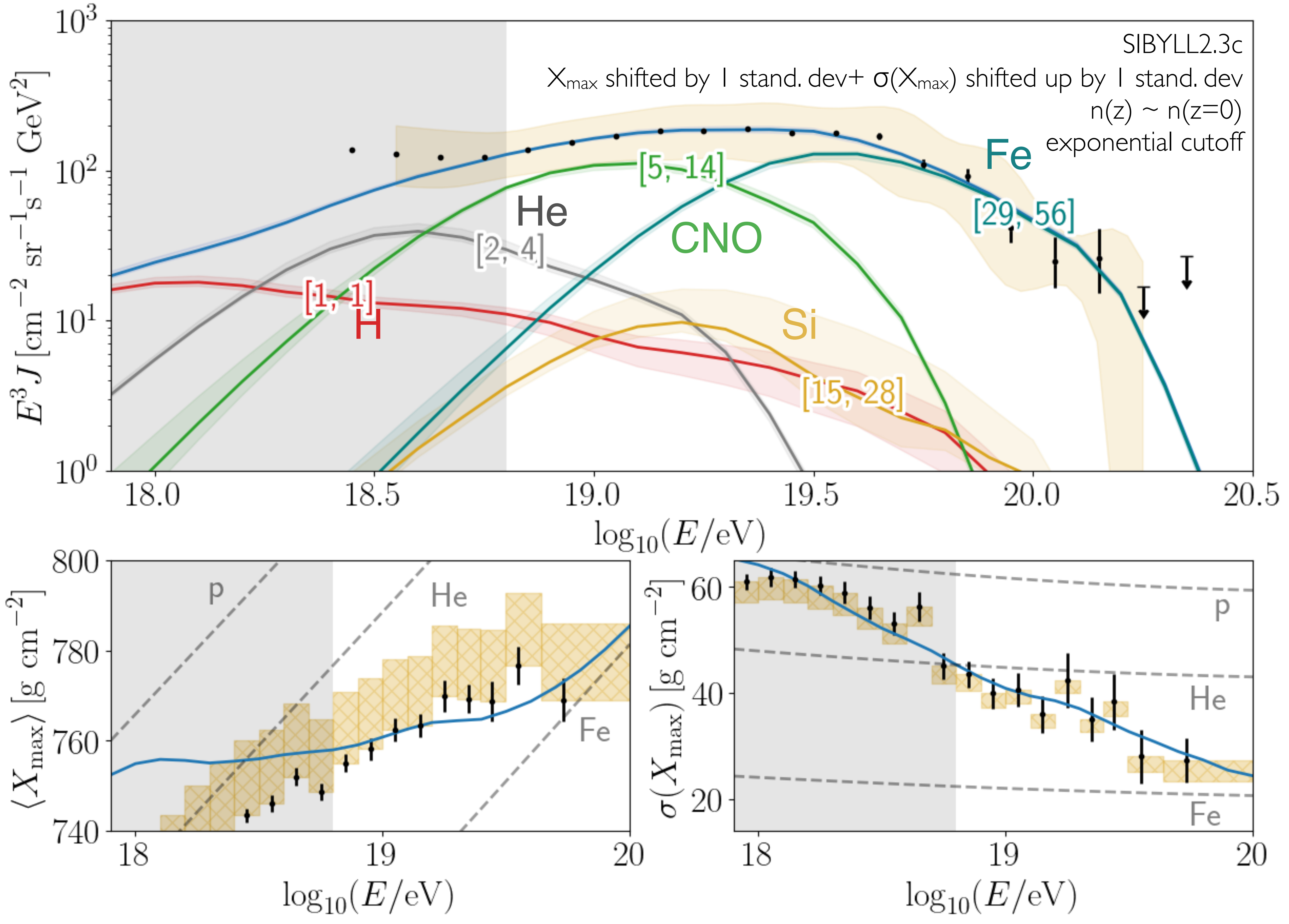

$$\frac{\mathrm{d}N}{\mathrm{d}R} \propto R^{-\gamma_{src}} \qquad \frac{\mathrm{d}N}{\mathrm{d}R_{max}} \propto R_{max}^{-\beta_{pop}} \qquad \phi_{pop} \propto \begin{cases} R^{-\gamma_{src}} & R \ll R_0 \\ R^{-\gamma_{src}-\beta_{pop}+1} & R \gg R_0 \end{cases}$$

Single-power-law distributed maximum rigidity

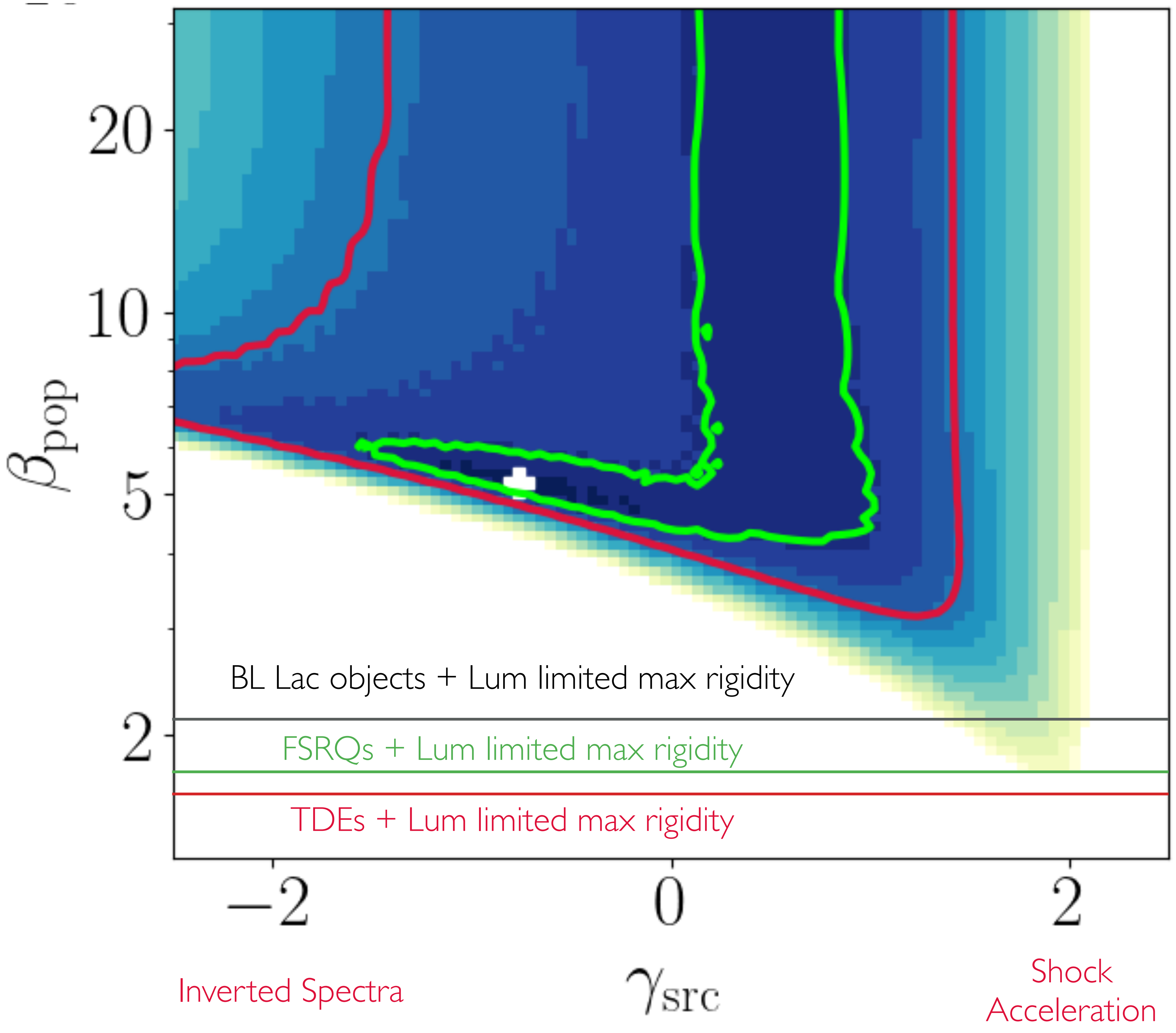

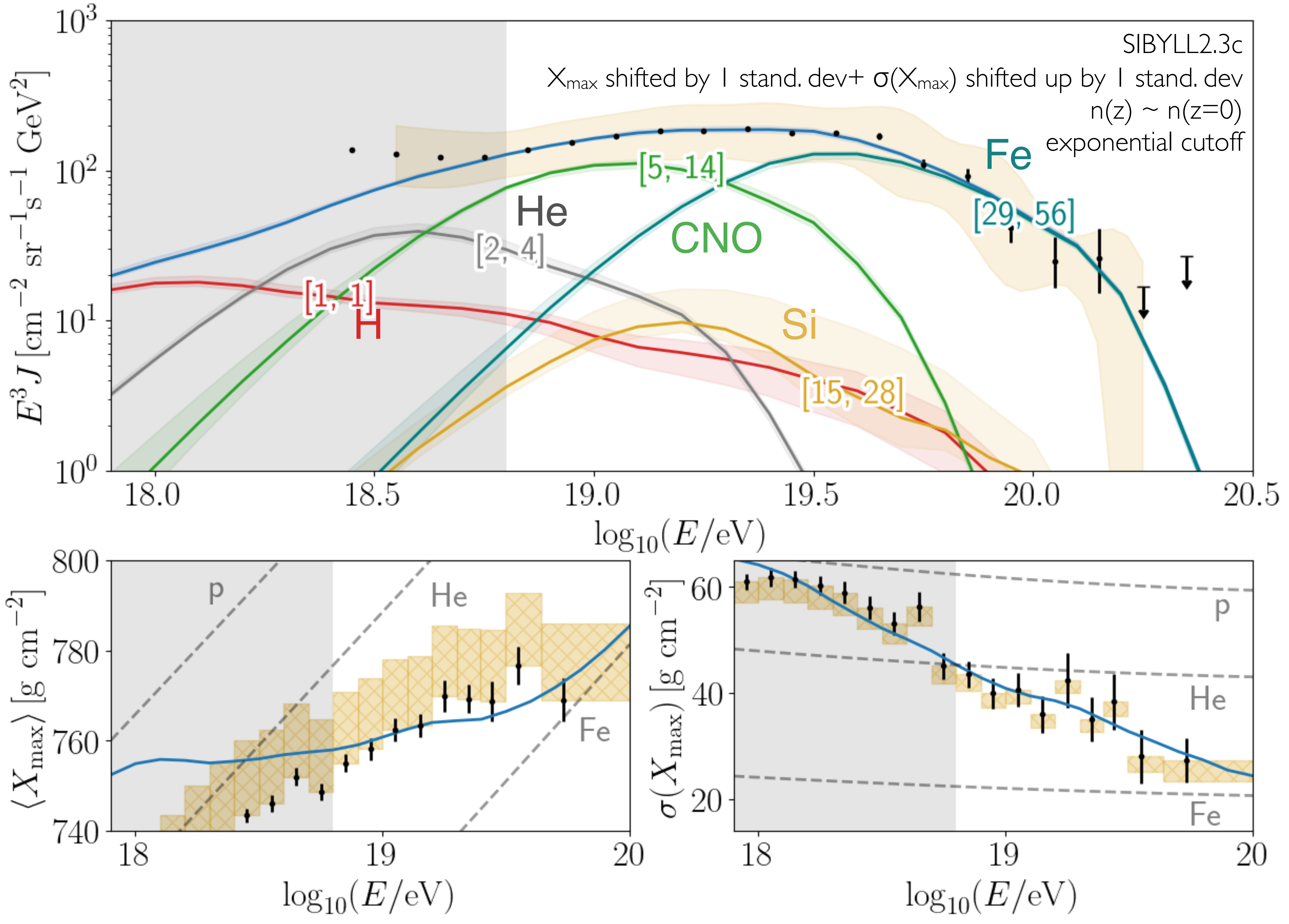

$$\frac{\mathrm{d}N}{\mathrm{d}R} \propto R^{-\gamma_{src}} \qquad \frac{\mathrm{d}N}{\mathrm{d}R_{max}} \propto R_{max}^{-\beta_{pop}} \qquad \phi_{pop} \propto \begin{cases} R^{-\gamma_{src}} & R \ll R_0 \\ R^{-\gamma_{src}-\beta_{pop}+1} & R \gg R_0 \end{cases}$$

Model variations

- R_{max} systematically changes with redshift
- Redshift evolution of source number density
- Minimum source redshift
- Super-exponential source spectrum cutoff
- Hadronic interaction models
- Injection composition fixed to Galactic

Model	Parameter	β_{pop}	γ_{src}	χ^2
fd		$5.2^{+26.4*}_{-0.5}$	$-0.8^{+1.4}_{-0.5}$	40.4
bp	β_1, β_2	$18.4^{+8.5}_{-11.2}$	$-3.5^{+0.2}_{-0.8}$	34.7
zr	$q \in [-5, 2]$	$4.8^{+26.9*}_{-0.5}$	$-0.19^{+0.89}_{-0.18}$	33.7
zn	$m = -3$	$4.4^{+23.9}_{-0.5}$	$0.2^{+0.8}_{-0.4}$	37.3
	$m = 3$	$6.46^{+0.36}_{-0.34}$	$-2.0^{+0.4}_{-0.5*}$	42.5
	$m = 6$	$6.46^{+0.36}_{-0.34}$	$-2.24^{+0.35}_{-0.18}$	68.9
zm	$z_{\min} = 0.01$	$29.9^{+1.7*}_{-25.5}$	$0.38^{+0.18}_{-1.22}$	46.2
sc	$\lambda \in [1, 50]$	$4.0^{+3.2}_{-0.4}$	$1.43^{+0.16}_{-0.16}$	33.6
fg	f_A^R	$4.9^{+0.5}_{-0.5}$	$0.73^{+0.16}_{-0.16}$	45.5
ex	EPOS-LHC	$3.17^{+0.18}_{-0.17}$	$1.43^{+0.09}_{-0.09}$	40.6
	SIBYLL2.3c	$3.5^{+0.6}_{-0.5}$	$1.69^{+0.09}_{-0.09}$	34.7

Model variations

$$\frac{dN}{dR_{max}} \propto R_{max}^{-\beta_{pop}}$$

- R_{max} systematically changes with redshift
- Decreasing R_{max} preferred (less elemental mixing)
- Redshift evolution of source number density
- Decreasing density preferred (less elemental mixing)
- Minimum source redshift
- Smaller z_{min} preferred (fewer interactions, less mixing)
- Super-exponential source spectrum cutoff
- Small preference for strong cutoff- almost Heaviside spectra
- Hadronic interaction models
- Worse fit with EPOS-LHC but more population variance allowed
- Injection composition fixed to Galactic
- Poorer fit - hard source spectra needed to compensate

Model	Parameter	β_{pop}	γ_{src}	χ^2
fd		$5.2^{+26.4*}_{-0.5}$	$-0.8^{+1.4}_{-0.5}$	40.4
bp	β_1, β_2	$18.4^{+8.5}_{-11.2}$	$-3.5^{+0.2}_{-0.8}$	34.7
zr	$q \in [-5, 2]$	$4.8^{+26.9*}_{-0.5}$	$-0.19^{+0.89}_{-0.18}$	33.7
zn	$m = -3$	$4.4^{+23.9}_{-0.5}$	$0.2^{+0.8}_{-0.4}$	37.3
	$m = 3$	$6.46^{+0.36}_{-0.34}$	$-2.0^{+0.4}_{-0.5*}$	42.5
	$m = 6$	$6.46^{+0.36}_{-0.34}$	$-2.24^{+0.35}_{-0.18}$	68.9
zm	$z_{min} = 0.01$	$29.9^{+1.7*}_{-25.5}$	$0.38^{+0.18}_{-1.22}$	46.2
sc	$\lambda \in [1, 50]$	$4.0^{+3.2}_{-0.4}$	$1.43^{+0.16}_{-0.16}$	33.6
fg	f_A^R	$4.9^{+0.5}_{-0.5}$	$0.73^{+0.16}_{-0.16}$	45.5
ex	EPOS-LHC	$3.17^{+0.18}_{-0.17}$	$1.43^{+0.09}_{-0.09}$	40.6
	SIBYLL2.3c	$3.5^{+0.6}_{-0.5}$	$1.69^{+0.09}_{-0.09}$	34.7

Model variations

$$\frac{\mathrm{d}N}{\mathrm{d}R_{\mathrm{max}}} \propto R_{\mathrm{max}}^{-\beta_{\mathrm{pop}}}$$

- R_{max} systematically changes with redshift
- Decreasing R_{max} preferred (less elemental mixing)
- Redshift evolution of source number density
- Decreasing density preferred (less elemental mixing)
- Minimum source redshift
- Smaller z_{min} preferred (fewer interactions, less mixing)
- Super-exponential source spectrum cutoff
- Small preference for strong cutoff- almost Heaviside spectra
- Hadronic interaction models
- Worse fit with EPOS-LHC but more population variance allowed
- Injection composition fixed to Galactic
- Poorer fit - hard source spectra needed to compensate

Model	Parameter	β_{pop}	γ_{src}	χ^2
fd		[illegible]	[illegible]	40.4
bp				34.7
zr				33.7
zn				37.3
				42.5
				58.9
zm				46.2
sc				33.6
fg				45.5
ex				40.6
	SIBYLL2.3c	$3.5^{+0.6}_{-0.5}$	$1.69^{+0.09}_{-0.09}$	34.7

For all model variations:

$$\beta_{\mathrm{pop}} \gtrsim 3$$

90% of UHECR sources have same R_{max} within a factor of three.

Broken-power-law distributed maximum rigidity

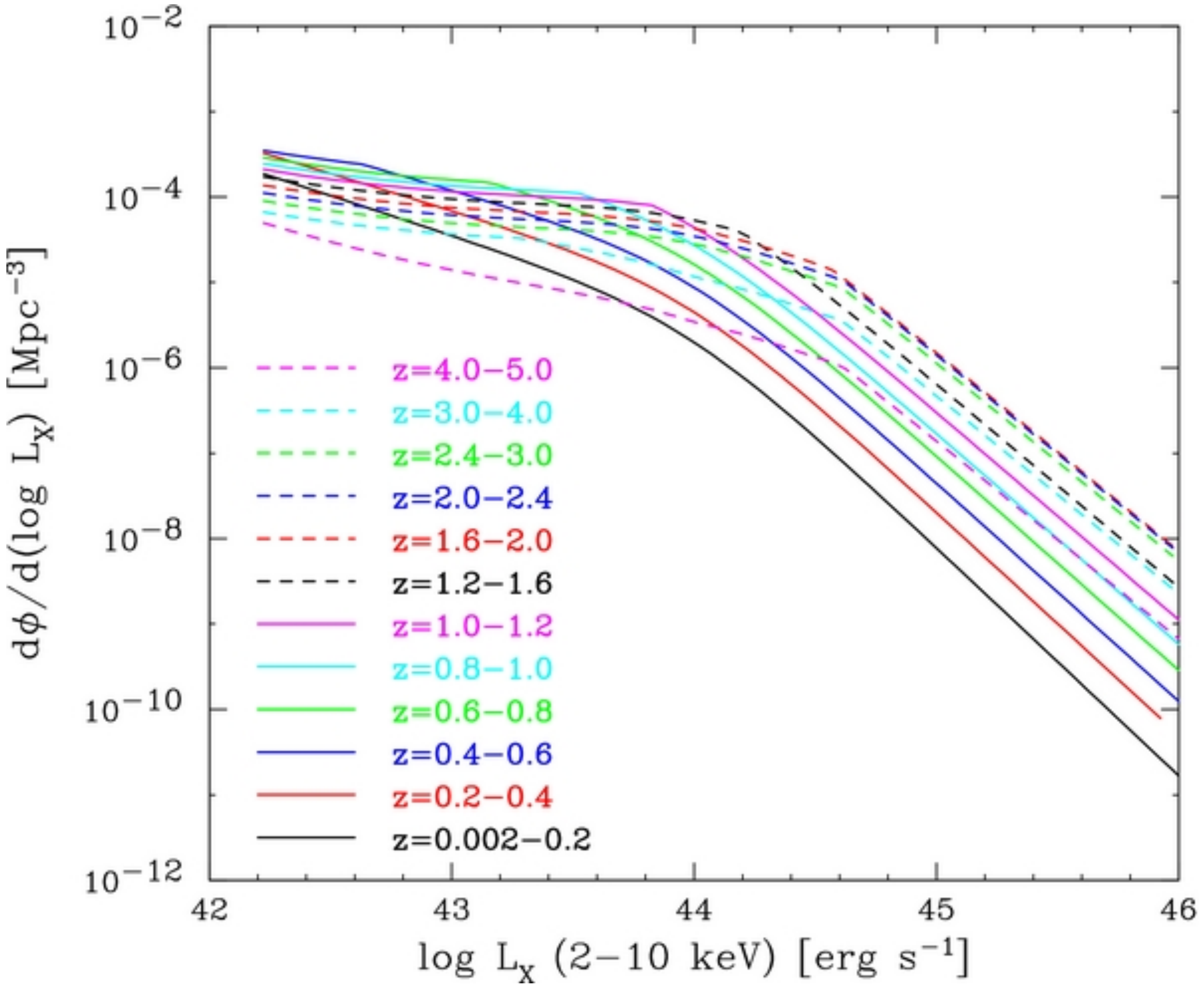

Hard X-ray luminosity function of Compton thick AGN, *Ueda et al 2014*

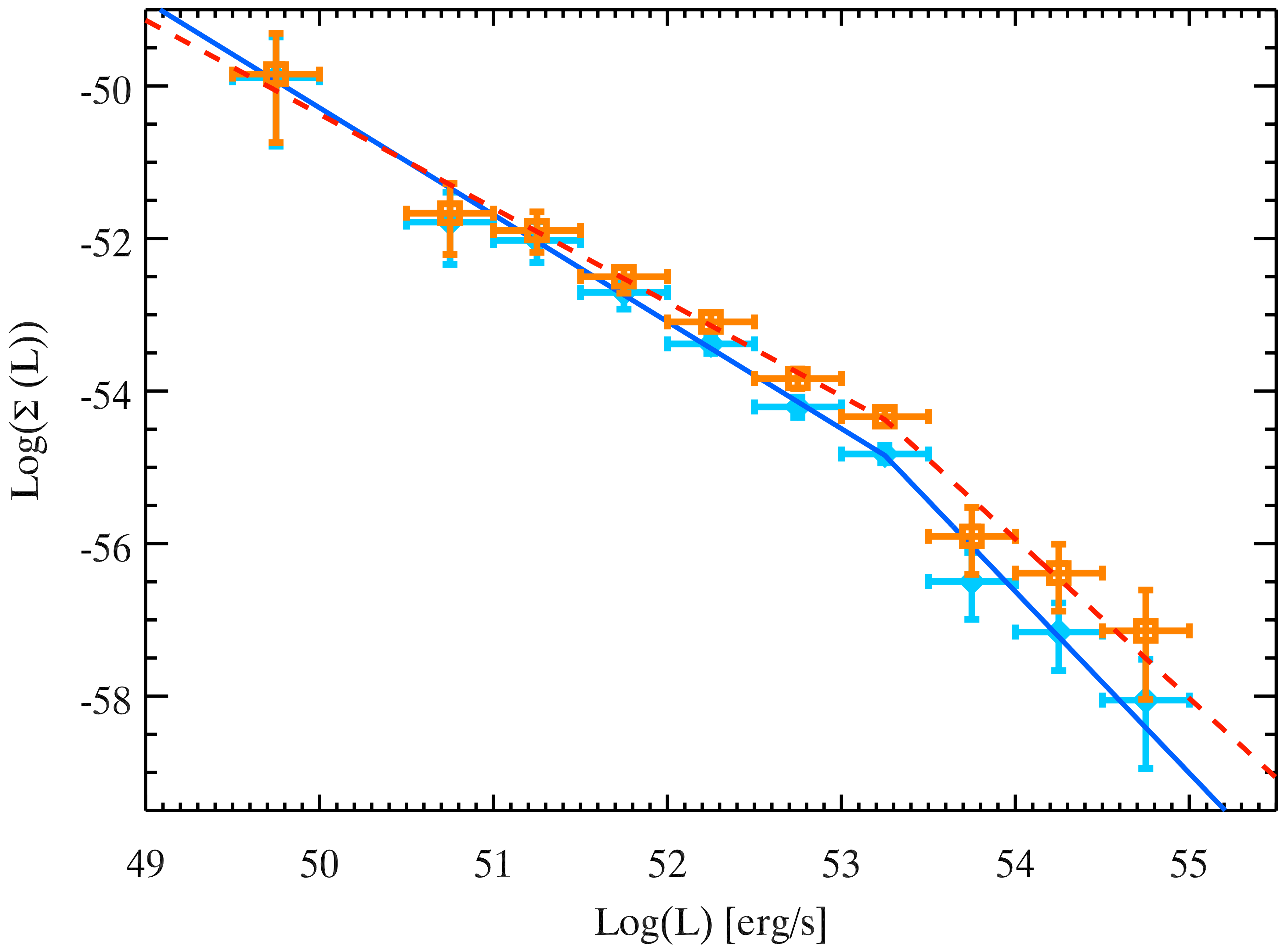

Swift-selected Long GRBs, *Pescalli et al 2016*

Broken-power-law distributed maximum rigidity

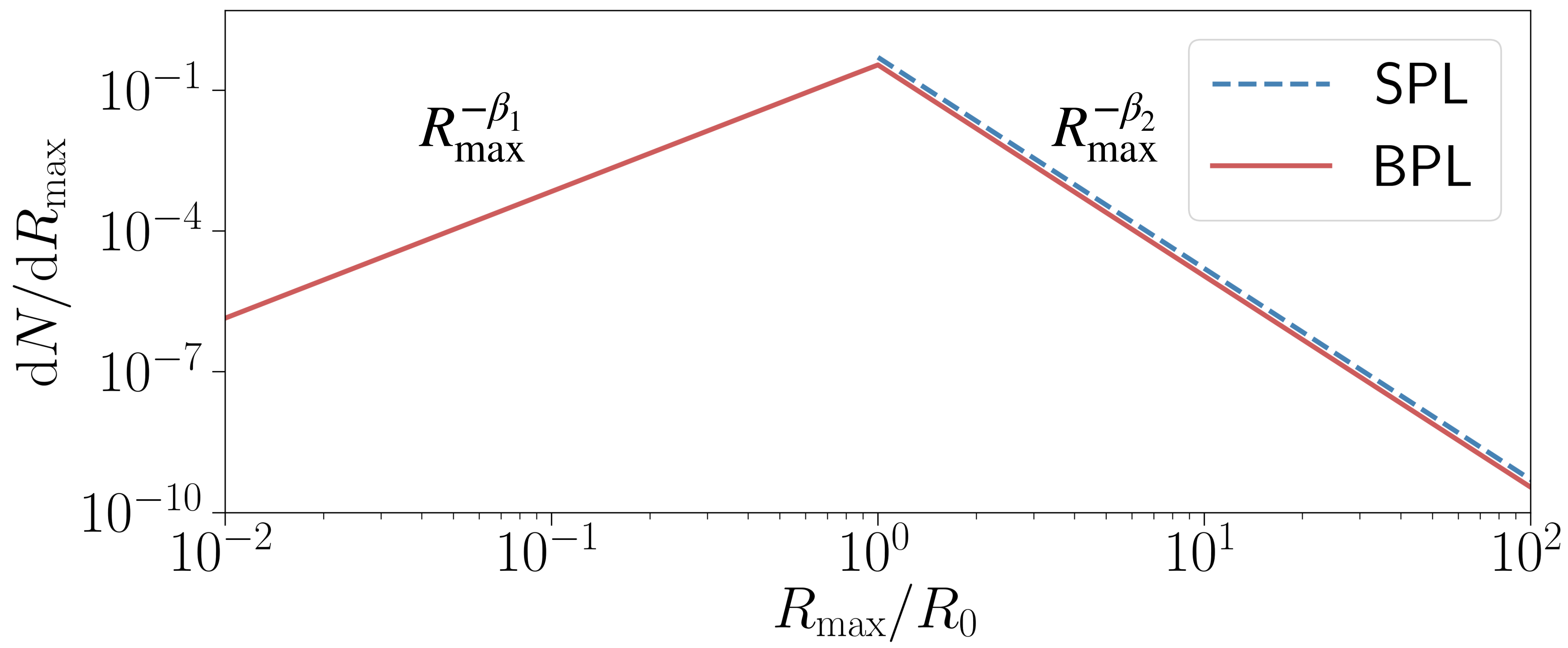

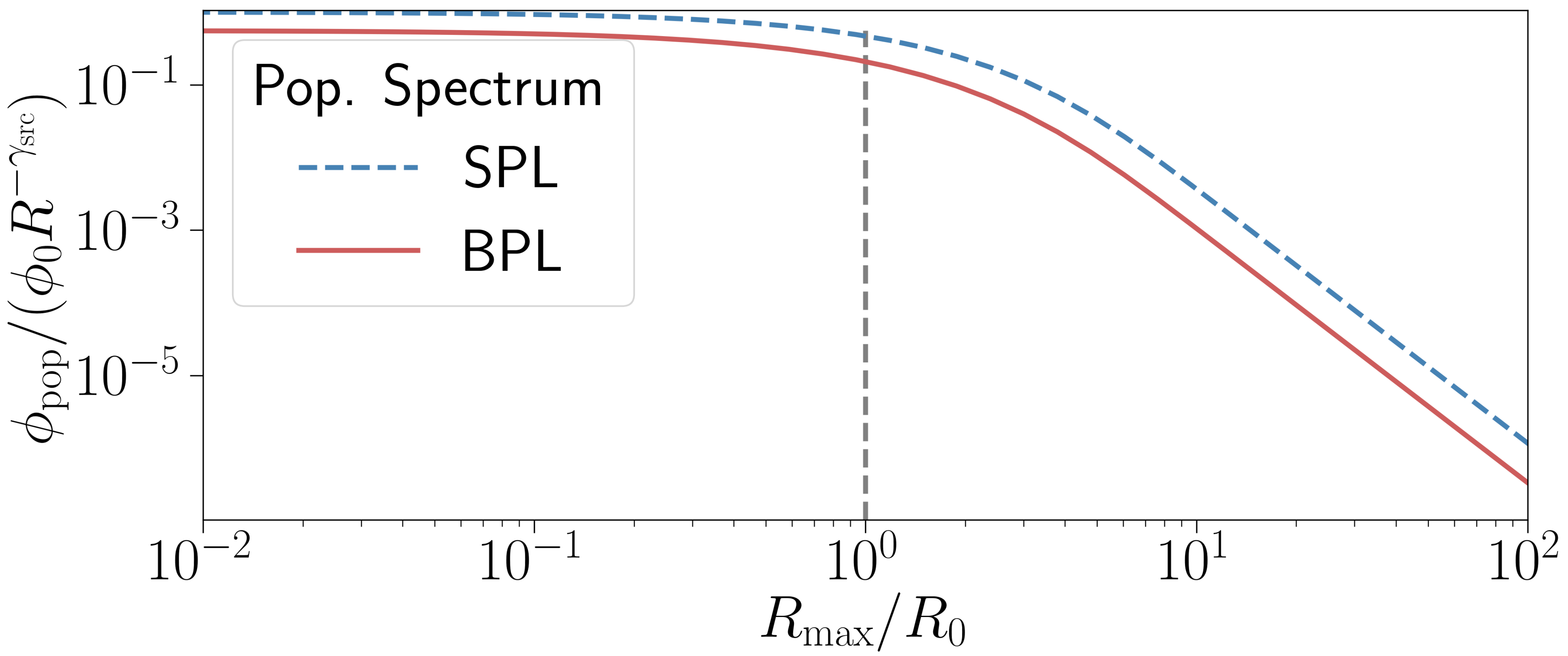

$$dN/dR_{max} \propto \begin{cases} \left(\frac{R_{max}}{R_0}\right)^{-\beta_1} & R_{max} < R_0 \\ \left(\frac{R_{max}}{R_0}\right)^{-\beta_2} & R_{max} > R_0 \end{cases}$$

$\beta_1 \leq 1$: Reduces to a single power-law

$$\phi_{pop} \propto \begin{cases} R^{-\gamma_{src}} & R \ll R_0 \\ R^{-\gamma_{src}-\beta_{pop}+1} & R \gg R_0 \end{cases}$$

Broken-power-law distributed maximum rigidity

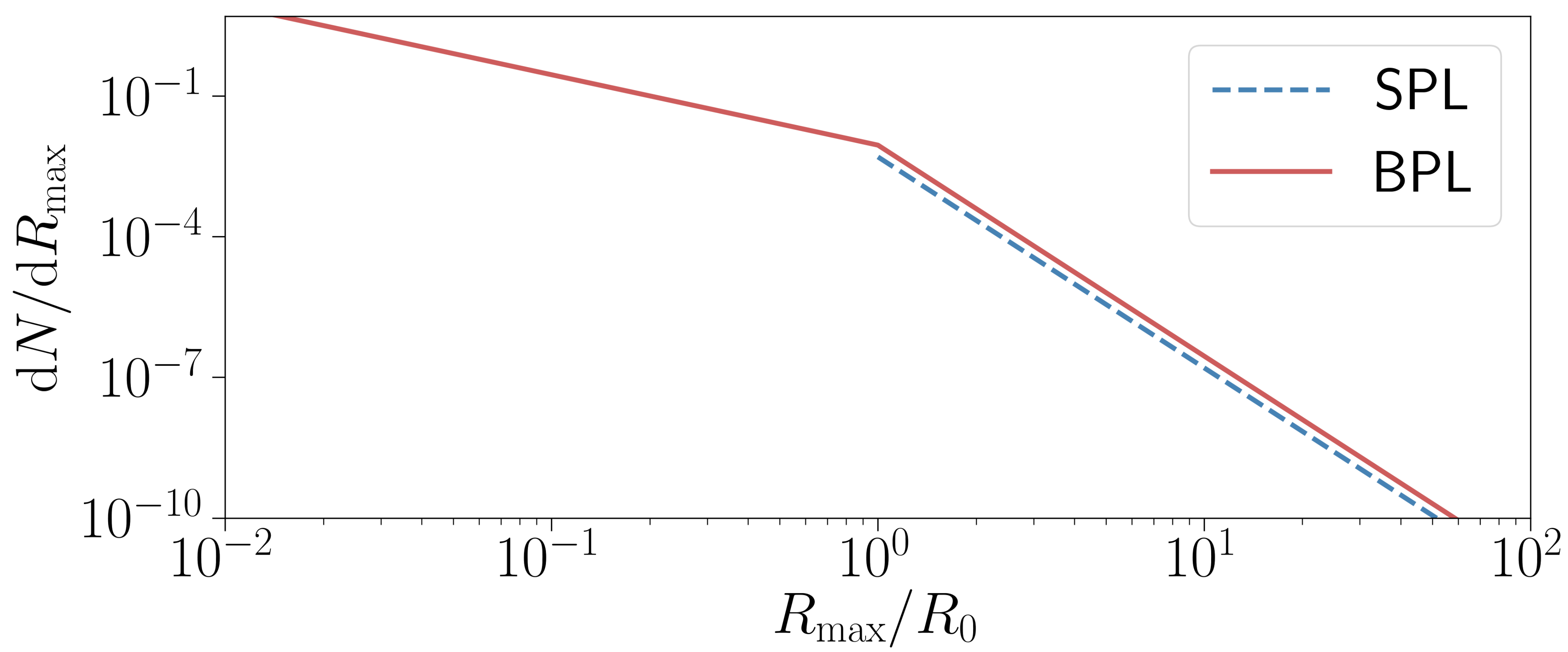

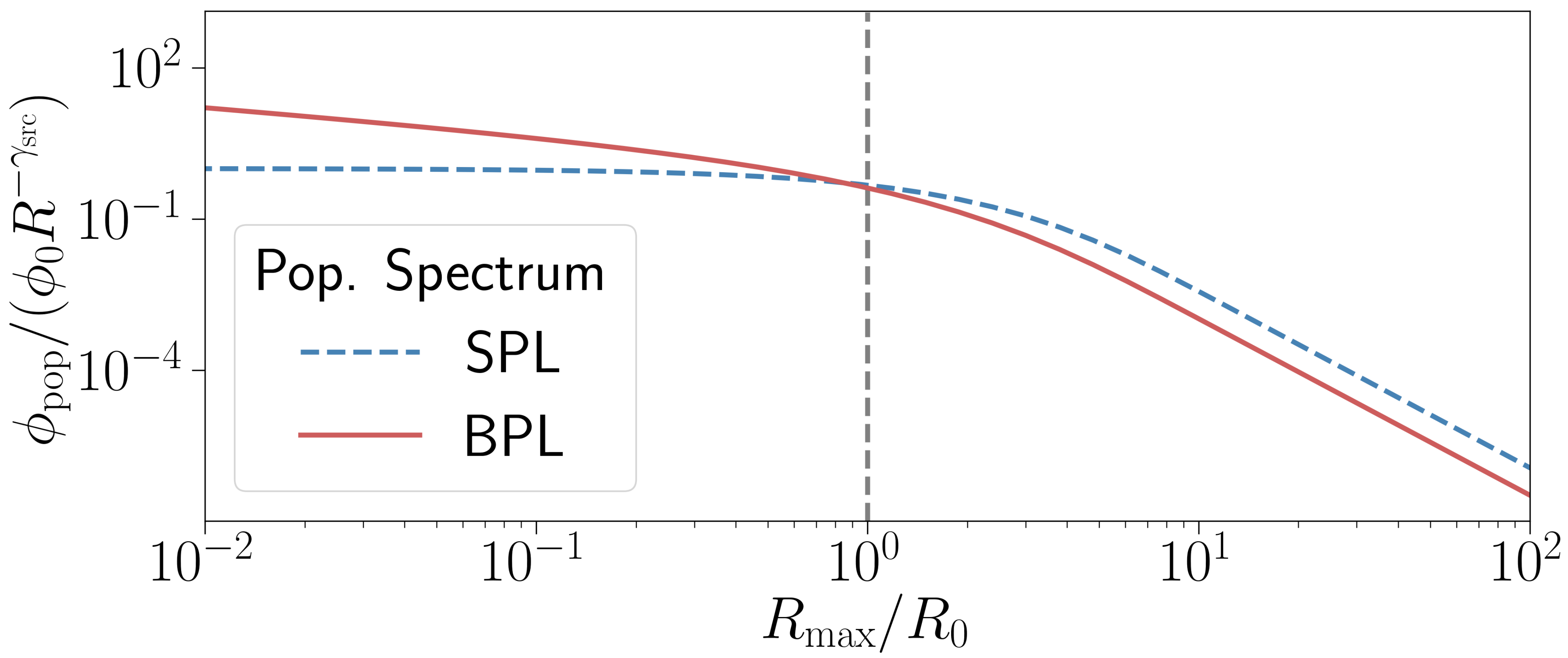

$$\mathrm{d}N/\mathrm{d}R_{\mathrm{max}} \propto \begin{cases} \left(\frac{R_{\mathrm{max}}}{R_0}\right)^{-\beta_1} & R_{\mathrm{max}} < R_0 \\ \left(\frac{R_{\mathrm{max}}}{R_0}\right)^{-\beta_2} & R_{\mathrm{max}} > R_0 \end{cases}$$

$\beta_1 > 1$: Full broken-power law treatment

Broken-power-law distributed maximum rigidity

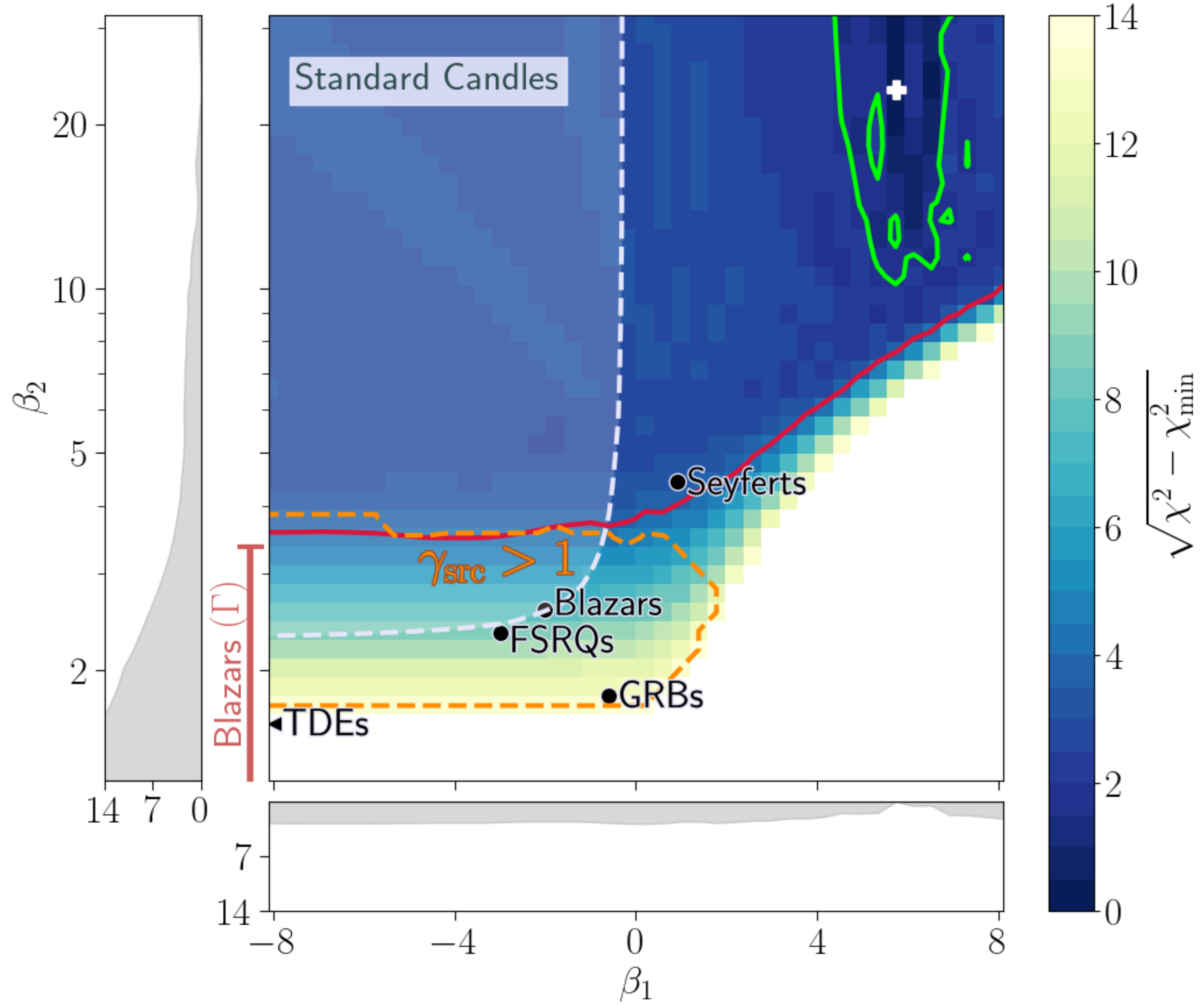

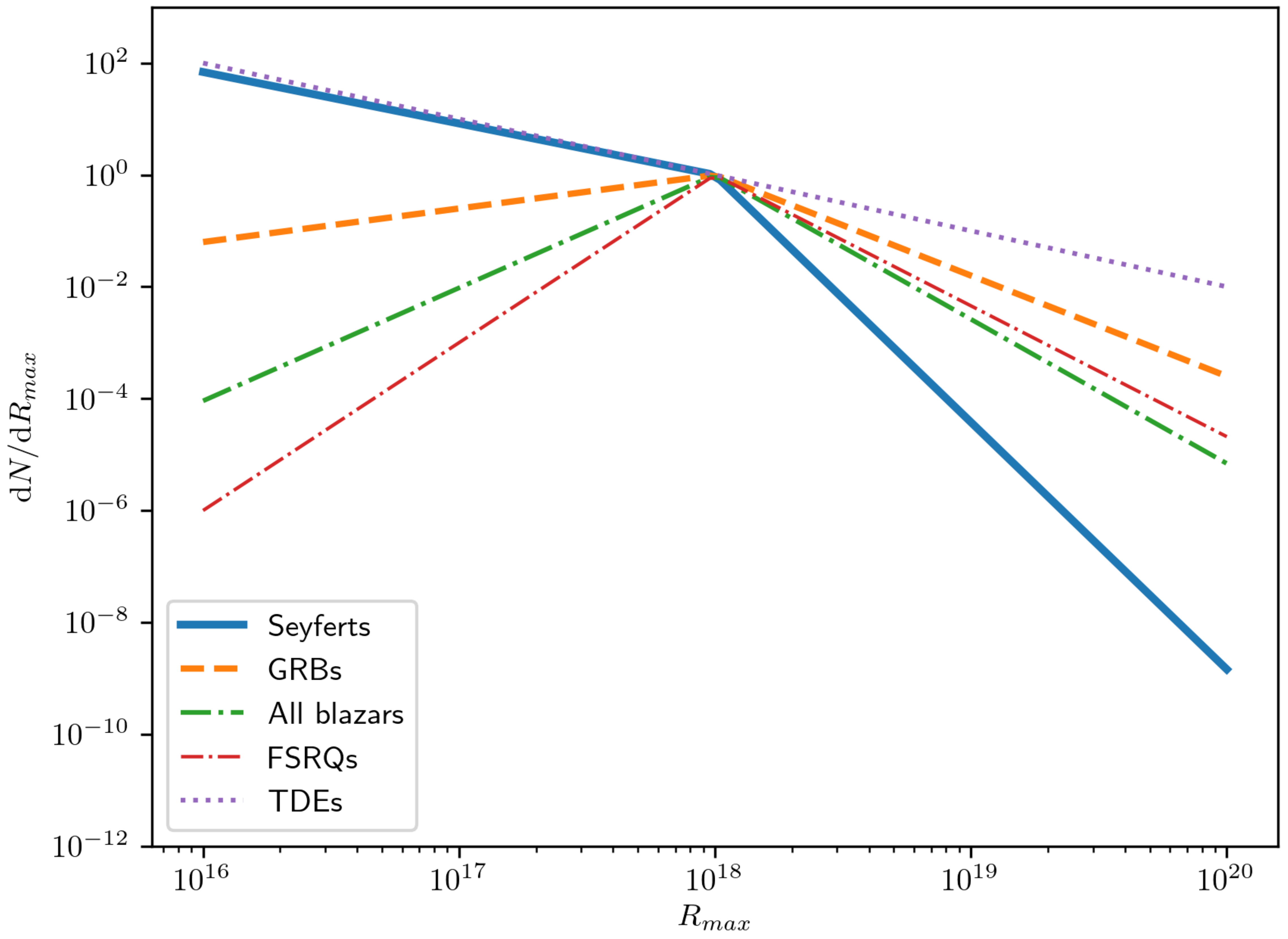

$$dN/dR_{\max} \propto \begin{cases} \left(\frac{R_{\max}}{R_0}\right)^{-\beta_1} & R_{\max} < R_0 \\ \left(\frac{R_{\max}}{R_0}\right)^{-\beta_2} & R_{\max} > R_0 \end{cases}$$

Broken-power-law distributed maximum rigidity

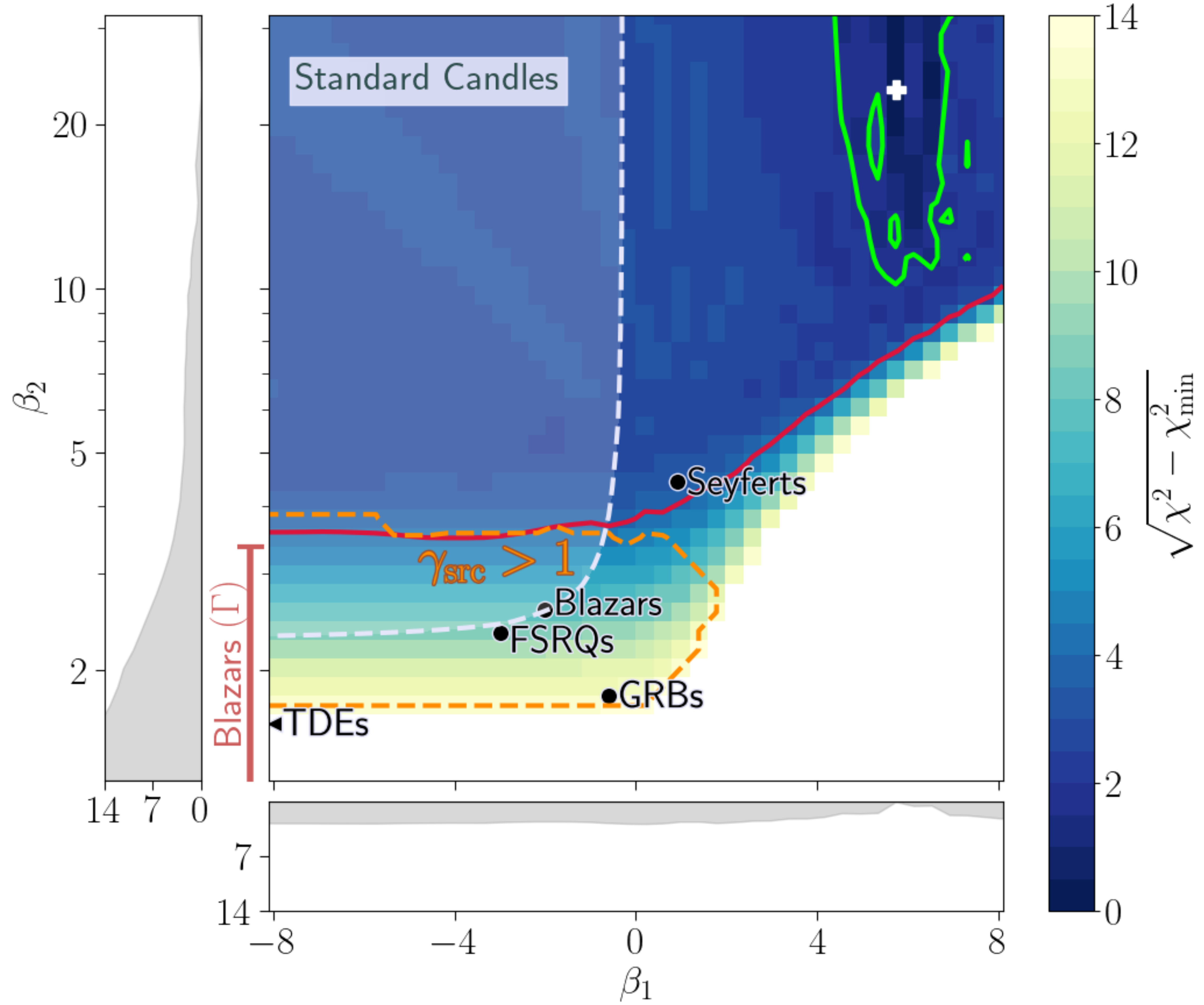

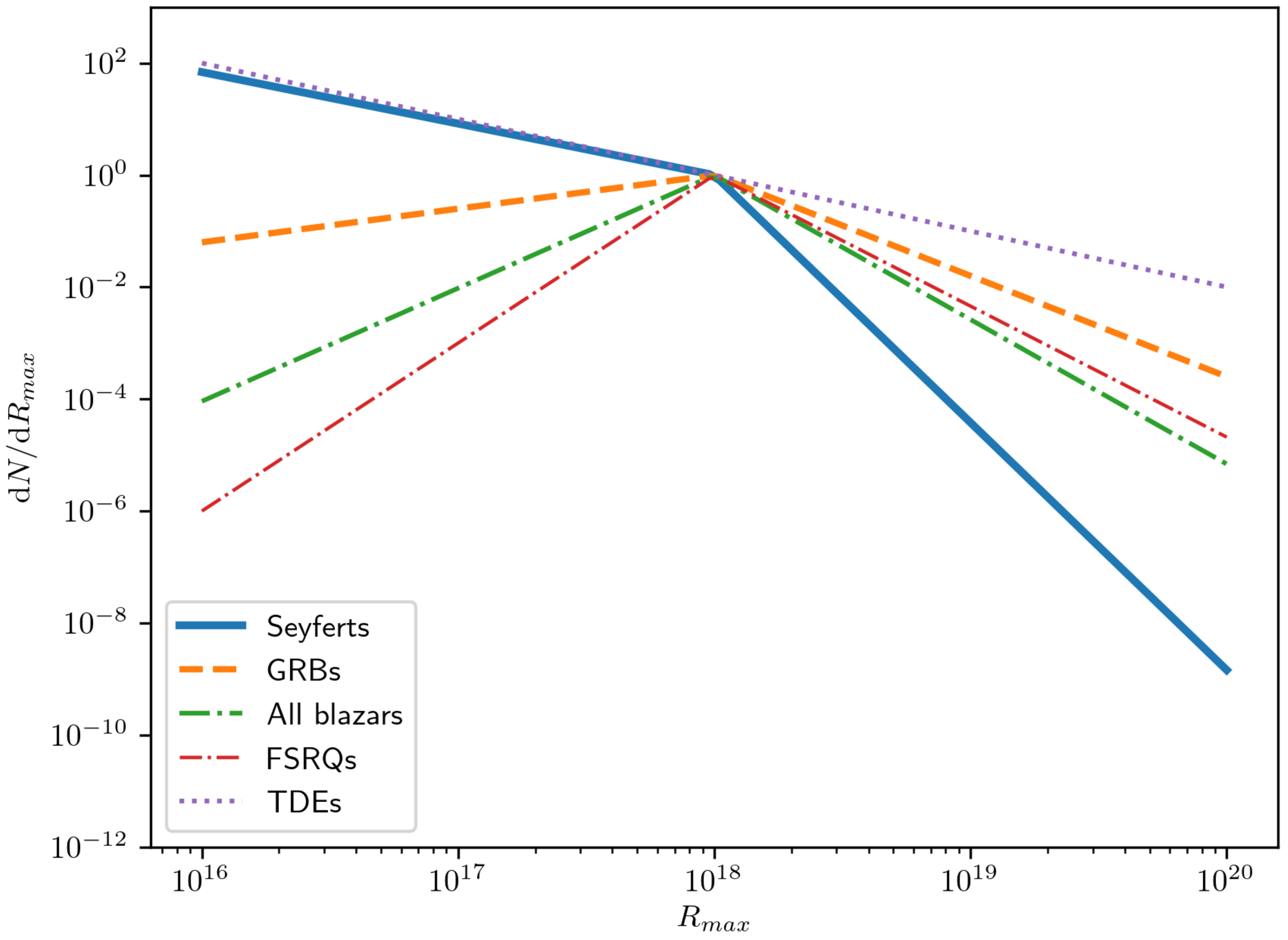

$$
dN/dR_{max} \propto \begin{cases} \left(\frac{R_{max}}{R_0}\right)^{-\beta_1} & R_{max} < R_0 \\ \left(\frac{R_{max}}{R_0}\right)^{-\beta_2} & R_{max} > R_0 \end{cases}
$$

Broken-power-law distributed maximum rigidity

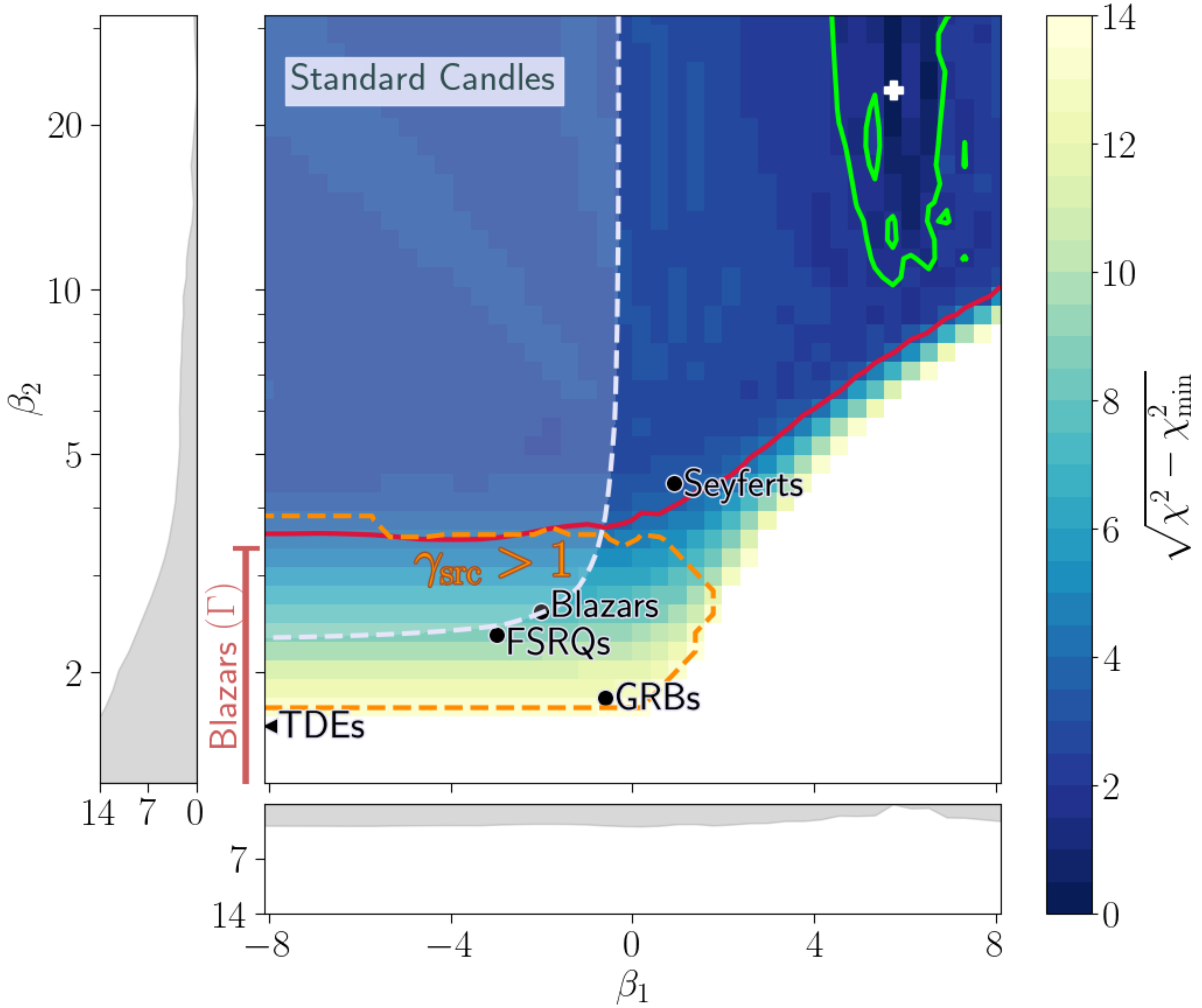

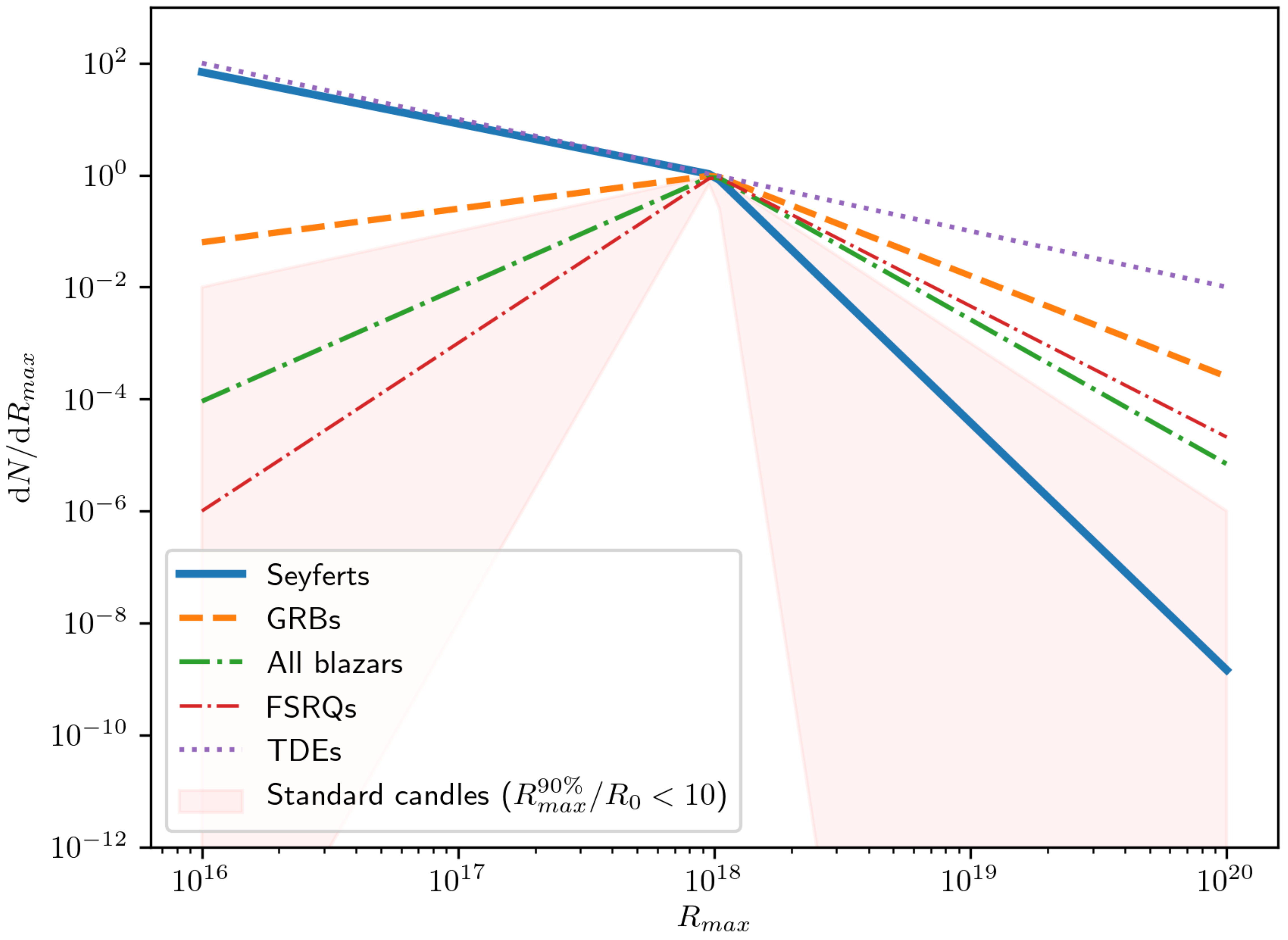

$$
dN/dR_{\max} \propto \begin{cases} \left(\frac{R_{\max}}{R_0}\right)^{-\beta_1} & R_{\max} < R_0 \\ \left(\frac{R_{\max}}{R_0}\right)^{-\beta_2} & R_{\max} > R_0 \end{cases}
$$

Broken-power-law distributed maximum rigidity

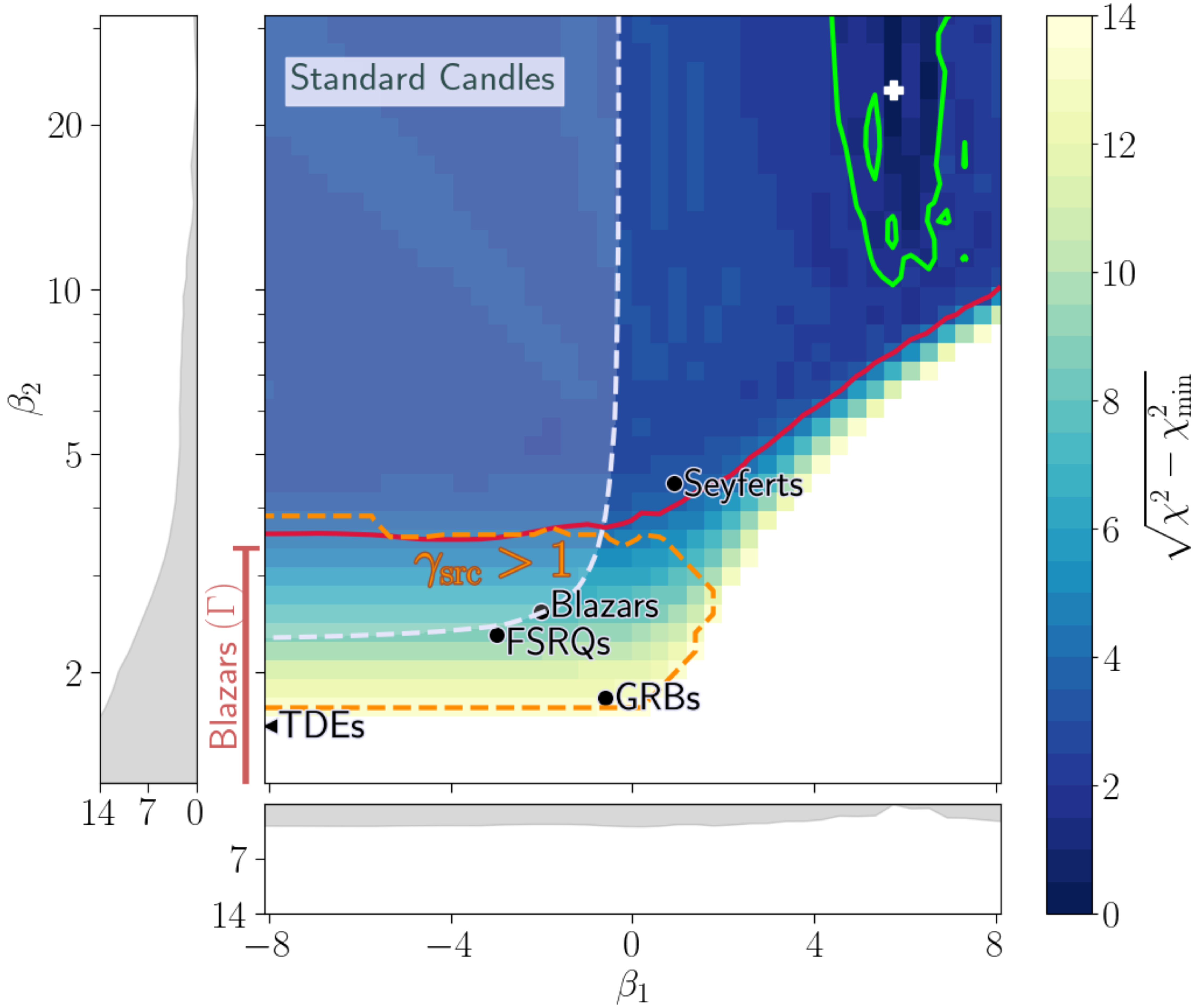

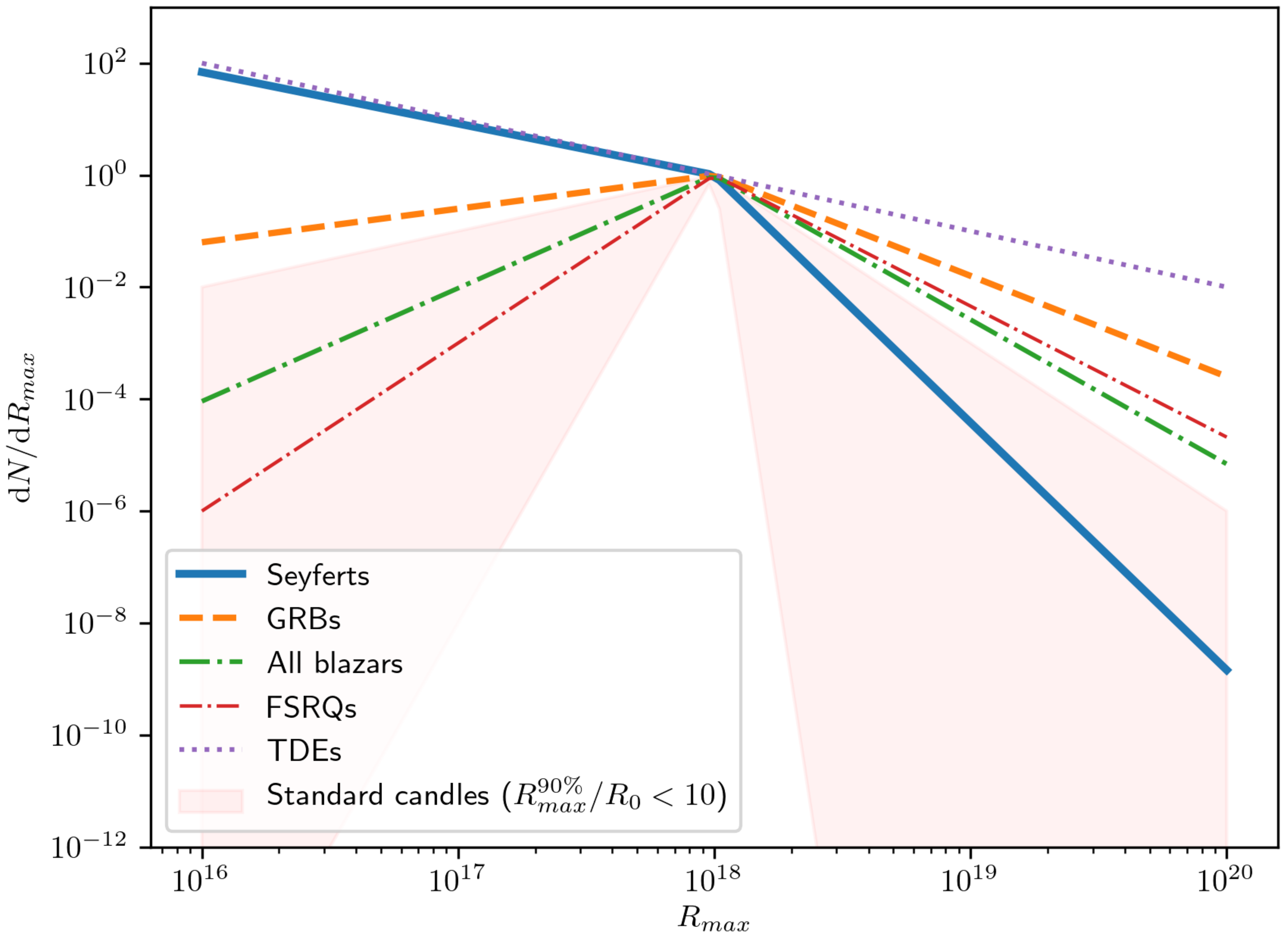

$$
dN/dR_{\max} \propto \begin{cases} \left(\frac{R_{\max}}{R_0}\right)^{-\beta_1} & R_{\max} < R_0 \\ \left(\frac{R_{\max}}{R_0}\right)^{-\beta_2} & R_{\max} > R_0 \end{cases}
$$

Broken-power-law distributed maximum rigidity

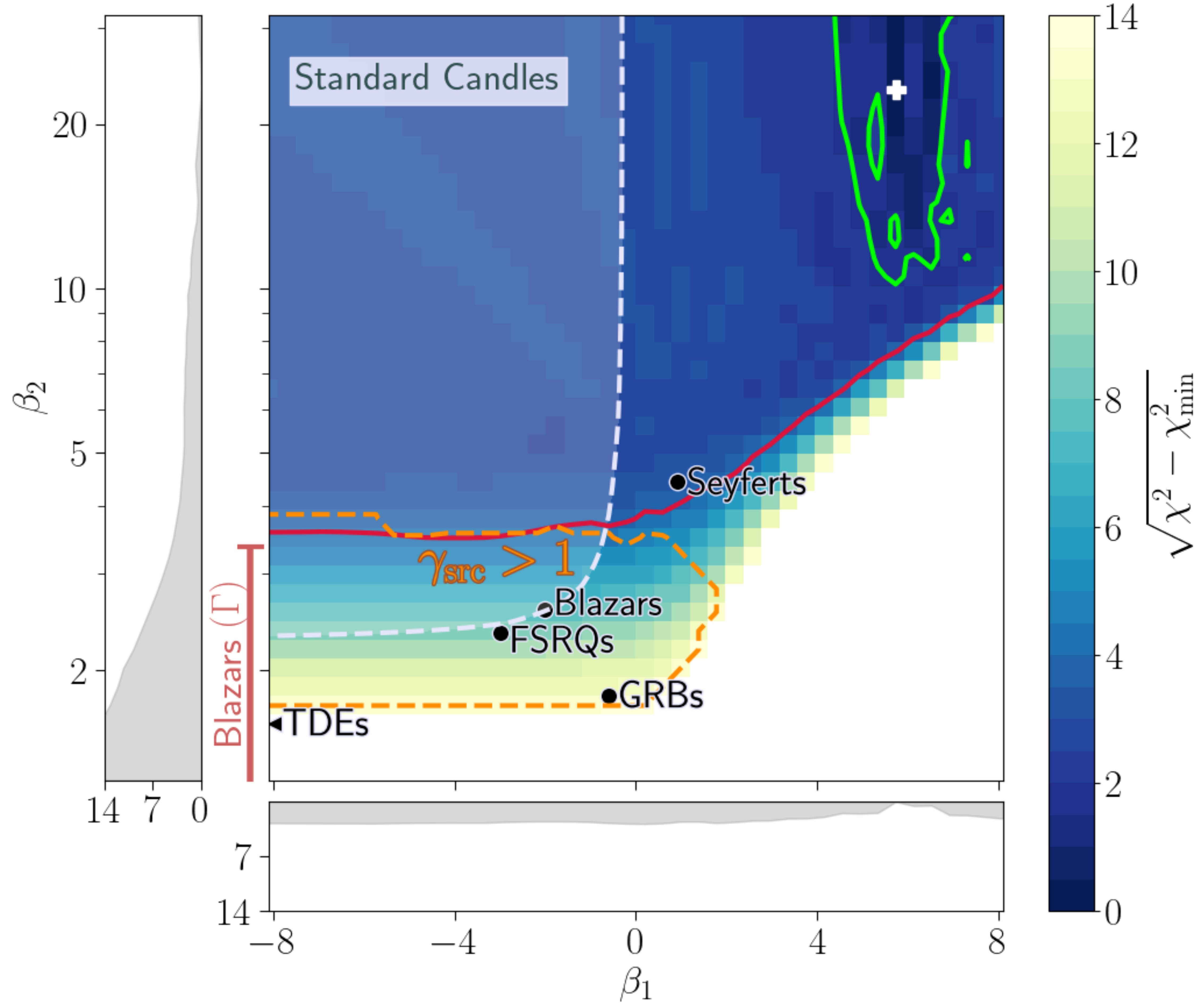

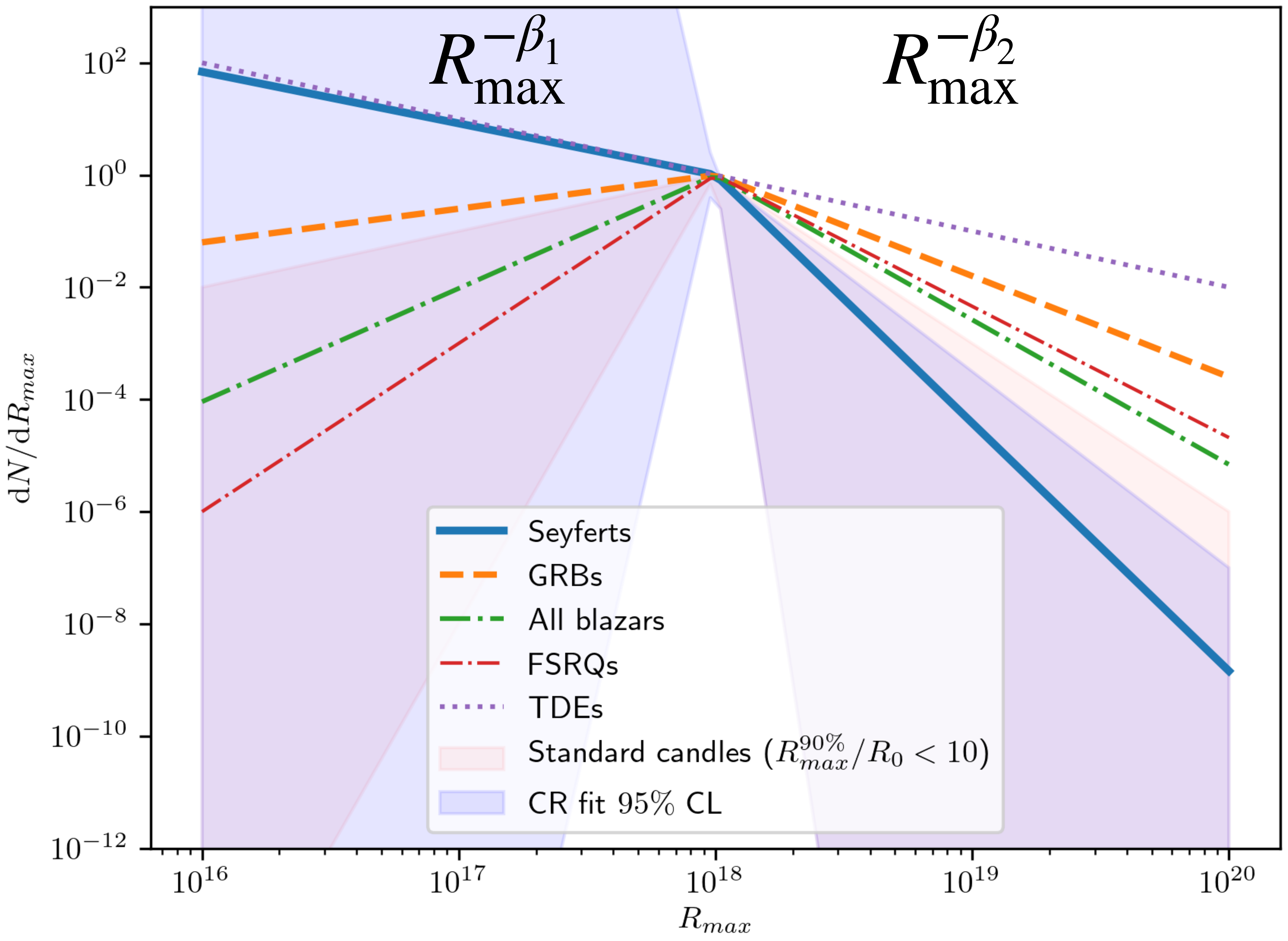

$$dN/dR_{\max} \propto \begin{cases} \left(\frac{R_{\max}}{R_0}\right)^{-\beta_1} & R_{\max} < R_0 \\ \left(\frac{R_{\max}}{R_0}\right)^{-\beta_2} & R_{\max} > R_0 \end{cases}$$

Broken-power-law distributed maximum rigidity

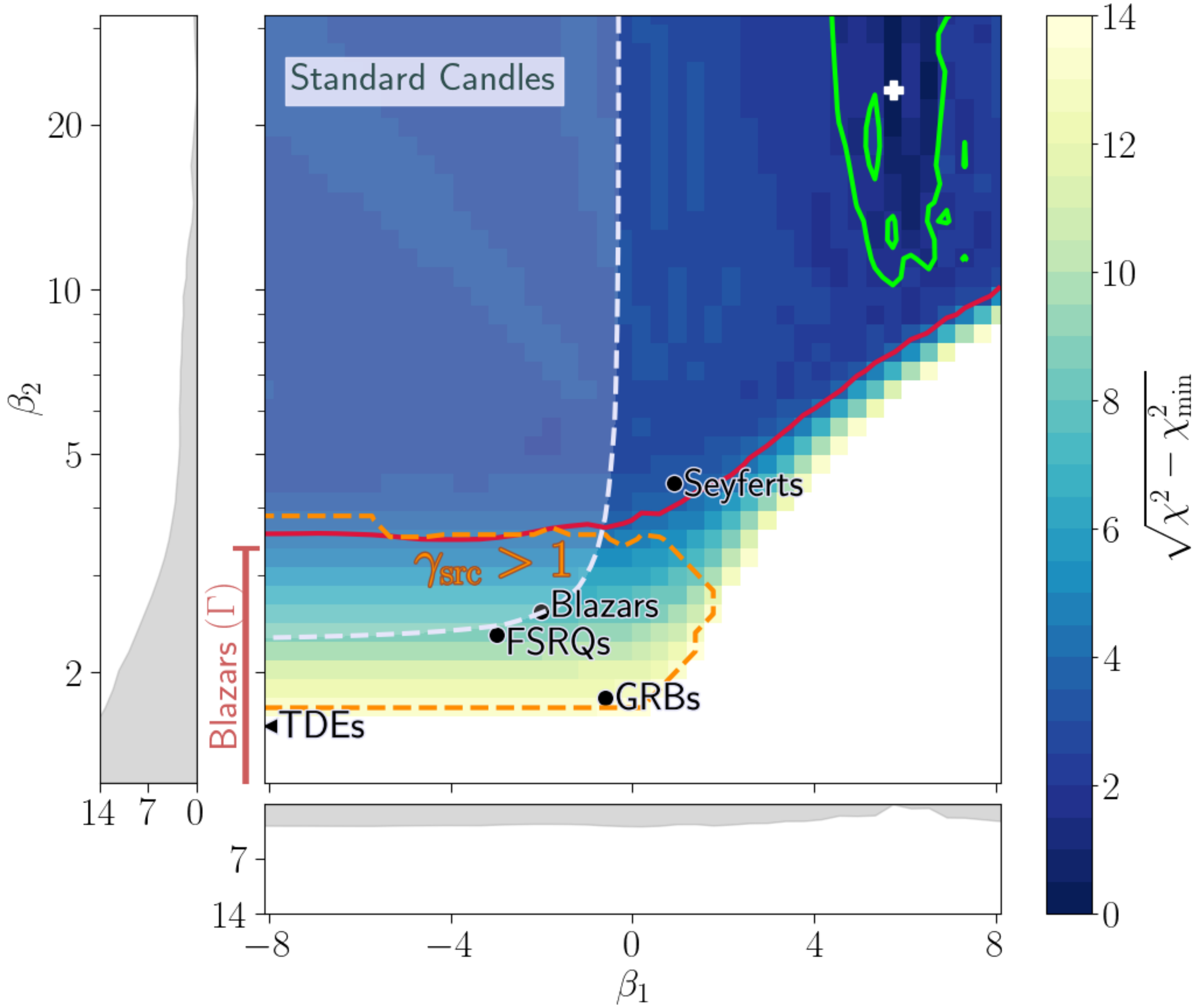

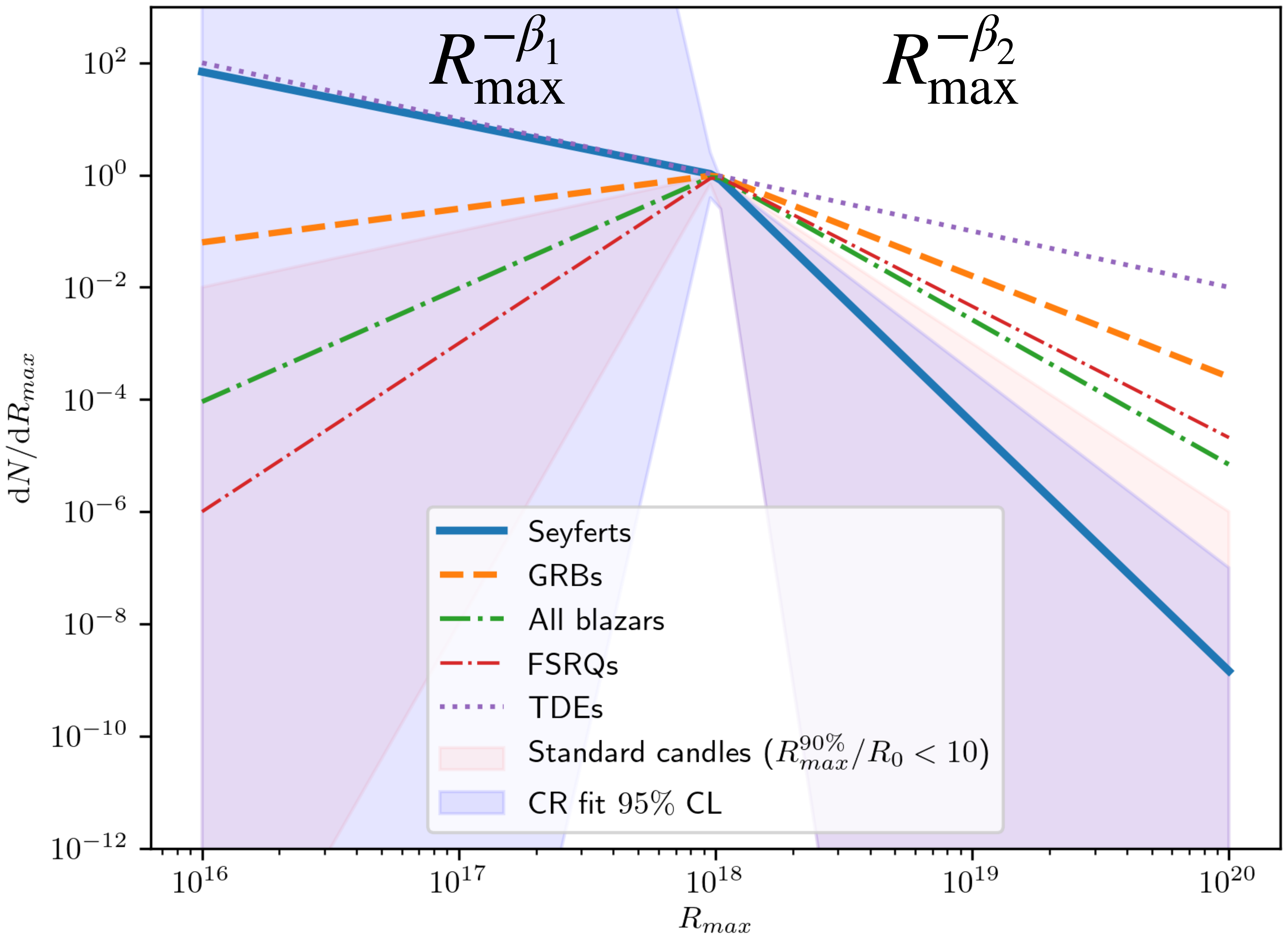

$$dN/dR_{\max} \propto \begin{cases} \left(\frac{R_{\max}}{R_0}\right)^{-\beta_1} & R_{\max} < R_0 \\ \left(\frac{R_{\max}}{R_0}\right)^{-\beta_2} & R_{\max} > R_0 \end{cases}$$

Broken-power-law distributed maximum rigidity

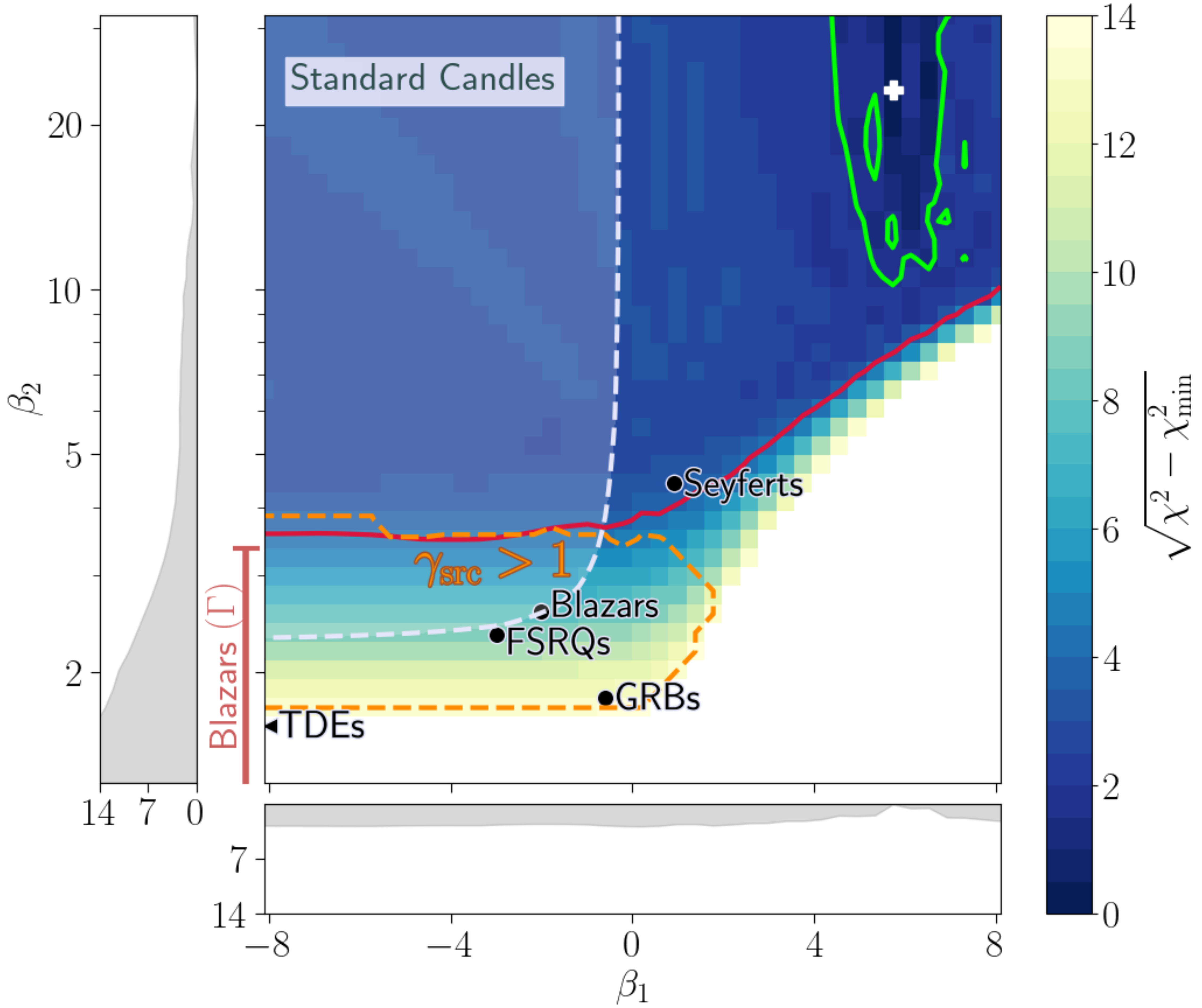

Individual source energy spectral index

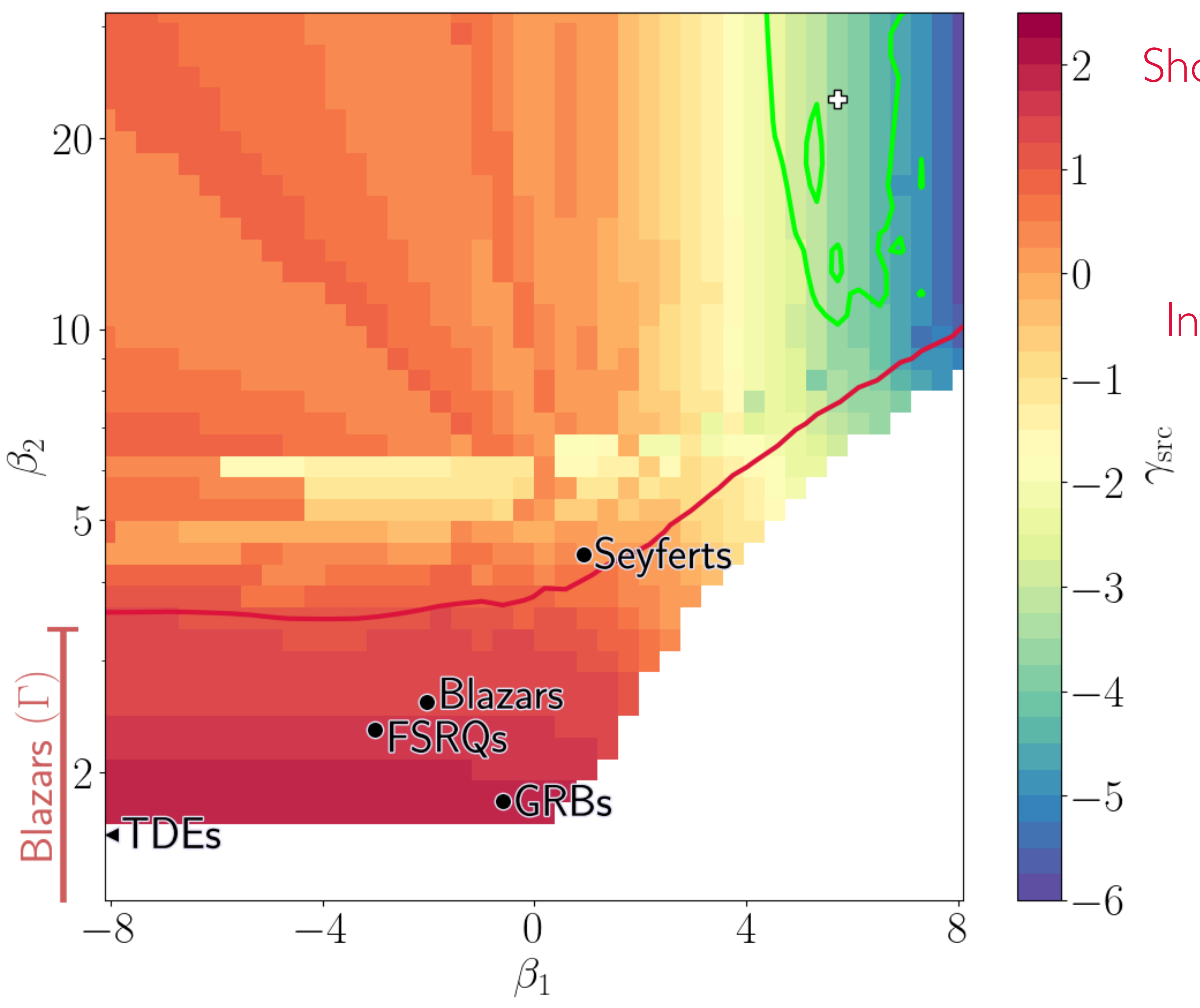

$$\mathrm{d}N/\mathrm{d}R_{\max} \propto \begin{cases} \left(\frac{R_{\max}}{R_0}\right)^{-\beta_1} & R_{\max} < R_0 \\ \left(\frac{R_{\max}}{R_0}\right)^{-\beta_2} & R_{\max} > R_0 \end{cases}$$

Broken-power-law distributed maximum rigidity

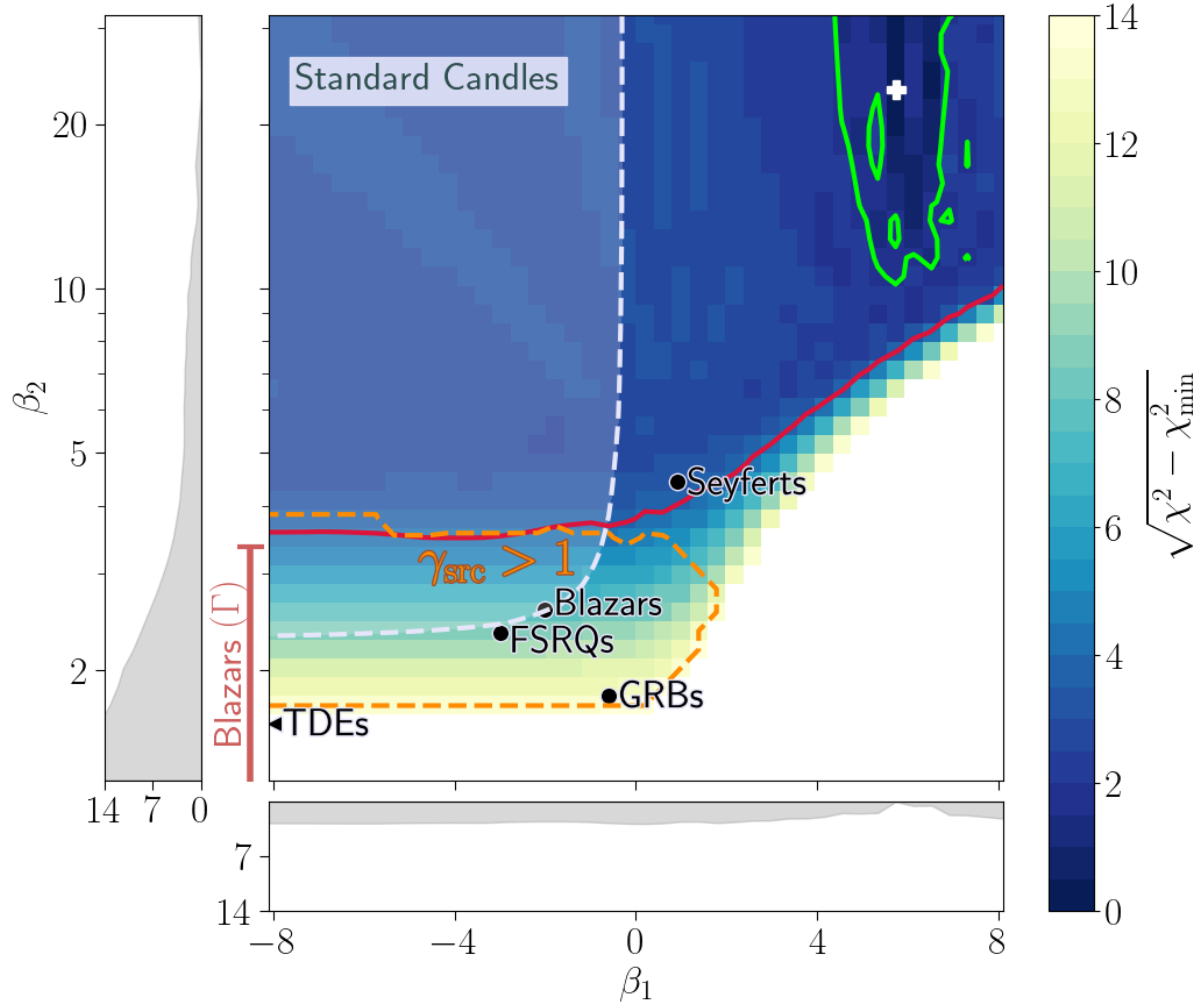

Individual source energy spectral index

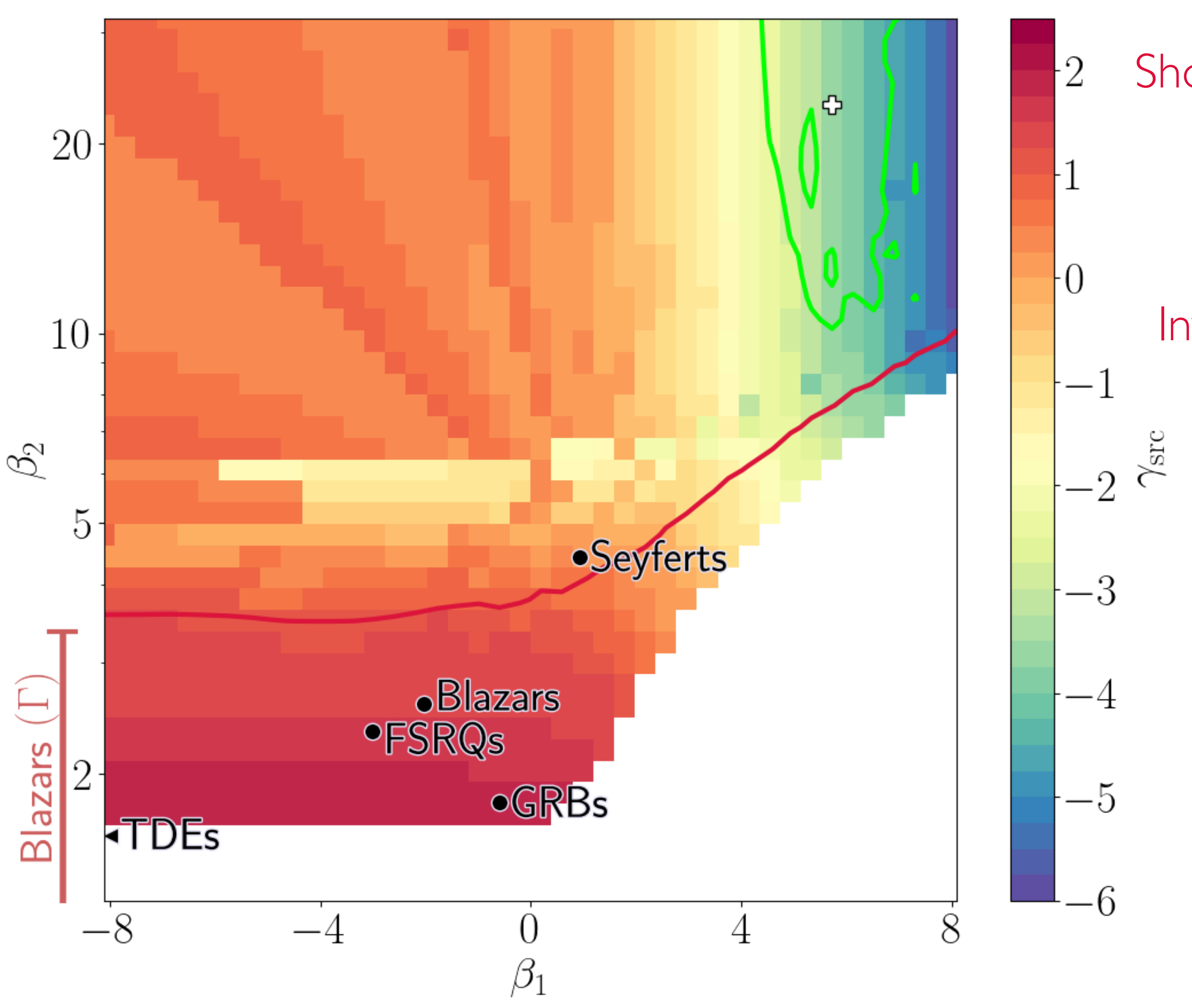

$$
\mathrm{d}N/\mathrm{d}R_{\max} \propto \begin{cases} \left(\frac{R_{\max}}{R_0}\right)^{-\beta_1} & R_{\max} < R_0 \\ \left(\frac{R_{\max}}{R_0}\right)^{-\beta_2} & R_{\max} > R_0 \end{cases}
$$

Summary

- First systematic investigation of allowed population variance in maximum UHECR rigidity

- Strong constraints on astrophysical sources
  - Near-identical sources or sharp cutoff in rigidity distrib.
  - Low rigidity tail exacerbates hard injection spectra

- NB: Additional variance expected from distribution of radius, magnetic field strength…

- Few sources? (in tension with source # density constraints)
- Seyferts with extra-hard injection spectra?
- Exotic physics?

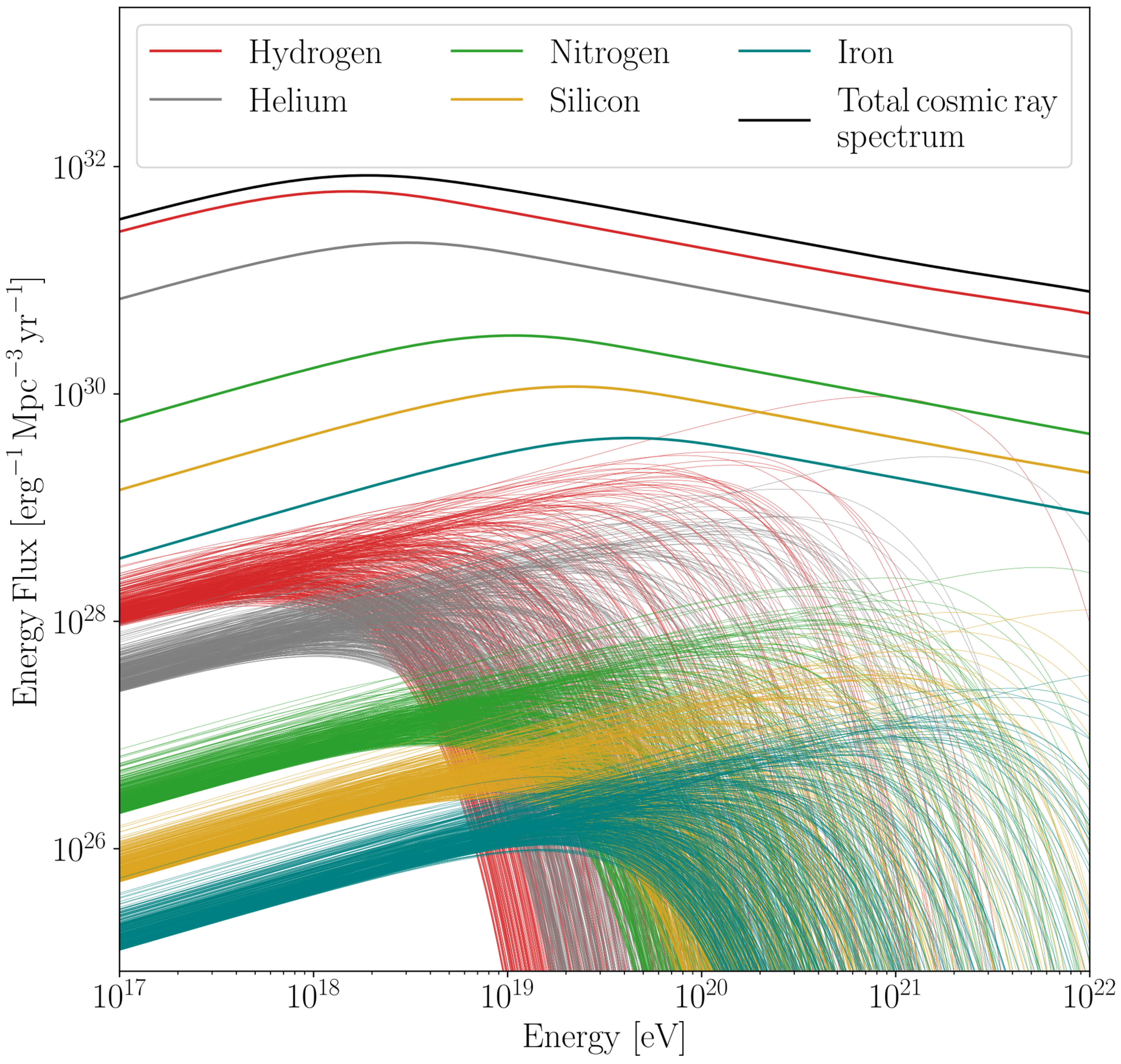

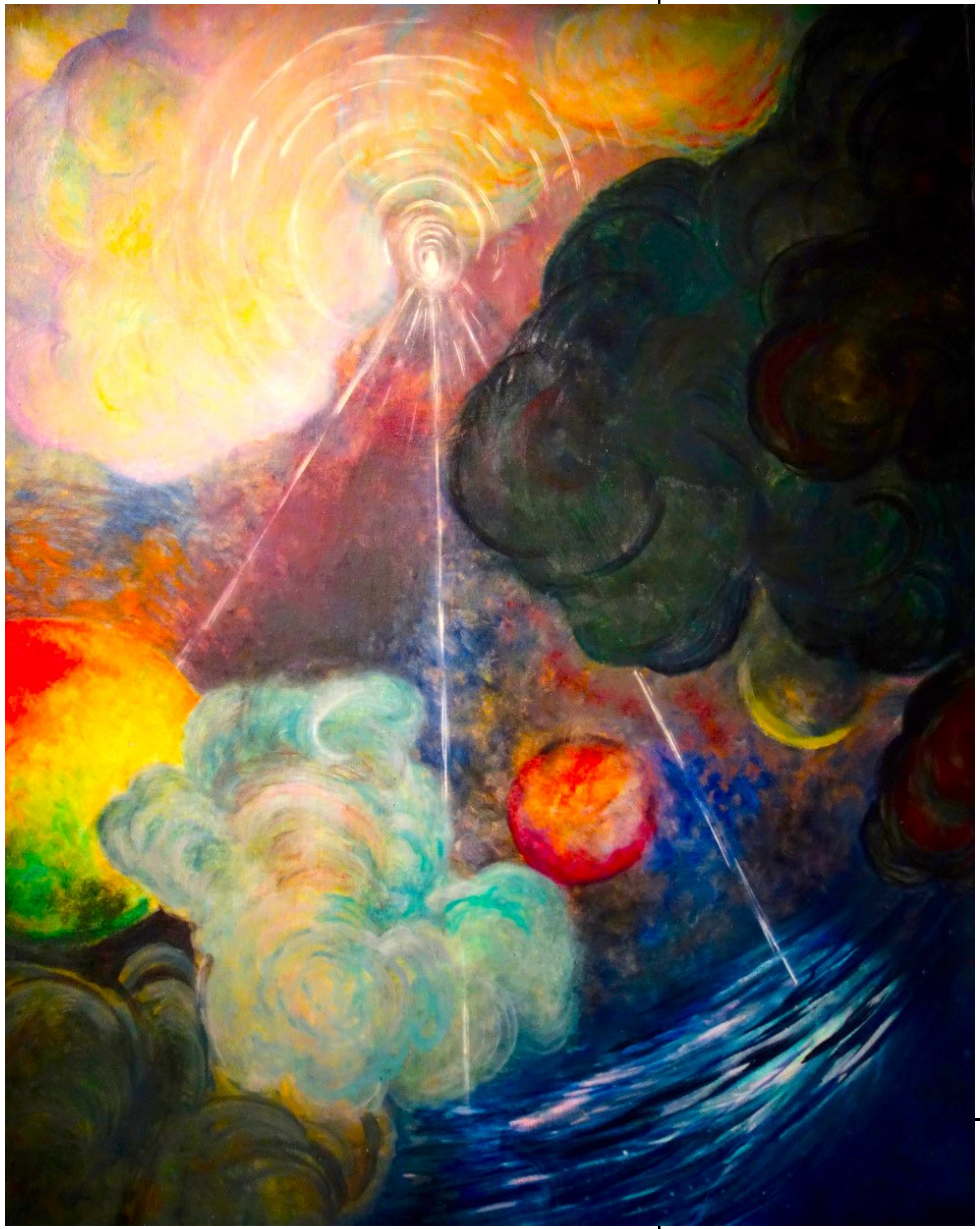

Back-up slides

Different hadronic interaction models

Model	Sibyll2.3c (no shifts)	Sibyll2.3c (fid. shifts)	Epos-LHC (fid. shifts)
R_0 [EV]	$1.73^{+0.20}_{-0.18}$	$0.57^{+1.88}_{-0.11}$	$1.6^{+0.6}_{-0.4}$
$\beta_{\rm pop}$	$29.9^{+1.7*}_{-18.1}$	$5.2^{+26.4*}_{-0.5}$	$4.4^{+0.5}_{-0.5}$
$\gamma_{\rm src}$	$-0.23^{+0.18}_{-0.26}$	$-0.8^{+1.4}_{-0.5}$	$0.1^{+0.4}_{-0.5}$
$f_A^R[\%]$	0^{+0}_{-0}	$0^{+36.4}_{-0}$	0^{+0}_{-0}
	$58.1^{+0.4}_{-1.9}$	$0^{+51.3}_{-0}$	$36.9^{+7.4}_{-22.8}$
	$35.0^{+1.6}_{-0.2}$	$93.7^{+0.5}_{-53.5}$	$50.3^{+16.3}_{-5.4}$
	$5.7^{+0.5}_{-0.6}$	$0.3^{+7.7}_{-0.3}$	$11.3^{+6.6}_{-3.8}$
	$1.16^{+0.12}_{-0.11}$	$6.0^{+0.2}_{-3.8}$	$1.41^{+0.27}_{-0.04}$
$R_{\rm max}^{0.90}$ $[R_0]$	$1.083^{+0.155}_{-0.005}$	$1.72^{+0.13}_{-0.64}$	$1.97^{+0.22}_{-0.17}$
χ^2/d.o.f.	45.0/26	40.4/26	56.3/26

Redshift evolution of source number density, $n(z) \sim n_0 \cdot (1+z)^m$

Redshift evolution m	-3	0	3	6
R_0 [EV]	$0.80^{+1.88}_{-0.16}$	$0.57^{+1.88}_{-0.11}$	$0.46^{+0.05}_{-0.09}$	$0.52^{+0.06}_{-0.05}$
$\beta_{\rm pop}$	$4.4^{+23.9}_{-0.5}$	$5.2^{+26.4*}_{-0.5}$	$6.46^{+0.36}_{-0.34}$	$6.46^{+0.36}_{-0.34}$
$\gamma_{\rm src}$	$0.2^{+0.8}_{-0.4}$	$-0.8^{+1.4}_{-0.5}$	$-2.0^{+0.4}_{-0.5}$	$-2.24^{+0.35}_{-0.18}$
$f_A^R[\%]$	$3.5^{+46.8}_{-3.5}$	$0^{+36.4}_{-0}$	$0^{+0.01}_{-0}$	0^{+0}_{-0}
	$8.7^{+49.8}_{-8.7}$	$0^{+51.3}_{-0}$	$2.6^{+17.0}_{-2.6}$	0^{+0}_{-0}
	$81.3^{+11.5}_{-46.7}$	$93.7^{+0.5}_{-53.5}$	$90.5^{+2.0}_{-16.2}$	$38.5^{+1.8}_{-15.7}$
	$1.7^{+3.7}_{-0.8}$	$0.3^{+7.7}_{-0.3}$	$0^{+0.9}_{-0}$	$53.0^{+16.2}_{-3.9}$
	$4.8^{+0.8}_{-2.8}$	$6.0^{+0.2}_{-3.8}$	$6.8^{+0.5}_{-1.3}$	$8.5^{+2.1}_{-0.5}$
$R^{0.90}_{\rm max}$ $[R_0]$	$1.97^{+0.22}_{-0.88}$	$1.72^{+0.13}_{-0.64}$	$1.53^{+0.04}_{-0.04}$	$1.53^{+0.04}_{-0.04}$
χ^2/d.o.f.	37.3/26	40.6/26	42.5/26	68.9/26

Redshift evolution of the maximum rigidity, $R_{\max}(z) \sim R_{\max}^{z=0}(1+z)^q$

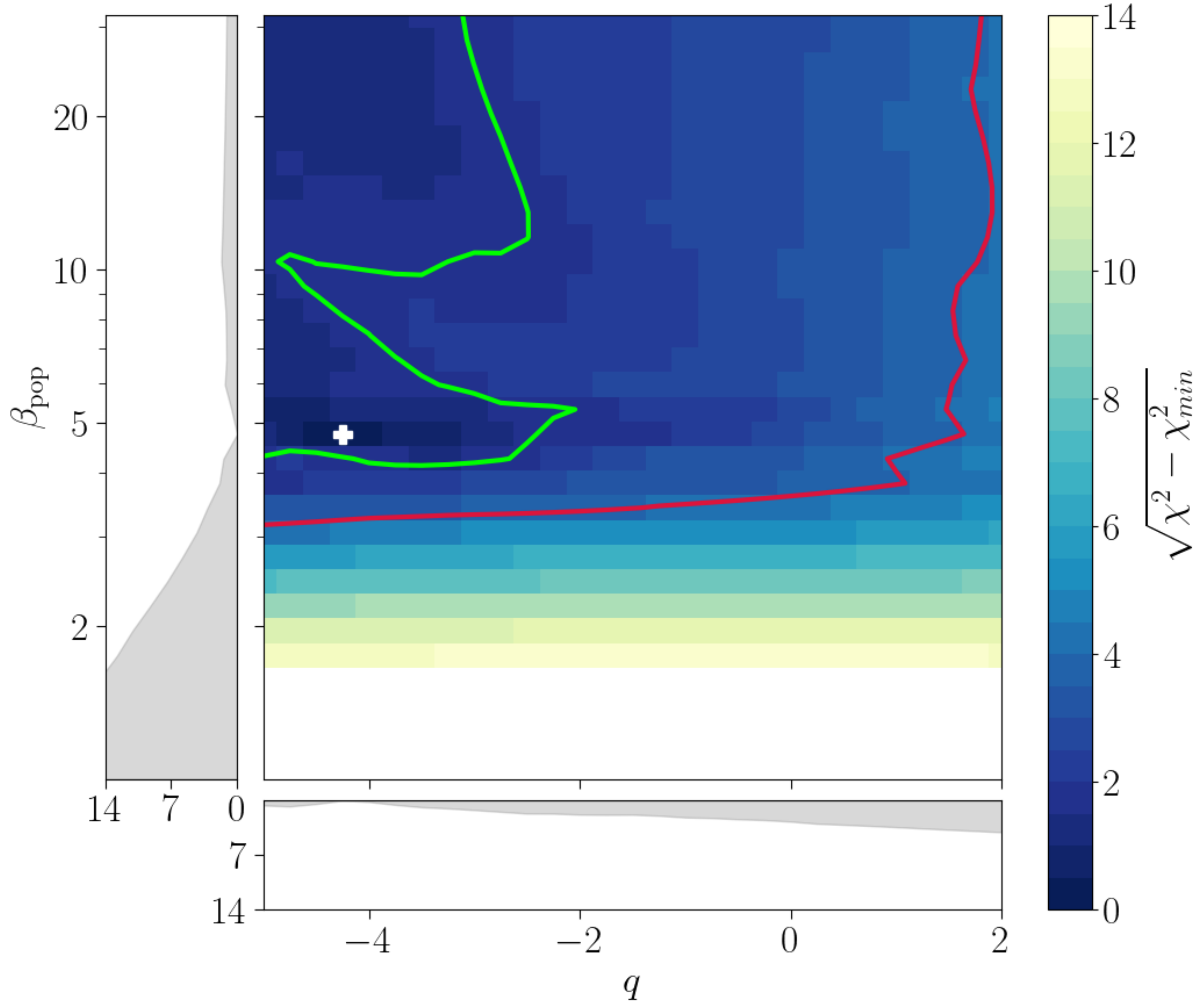

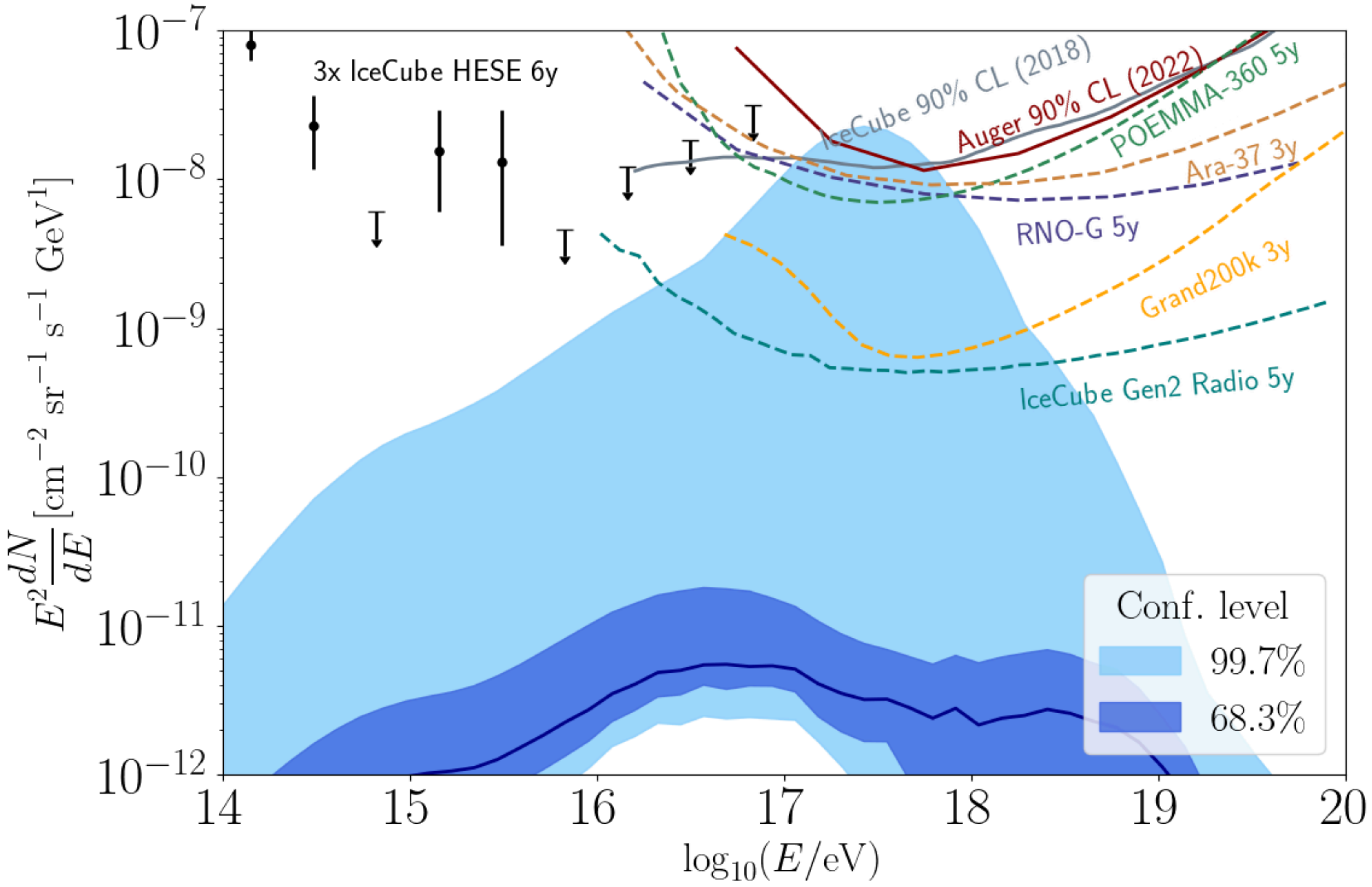

Different cutoff functions (super exponential)